Spring 5-2011

Microarray Data Mining and Gene Regulatory Network Analysis

Ying Li
University of Southern Mississippi

The University of Southern Mississippi

MICROARRAY DATA MINING AND GENE REGULATORY NETWORK ANALYSIS

by

Ying Li

A Dissertation
Submitted to the Graduate School
of The University of Southern Mississippi
in Partial Fulfillment of the Requirements
for the Degree of Doctor of Philosophy

May 2011

ABSTRACT

MICROARRAY DATA MINING AND

GENE REGULATORY NETWORK ANALYSIS

by Ying Li

May 2011

The novel molecular biological technology, microarray, makes it feasible to obtain quantitative measurements of expression of thousands of genes present in a biological sample simultaneously. Genome-wide expression data generated from this technology are promising to uncover the implicit, previously unknown biological knowledge. In this study, several problems about microarray data mining techniques were investigated, including feature(gene) selection, classifier genes identification, generation of reference genetic interaction network for non-model organisms and gene regulatory network reconstruction using time-series gene expression data. The limitations of most of the existing computational models employed to infer gene regulatory network lie in that they either suffer from low accuracy or computational complexity. To overcome such limitations, the following strategies were proposed to integrate bioinformatics data mining techniques with existing GRN inference algorithms, which enables the discovery of novel biological knowledge. An integrated statistical and machine learning (ISML) pipeline was developed for feature selection and classifier genes identification to solve the challenges of the curse of dimensionality problem as well as the huge search space. Using the selected classifier genes as seeds, a scale-up technique is applied to search through major databases of genetic interaction networks, metabolic pathways, etc.

By curating relevant genes and blasting genomic sequences of non-model organisms against well-studied genetic model organisms, a reference gene regulatory network for less-studied organisms was built and used both as prior knowledge and model validation for GRN reconstructions. Networks of gene interactions were inferred using a Dynamic Bayesian Network (DBN) approach and were analyzed for elucidating the dynamics caused by perturbations. Our proposed pipelines were applied to investigate molecular mechanisms for chemical-induced reversible neurotoxicity.

The University of Southern Mississippi

MICROARRAY DATA MINING AND GENE REGULATORY NETWORK ANALYSIS

by

Ying Li

A Dissertation
Submitted to the Graduate School
of The University of Southern Mississippi
in Partial Fulfillment of the Requirements
for the Degree of Doctor of Philosophy

Approved:

Chaoyang Zhang
Director

Nan Wang

Ping Gong

Edward J Perkins

Andrew Strelzoff

Susan A Siltanen
Dean of the Graduate School

May 2011

ACKNOWLEDGMENTS

I would like to thank Dr. Nan Wang, Dr. Chaoyang Zhang, and all the other committee members, Dr. Ping Gong, Dr. Edward J. Perkins, and Dr. Andrew Strelzoff, for their suggestions and advice to improve my work during the whole process. I gratefully acknowledge my advisors, Dr. Wang and Dr. Zhang, for their generous help in the past four years. Along the path of research that has led to this dissertation, they have constantly been there to provide me guidance, support and suggestions. I also would like to thank Dr. Ping Gong and Dr. Edward Perkins for their comments and for providing high-quality data during my doctoral research.

I am forever indebted to my parents, who have been extremely supportive and helpful despite living thousands miles away. My father always encourages me to do what I want to do, and my mother believes I am the best in the world, which gives me a lot of confidence. I am especially thankful to all other collaborators in Engineer Research and Development Center Environmental Lab in Vicksburg, MS. They gave me a lot of help when I was working there during my Ph.D. program.

TABLE OF CONTENTS

LIST OF TABLES

Table

LIST OF ILLUSTRATIONS

Figure

CHAPTER I

INTRODUCTION

Biological Background

Central Dogma of Molecular Biology

The Central Dogma of genetics [1] is: DNA is transcribed to RNA which is translated to protein. Protein is never back-translated to RNA or DNA, and DNA is never directly translated to protein. This dogma forms the backbone of molecular biology and is represented by four major stages: (1) replication: the DNA replicates its information in a process that involves many enzymes; (2) transcription: the DNA codes for the production of messenger RNA (mRNA); (3) In eukaryotic cells, the mRNA is processed (essentially by splicing) and migrates from the nucleus to the cytoplasm; (4) translation: messenger RNA carries coded information to ribosome. The ribosome "read" this information and uses it for protein synthesis. Proteins do not code for the production of protein, RNA or DNA. They are involved in almost all biological activities, structural or enzymatic. We often concentrate on protein coding genes, because proteins are the building blocks of cells and the majority of bio-active molecules. Figure 1.1 shows the central dogma of molecular biology [1].

The relationships of DNA, RNA, and Proteins are: Proteins determines the activity of the cells. They are the physical format of the abstract information integrated in the genome. DNA contains the genetic information and each cell has a copy. It is stable, packaged, and inert. RNA is the messenger and translator. It is unstable and lacks secondary structure. Some RNA has enzymatic activity.

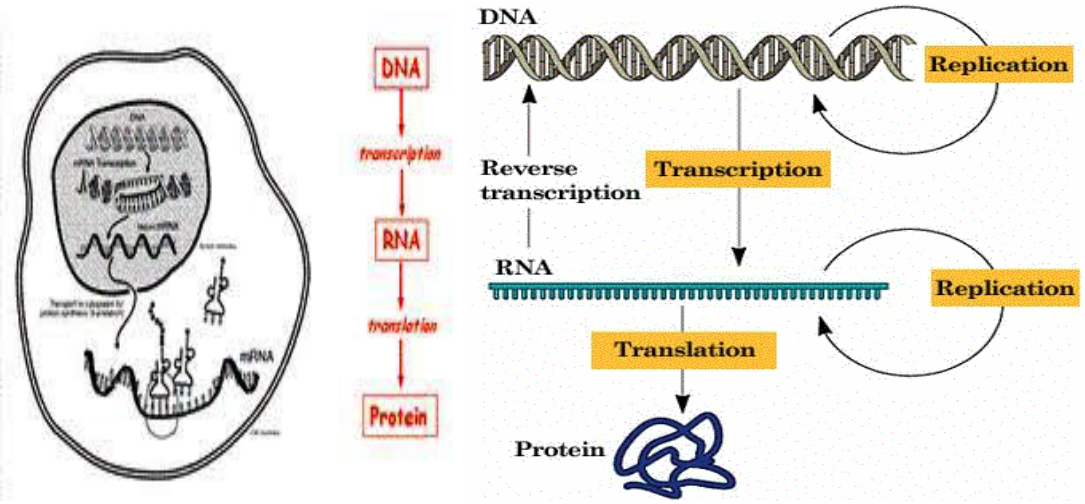

Figure 1.1. Central dogma of molecular biology [1].

Genes and Proteins

Genes are made of millions of deoxyribonucleic acid (DNA) molecules. A DNA molecule is constructed like a spiral staircase, or a double helix. The rails of the staircase are made of a backbone structure of phosphates and sugars, and the steps are pairs of four nitrogen-containing bases: adenine (A), cytosine (C), guanine (G), and thymine (T). Through hydrogen bonds the two rails of the staircase are kept together, A and T pair together, and C and G are partners [2].

A gene is made of a unique sequence of DNA bases. It is like a message containing a unique combination of letters. Then a translation of this message into information for protein production is performed. A protein is a folding chain of amino acids following a specific order. Altogether there are 20 different amino acids exist. The message for each amino acid within a protein is coded by a combination of three nucleotide bases. If the sequence in the message is misspelled, it will have a point mutation. As a result, the gene may produce a protein that has an incorrect shape so it won't combine with another protein (e.g., a receptor), leading to a mistake in the resulting message due to the unfitting

shape. In other words, if the message in the gene is misspelled, the protein it encodes may be wrong and its function in the body may be changed. In general, experimental and computational evidence shows that many genes produce an average of three different proteins and as many as ten protein products. The protein-coding regions of a gene are called exons, while the non-coding regions are called introns. Due to alternative splicing, the exons of a gene can be combined in different ways to make variants of the complete protein [3].

Gene Expression

By using the information from the DNA sequence of a gene, the synthesis of functional gene products is usually called gene expression. In Figure 1.2, it shows that there are two major steps in gene expression: transcription of DNA and translation of mRNA into protein. Here, the products are often proteins or functional RNA. Protein is considered the most basic building block of life. The roles that proteins play in the process of life include constituting cell structures, regulating cellular processes, catalyzing biochemical reactions in metabolic pathways, etc. The specific functions of a certain protein are determined by its particular physical structure and chemical properties.

Several steps in the gene expression process may be modulated, including the transcription, RNA splicing, translation, and post-translational modification of a protein. Gene regulation gives the cell control over structure and function, and is the basis for cellular differentiation, morphogenesis and the versatility and adaptability of any organism. Gene regulation may also serve as a substrate for evolutionary change, since control of the timing, location, and amount of gene expression can have a profound effect on the functions of the gene in a cell or in a multicellular organism.

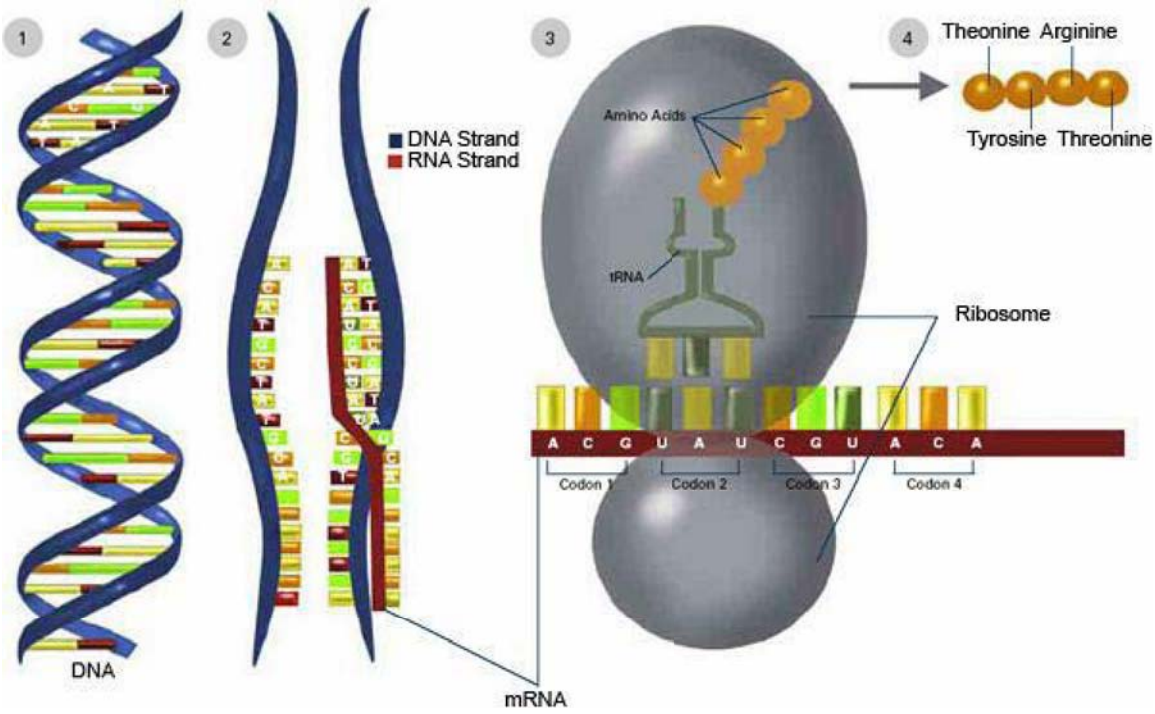

Figure 1.2. Transcription and translation process. Source from http://publications.nigms.nih.gov/thenewgenetics/chapter1.html

Gene Regulation

Gene regulation is the processes of cells regulate the information in genes to be turned into gene products. The majority of known mechanisms regulate protein coding genes although the product of a functional gene may be RNA or protein. A gene's expression could be modulated at any step, for instance, DNA-RNA transcription, or post-translational modification of a protein, etc. The regulation of gene's expression plays vial roles due to its increase of the versatility and adaptability of an organism by allowing the cell to express proteins when needed. Besides, the processes of cellular differentiation and morphogenesis are driven by gene regulation. Such processes lead to the creation of different cell types in multicellular organisms.

A gene regulation system consists of genes, cis-elements, and regulators [3]. The regulatory process of genes is illustrated in Figure 1.3. The regulators in the system could

be proteins in most cases, but small molecules such as miRNAs and metabolites may also be regulators sometimes. Such proteins that participate in the process of regulation are called transcription factors (TFs), or they are also referred to as trans-elements. The cis-elements, which are the complementary to trans-elements, are DNA segments that control the expression of corresponding genes.

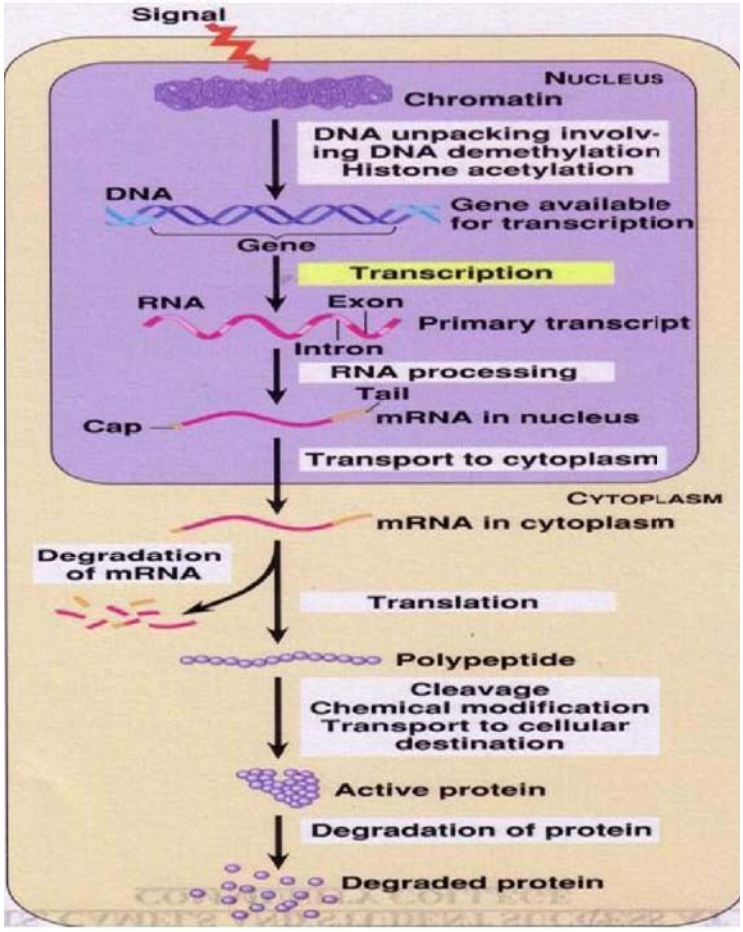

Figure 1.3. Regulations of genes.

There are six stages where gene expression is regulated: chromatin, domains, transcription, post-transcriptional modification, RNA transport, translation, and mRNA degradation. Any step of gene expression could be modulated. Among these stages, the most extensively utilized point is transcription initiation. There two major cases of regulation of gene expression, namely up-regulation and down-regulation. Up-regulation

occurs within a cell, which results in increased expression of one or more genes while down-regulation results in decreased gene expression and corresponding protein expression. The regulation mechanism includes the binding of certain TFs to cis-elements and then controls the level of target gene's expression during transcription. A gene's expression is regulated by some regulators, while its own expressed products can be regulators of another gene. The gene regulatory network (GRN) is formed by such complex regulatory connections [3].

DNA Microarray Technology

Functional genomics involves the analysis of large datasets of information derived from various biological experiments. One such type of large-scale experiment involves monitoring the expression levels of thousands genes simultaneously under a particular condition, called gene expression analysis. Microarray technology makes use of the sequence resources created by the genome projects and other sequencing efforts to answer the question, what genes are expressed in a particular cell type of an organism, at a particular time, under particular conditions.

DNA Microarray

A DNA microarray is a multiplex technology used in molecular biology, which consists of an arrayed series of thousands of microscopic spots of DNA oligonucleotides, called features (genes). Each feature contains picomoles (10^{-12} moles) of a certain DNA sequence, which are also known as probes. Such probes can be a fragment of a gene or other DNA element which are used to hybridize with a cDNA/cRNA sample under experimental designed conditions. A microarray experiment is able to accomplish several genetic tests in parallel because tens of thousands of probes can be included in an array. Thus, microarray technology allows us to monitor tens of thousands of gene expressions

and have significantly accelerated the investigations of many types of biology experiments. Figure 1.4 illustrated the overall workflow of a microarray experiment.

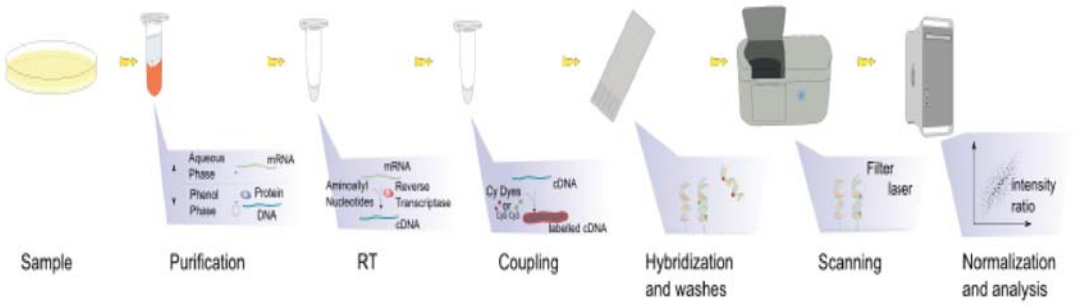

Figure 1.4. Workflow of microarray experiment. Source from http://images-mediawiki-sites.thefullwiki.org/06/3/9/3/8878261581107656.png

Microarray technology evolved from Southern blotting, where fragmented DNA is attached to a substrate and then probed with a known gene or fragment. The use of a collection of distinct DNAs in arrays for expression profiling was first described in 1987, and the arrayed DNAs were used to identify genes whose expression is modulated by interferon [4]. These early gene arrays were made by spotting cDNAs onto filter paper with a pin-spotting device. The use of miniaturized microarrays for gene expression profiling was first reported in 1995 [5], and a complete eukaryotic genome on a microarray was published in 1997 [6].

Microarray Types and Applications

There exist many types of microarrays and they are differed by whether being spatially arranged on a surface or on coded beads. The early-stage array is a collection of orderly microscopic spots. Each spot is combined with a specific probe attached to a solid surface, such as silicon, glass or plastic biochip. The location of a certain probe has been arranged and thousands of these probes are placed on a single DNA microarray. On the alternative, bead array is a collection of microscopic polystyrene beads. A specific probe

and a ratio of two or more dyes are combined with each bead. Thus, they do not interfere with the fluorescent dyes used on the target sequence. DNA microarrays technology can be used in many areas such as gene expression profiling, comparative genomic hybridization, chromatin immunoprecipitation on Chip (ChIP), SNP detection, alternative splicing detection [4, 5, 7, 8] and etc.

Microarray Data Analysis

Microarray experiments are inexpensive compare to many other biological experimental technologies. However, there exist several specific bioinformatics challenges as follows: first one is the multiple levels of replication in experimental design. Due to the biological complexity of gene expression, experiment design of a microarray experiment is critically important if statistically and biologically valid conclusions need to be elucidated from the data [9]. The second challenge is the number of platforms and distinct groups and data format. Microarray data is impossible to be exchanged due to the lack of standard protocols in platform fabrication, assay types, and analysis approaches. The "MicroArray Quality Control (MAQC) Project" is being conducted by the US Food and Drug Administration (FDA) to form standards and quality control metrics which will allow the use of microarray data in many fields such as drug discovery, clinical practice and regulatory decision-making [10, 11]. The third challenge is statistical analysis regards to accuracy and precision. Microarray data sets are normally of huge amount, and its analytical precision is influenced by several variables. Statistical challenges include effects of image background noise, whether appropriate normalization and transformation techniques are conducted, identification of significantly differentially expressed genes (DEGs) [12, 13, 14, 15] as well as inference of gene regulatory networks

[16]. How to reduce the dimensionality of microarray dataset in order to obtain more comprehension and focused analysis requires further preprocess of microarray data [17].

Contributions

In this dissertation, we have made a number of contributions in identification and optimization of classifier genes and significant pathways. Based on such information, reconstruction of gene regulatory networks of interested pathways was performed, and all above work were summarized below.

Identification and Optimization of Classifier Genes

One important goal of microarray experiments is to discover novel classifier genes which play vital roles in genetic and molecular interactions. Microarrays have been successfully served as a research tool in discovering novel drug targets [18] and disease- or toxicity-related biomarker genes for cancer classification [19]. A challenge in classifying or predicting the diagnostic categories using microarray data is the curse of dimensionality problem coupled with sparse sampling. That is, the number of examined genes per sample is much greater than the number of samples that are involved in classification [20]. The other crucial challenge is that the huge search space for an optimal combination of classifier genes renders high computational expenses [21]. To address these two issues, we developed the new Integrated statistical and machine learning (ISML) pipeline, which integrates statistical analysis with supervised and unsupervised machine learning techniques. A set of classifier/biomarker genes from high dimensional datasets were identified and classification models of acceptable precision for multiple classes were generated as well by our pipeline. More details will be discussed in Chapter III.

Reference Network Builder

Gene Regulatory Networks (GRNs) provide integrated views of gene interactions that control biological processes. Many public databases contain biological interactions extracted from literature with experimental validations, but most of them only provide information for a few genetic model organisms. A number of computational models have been developed to infer GRN from microarray data, and these models are often evaluated on model organisms. Researchers who work with non-model organisms rely on these computational models to build GRN for less-studied organisms. However, they can only evaluate GRNs built by computational models based on the evaluation criteria such as recall, precision tested on model organisms. The accuracy and reliability of the tools are critical for non-model organisms. The researchers also are interested in evaluating the GRN based on “true” GRN of their organisms. Although, some public network databases provide experimentally validated interactions among genes or proteins, there are limitations in accessibility and scalability. Thus, we developed a cyber-based integrated environment, called "reference network (RefNet)", to build a reference gene regulatory network for less-studied organisms. The resulting reference network could be used for validation of inferred GRNs or as prior knowledge for further inference.

Gene Regulatory Network Reconstruction

In the past, many computational models have been proposed to infer gene regulatory networks. Among them Probabilistic Boolean Network (PBN) [22, 23, 24, 25, 26] and Dynamic Bayesian Network (DBN) [27, 28, 29, 30, 31] are two popular and powerful models. PBN is a discrete state space model which characterizes a system using quantized data, while DBN is an extension of Bayesian network model to incorporate temporal concept. Previous studies showed that both PBN and DBN approaches had good

performance in modeling the gene regulatory network, but DBN identified more gene interactions and gave better accuracy than PBN [32]. Besides, *Zou et al.* [28] used DBNs with various time-delays, by shifting time-series profiles with properly predicted amount of time steps. Therefore, we used the time-lagged DBN to reconstruct those chemical-induced networks/pathways which were identified by the RefNet (see Chapter IV) to analyze the dynamics caused by perturbations.

Dissertation Organization

This dissertation is organized as follows: In Chapter II, we introduce some basic concepts and backgrounds of microarray experiments and gene regulatory networks. Then some data preprocessing methods and techniques based on microarray data are introduced, such as transformation, normalization, etc. We also discuss some statistical models to identify differentially expressed genes such as t-test, ANOVA and others for either two-class comparison or multi-class comparison. Then, some machine learning methods such as clustering, classification based on microarray data for feature selection and identification of biomarker genes are reviewed.

In Chapter III, we proposed an integrated pipeline combining statistical analysis and machine learning approaches to identify a set of classifier genes for disease diagnostic and toxicity evaluation. We assembled an integrated statistical and machine learning pipeline consisting of several well-established feature filtering/selection and classification techniques to analyze microarray dataset in order to construct classifier models that can separate samples into different treatment groups such as evaluating toxicity exposure in certain environment or diagnosing cancer patients from normal people, etc.

In Chapter IV, a cyber-based environment to retrieve reference genetic interaction network (RefNet) is proposed. Our RefNet toolbox provides the following services: (1) to

build reference GRN/Pathway for non-model organisms; (2) to provide biological prior knowledge of GRN to improve computational models; (3) to interpret and compare the GRNs built from computational models with wet-lab experiments; and (4) to serve as a gene selection tool for GRN reconstruction.

In Chapter V, we introduced and discussed various computational methodologies to infer gene regulatory network. A review of existing inferring algorithms such as Boolean networks, Bayesian networks, and Dynamic Bayesian network is given. The time-lagged dynamic Bayesian network model was used to reconstruct sets of genes from selected pathways by RefNet. Results showed that our strategy helped with the improvement of accuracy as well as computational cost of GRN reconstruction and novel biological knowledge was discovered. In Chapter VI, by integrating all the toolkits and services for microarray data mining and gene regulatory network analysis, we presented two case studies to present the detailed contextual analysis.

We complete the dissertation by summarizing our work, and providing sets of issues appropriate for future work in Chapter VII.

CHAPTER II

REVIEW OF MICROARRAY DATA MINING

Microarray Experiments and Data Generation

A microarray experiment requires a number of cDNA or oligonucleotide DNA sequences (probes) that are affiliated to a glass, nylon, or quartz wafer (adopted from the semiconductor industry and used by Affymetrix, Inc. [33]). Then material containing RNA, which is acquired from the biological samples to be studied, is mixed with this array. For example, the mixture of samples from normal tissues with samples from cancer tissues. Figure 2.1 illustrates the basic process of cDNA microarray experiments.

Microarrays can be manufactured using various technologies. In spotted microarrays, the probes are oligonucleotides, cDNA or small fragments of PCR products that correspond to mRNAs. The probes are synthesized prior to deposition on the array surface and are then "spotted" onto glass. The resulting grid of probes represents the nucleic acid profiles of the prepared samples. This provides a relatively low-cost microarray that may be customized for each study, and avoids the costs of interest to the investigator. However, publications exist which indicate such microarrays may not provide the same level of sensitivity compared to commercial oligonucleotide arrays [34]. In oligonucleotide microarrays, the probes are short sequences designed to match parts of the sequence of known or predicted Expressed Sequence Tags (ESTs), which is a short sub-sequence of a transcribed cDNA sequence [35]. Oligonucleotide arrays are produced by printing short oligonucleotide sequences designed to represent a single gene or family of gene splice-variants by synthesizing this sequence directly onto the array surface instead of depositing intact sequences. Sequences may be longer (60-mer probes such as the Agilent design) or shorter (25-mer probes produced by Affymetrix) depending on the

desired purpose; longer probes are more specific to individual target genes, shorter probes may be spotted in higher density across the array [36].

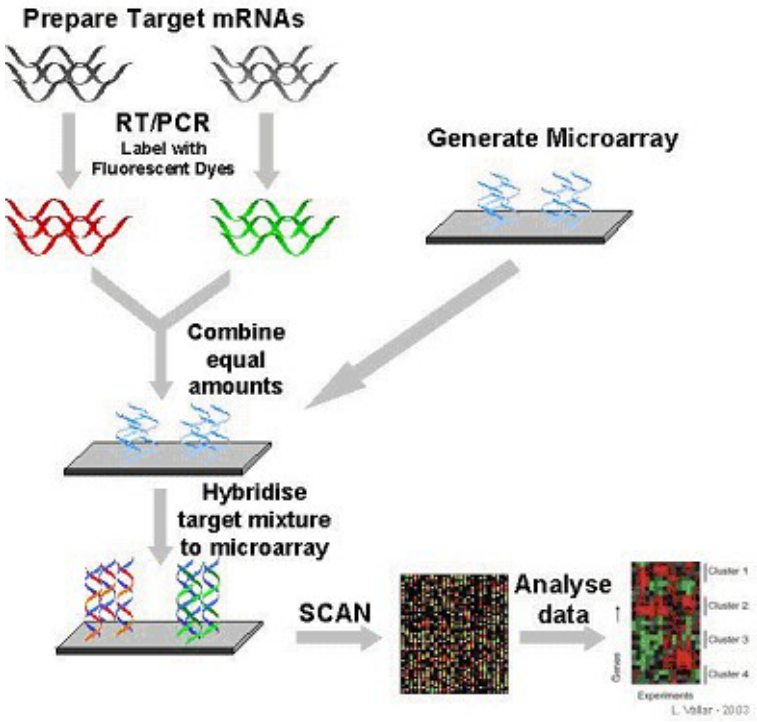

Figure 2.1. Process of cDNA microarray experiment design. Source from http://www.microarray.lu/en/MICROARRAY_Overview.shtml

Two-color microarrays or two-channel microarrays are typically hybridized with cDNA prepared from two types of samples to be compared (i.e., chemical-treated sample versus un-treated sample) and they are labeled with two different fluorophores [37]. *Cy3* and *Cy5* are two common fluorescent dyes that are used for cDNA labeling. The two Cy-labeled cDNA samples are mixed and hybridized to a single microarray which is then scanned in a microarray scanner to measure the intensities of fluorescence of the two fluorophores after excitation with a laser beam of a defined wavelength. Relative intensities of each fluorophore are then used to identify up-regulated and down-regulated genes [38]. In single-channel or one-color microarrays, the array provides intensity data for each probe indicating a relative level of hybridization with the labeled target.

However, this intensity data is not true indicator of abundance level of a gene, but rather a relative abundance when compared with other samples processed in the same experiment. Since each chip is exposed to only one sample as opposed to two-channel platform, the single-channel system is more accurate. In one-color array chip, an aberrant sample cannot affect the raw data derived from other samples. While in two-color array chip, a single low-quality sample may drastically impinge on the precision of overall data set even if the other sample was of high quality. Another advantage of single-channel chip is that it is much easier when comparing data to arrays from different experiments as long as batch effects are taken care of.

Microarray Data Preprocessing

Image Processing Analysis

The population of mRNA in a certain sample can be stored as an image with intensity values indicating the relative expression level for each gene. The array chips are scanned by microarray scanners, which are provided by microarray manufacturers, and the intensity values of each spot on the chip are recorded. Image processing involves the following steps: (1) Identification of the spots and distinguishing them from spurious signals. The microarray is scanned following hybridization and an image file is generated. Once image generation is completed, the image is then analyzed to identify spots and used to identify regions that correspond to spots; (2) Determination of the spot area will be studied and identification of the local region is used to estimate background noise. After identifying regions that correspond to sub-arrays, in order to get a measurement of the spot signal and estimated for background intensity, a region within the sub-array needs to be selected; (3) Reporting statistics summary and generate spot intensity by subtracting background intensity. In this step, once the center and

background areas have been determined, a number of statistics summary for each spot are reported. Another concern in image processing is the number of pixels to be included for measurement in the spot image [39]. For many scanners, the default pixel size is 10μm. However, it is better to use a smaller pixel size to make sure enough pixels included. Even though using a smaller pixel size increases the confidence in the measurement, the image size tends to be bigger when compared with ones using larger pixel size.

Data Normalization and Transformation

The purpose of normalization is to eliminate variations to allow appropriate comparison of data that is obtained from each sample. Comparison of different arrays/samples normally involves making adjustments for systematic errors which is introduced by different procedures and effects. The order of operations for filtering the data is that spot filters are applied first, then data normalization, and then truncation of extreme values, then gene screening.

Spot filtering refers to filters on spots in individual arrays. Spot filtering is used for quality control purposes, i.e., to filter out "bad" spots. Unlike gene screening, Spot filtering does not filter out the entire gene (a row), but replaces the existing values of a spot within any given array with a missing value. There exist four types of spot filters: intensity filter, spot flag filter, spot size filter and detection call filter. The intensity filter is applied to the background adjustment of signals and different parameters are adopted for dual-channel or single-channel data. The spot flag filter can contain both numeric and character values. Outside of a specified numeric range, a flag is considered to be "excluded". For example, in Affymetrix array, a Detection Call column is used to designate as the spot flag at the time of collating, which allows the users to filter out expression values that have an "A" (Absent) call. Additionally, the spot flag is also used

to filter out spots with a large percentage of expression values that have a spot flag value of "A".

In general, a logarithmic (base 2) transformation is applied to the signal intensities (for single-channel data) or intensity-ratios (for dual-channel data) before they are normalized and truncated. There are currently four major normalization options: median normalization, housekeeping gene normalization, lowess normalization as well as print-tip group normalization. The first two are available for both single-channel and dual-channel data, but the last two are only for dual-channel data. For single-channel data, the user needs to choose a reference array against which all other arrays will be normalized. The "median" reference array is selected as following algorithm:

(1) Let N be the number of experiments, and let i be an index of experiments running from 1 to N.

(2) For each array i, the median log-intensity of the array (denoted M_i) will be computed.

(3) A median M will be selected from the $\{M_1,\ldots,M_N\}$ values. If N is even, then the median M will be the lower of the two middle values.

(4) The array whose median log-intensity M_i equals the overall median M will be chosen as the median array.

Then, the median normalization is performed by subtracting out the median log-ration for each array, so that each normalized array has a median log-ration of 0. Such median normalization is called per-gene normalization. Besides, per chip normalization is performed by computing a gene-by-gene difference between each array and the reference array, and subtracting the median difference from the log-intensities on that array, so that the gene-by-gene difference between the normalized array and the reference array is 0.

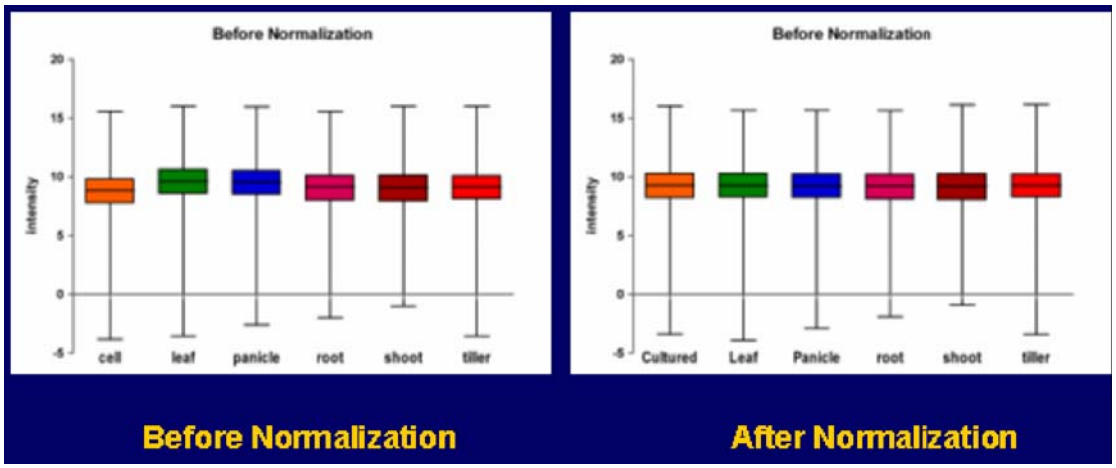

Figure 2.2. Intensity distribution of arrays before and after median normalization.

For dual-channel data, locally weighted linear regression (LOWESS) normalization is normally used. In the lowess normalization, a non-linear lowess smoother function is fit to the graph of un-normalized log-ratio on the y-axis versus average log intensity (i.e., *[log(R)+log(G)]/2*) on the x-axis. That is, lowess normalization assumes that the dye bias appears to be dependent on spot intensity. The adjusted ratio is computed by the following Equation 2.1:

$$\log\frac{R}{G} \rightarrow \log\frac{R}{G} - c(A) \quad (2.1)$$

where *c(A)* is the lowess fit to the $\log R/G$ versus $\log \sqrt[2]{R \times G}$ plot. Lowess regression is a technique for fitting a smoothing curve to a dataset. The degree of smoothing is determined by the window width parameter. In general, a larger window width results in a smoother curve, while a smaller window results in local variation [40, 41, 42, 43]. Figure 2.3 shows the plots under different lowess window width.

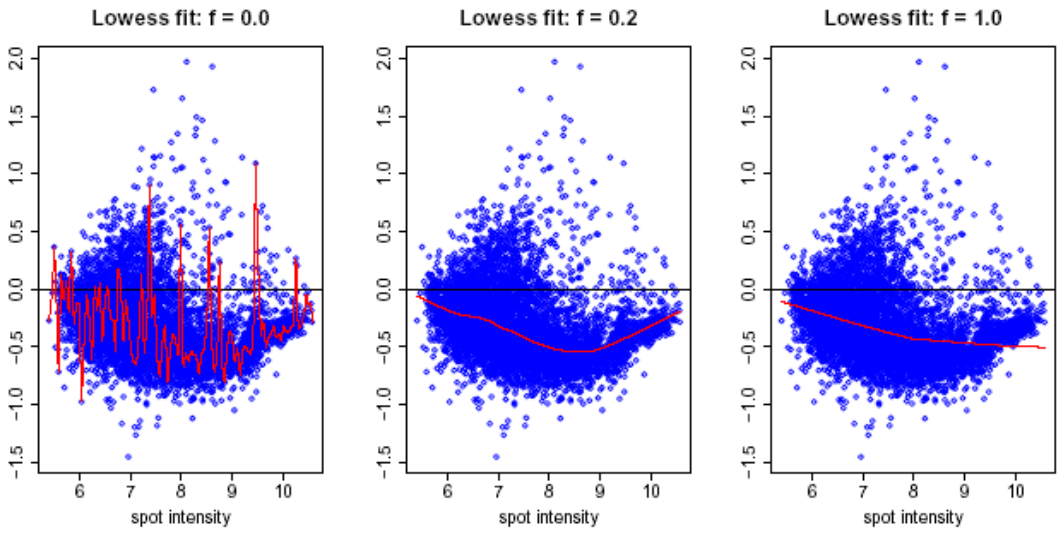

Figure 2.3. Spot intensity plots with different lowess window width.

Missing Values

After applying various techniques of normalization or filtering, missing expression values may exists in the data sets. However, many further gene expression analysis require a complete matrix of array values. Even missing values are allowed for some analysis algorithms, they are treated as intensity value of zero when calculated, which will certainly affect the accuracy and validity of analysis results. Therefore, methods for imputing missing data are needed to minimize the effect of incomplete data sets. Previously, three most popular methods to impute missing values are proposed, namely, Singular Value Decomposition (SVD) based method (SVDimpute) [45, 46, 47], weighted *K*-nearest neighbors (KNNimpute) [44], as well as row average. The KNN-based method selects genes whose expression profiles are similar to the gene of interest to impute missing values. Suppose there is a missing value in experiment 1 for gene A, KNNimpute will find *K* other genes whose expression values are most similar to A in experiments *2* to *N*. Euclidean distance, which is the metric for gene similarity is used during the imputing process. The row average technique is trivial as calculating the average of the row

containing missing values and filling them with it. SVDimpute method can only be performed on complete matrices, so row average is imputed for all missing values and then utilize an expectation maximization method to arrive at the final estimate. *Troyanskaya et al.* compared the above three missing value imputation techniques and KNN-based estimations turned out to have best performance among the three on the same data set.

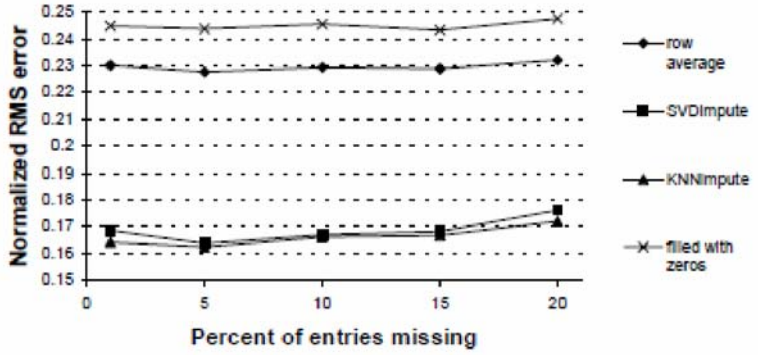

Figure 2.4. Comparison of KNN, SVD, and row average based estimations' performance on the same data set [44].

Identification of Differentially Expressed Genes (DEGs)

One of the common interests of microarray analysis is to identify genes that are significantly differentially expressed. Such DEGs are ones with expression ratio significantly different from 1 and are considered as important genes in later analysis study such as classification, clustering, or gene regulatory network reconstruction. Although some clustering techniques are used to find groups of genes with similar patterns [48, 49, 50], it is still very useful to find those genes that are changed significantly between different samples or conditions. A number of methods are proposed to identify the largely varied genes such as fold-change cut-off (usually two folds is used) method or a statistical approach called "Z-score", which calculates the mean and standard

deviation of the distribution of intensity values and defines a global fold change difference and confidence level. Therefore, if the confidence level is chosen at 95%, DEGs will have a Z-score value of $Z > 1.96$ [51]. Figure 2.5 illustrates an example of a *Z*-score selection application.

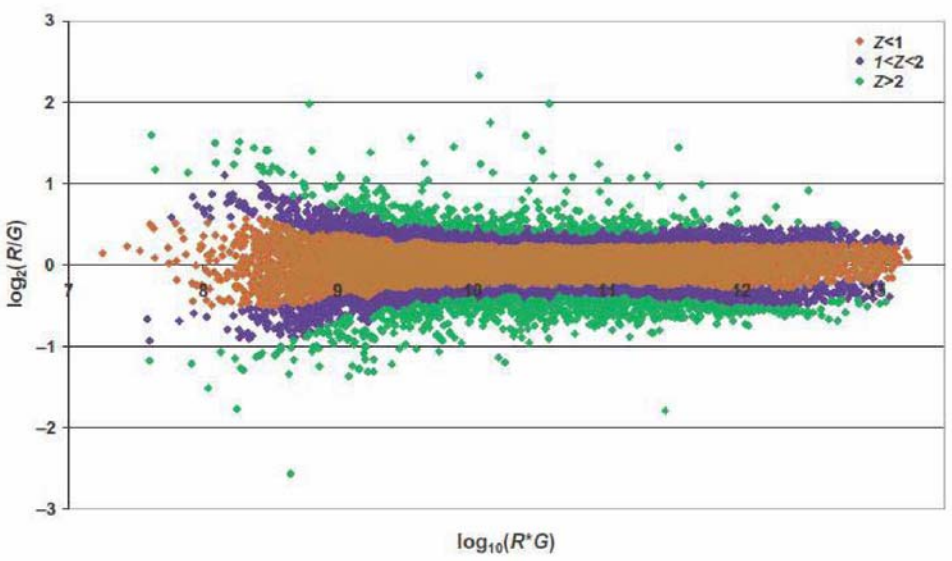

Figure 2.5. Intensity-dependent *Z*-scores for identifying differential expression.

In general, if two classes are compared and the experiments are paired, the paried t-test could be used to find DEGs. For example, DEGs can be found by comparing samples from cancer tissues with normal tissues. Here, either a single replicate for each RNA sample is used or the averaging mean of all replicates should be used. T-test (or F-test) is based on the comparison of differences in the mean log-ratios / log-intensities between classes relative to the variation expected in the mean differences. It is assumed that all the samples are independent. Alternatively, if multivariate permutation classes need to be compared (i.e., more than two classes), analysis of variance (ANOVA) is used, usually one-way ANOVA. The ANOVA test the null hypothesis that samples in multiple groups are drawn from the same population. Two estimates, which are made of the population variance, rely on various assumptions such as independent samples, equal variances of

populations, etc. The ANOVA calculates an F-score, which is the ratio of the variance among the means to the variance within the samples.

Feature Selection

Due to the "curse-of-dimensionality," i.e., the large dimensionality (usually contain tens of thousands of genes) and their relatively small sample sizes [52], it is of great challenge to analyze microarray data using data mining techniques. Furthermore, experimental complications such as systematic noise and variability add more difficulties to the analysis. Thus, one of the effective ways to deal with these particular characteristics of microarray data is to reduce the dimension and select "useful" features [53, 54, 55, 56]. A number of feature selection techniques has been proposed and studied to contribute to feature selection methodologies [57]. There are two major types of feature selection methods: univariate filtering and multivariate filtering. Figure 2.6 summarizes the most widely used techniques [58].

Univariate Filtering

Due to the high dimensionality of microarray data set, fast and efficient feature selection techniques such as univariate filtering methods are widely used. Previously and nowadays, comparative evaluations of different classification and feature selection techniques over DNA microarray datasets are normally focused in the univariate cases [59, 60, 61, 62]. Some trivial heuristics for the identification of DEGs include choosing a threshold for the fold-change differences in gene expression, and detection of the threshold point in each gene that minimizes the misclassification of training sample numbers [63]. Furthermore, new or adapted univariate feature ranking techniques has been developed, which is divided into two classes: parametric and model-free methods. Parametric methods assume a given distribution from which the samples have been

generated. Among them, t-test and ANOVA are the most widely used approaches in microarray analysis. Dominating the parametrical analysis field by Gaussian assumptions, other parametrical approaches such as regression modeling technique [64] and Gamma distribution models [65] are also useful.

Filter methods			Wrapper methods	Embedded methods
Univariate		Multivariate		
Parametric	Model-free			
t-test (Jafari and Azuaje, 2006)	Wilcoxon rank sum (Thomas *et al.*, 2001)	Bivariate (Bø and Jonassen, 2002)	Sequential search (Inza *et al.*, 2004; Xiong *et al.*, 2001)	Random forest (Díaz-Uriarte and Alvarez de Andrés, 2006; Jiang *et al.*, 2004)
ANOVA (Jafari and Azuaje, 2006)	BSS/WSS (Dudoit *et al.*, 2002)	CFS (Wang *et al.*, 2005; Yeoh et al., 2002)	Genetic algorithms (Jirapech-Umpai and Aitken, 2005; Li *et al.*, 2001; Ooi and Tan, 2003)	Weight vector of SVM (Guyon *et al.*, 2002)
Bayesian (Baldi and Long, 2001; Fox and Dimmic, 2006)	Rank products (Breitling *et al.*, 2004)	MRMR (Ding and Peng, 2003)	Estimation of distribution algorithms (Blanco *et al.*, 2004)	Weights of logistic regression (Ma and Huang, 2005)
Regression (Thomas *et al.*, 2001)	Random permutations (Efron *et al.*, 2001; Pan, 2003; Park *et al.*, 2001; Tusher *et al.*, 2001)	USC (Yeung and Bumgarner, 2003)		
		Markov blanket (Gevaert *et al.*, 2006; Mamitsuka, 2006; Xing *et al.*, 2001)		
Gamma (Newton *et al.*, 2001)	TNoM (Ben-Dor *et al.*, 2000)			

Figure 2.6. Key references for feature selection technique in microarray domain [58].

Multivariate Filter Paradigm

Univariate filtering approaches have specific restrictions and may cause less accurate classifiers. For example, gene to gene regulatory interactions are not considered. Therefore, techniques that capture such correlations between genetic interactions are proposed. The widely used applications of multivariate filter methods includes simple bivariate interactions [66], correlation-based feature selection (CFS) [67, 68] as well as some variants of the Markov blanket filter method [69, 70, 71]. An alternative way to perform a multivariate gene selection is to use wrapper or embedded methods. This could incorporate the classifier's bias into the search space and more accurate classifiers might

be constructed. Most wrapper approaches use population-based, randomized search heuristics [72, 73, 74, 75] while others use sequential search techniques [76, 77].

Inference of Gene Regulatory Networks (GRNs)

Inference of gene regulatory network is yet another major application of analysis of gene expression data. Such study is also known as reverse engineering problem, specifically, reverse engineering of gene regulatory networks. Previous studies [78, 79] indicate that microarray expression data can be used to make predictions about the genetic transcriptional regulation relationships. In a gene regulatory network, the nodes of this network could be protein products, their coded genes/mRNAs, and complexes of groups of proteins. While the edges between nodes represent protein-to-protein interactions, protein-to mRNA interactions, or molecular reactions. The structure of gene regulatory network is an abstraction of the system's chemical dynamics, describing the mechanisms how one substance affects all the others to which it is connected. Such gene regulatory networks are inferred from the biological knowledgebase for a certain system and represent a distillation of the collective knowledge regarding a set of related biochemical reactions. Figure 2.7 is an example of a gene regulatory network.

Mathematical models of GRN have been developed to capture the behavior of the modeled system, and generate predictions corresponding with experimental observations in some cases. In some other cases, models could make accurate novel predictions, which can be tested experimentally. Therefore, to explore in an experiment by suggesting novel approaches are not considered in the design of the protocol of an experimental laboratory. Several approaches are used for reconstruction or inference of gene regulatory networks from gene expression data such as clustering, classification, and visualization, etc. These methods generally group genes based on the similarity of expression patterns. In addition, many

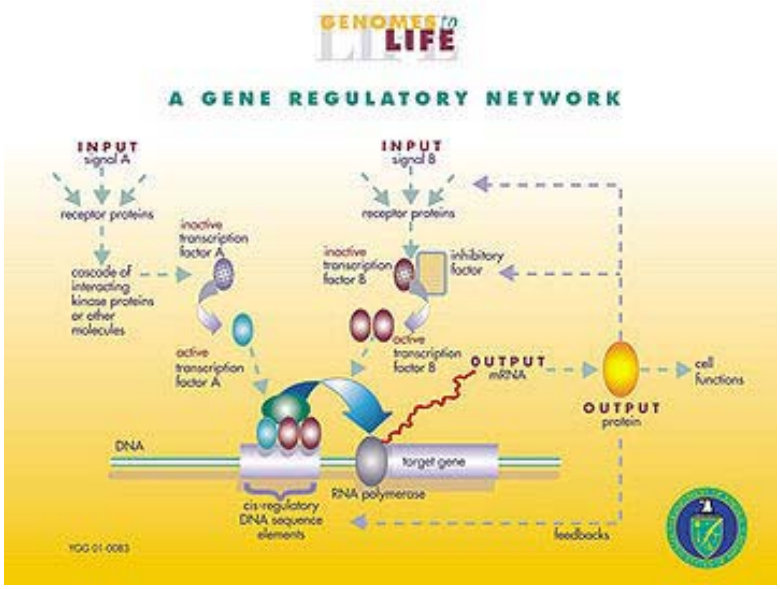

Figure 2.7. A typical gene regulatory network. Source from http://upload.wikimedia.org/wikipedia/commons/thumb/c/c4/Gene_Regulatory_Network.jpg/360px-Gene_Regulatory_Network.jpg

computational approaches have been proposed to reconstruct gene regulatory networks based on large-scale microarray data retrieved from biological experiments such as information theory [80, 81, 82, 83, 84], Boolean networks [23, 26, 85, 86, 87, 88], differential equations [89, 90, 91, 92, 93], Bayesian networks [27, 28, 29, 30, 94, 95, 96] and neural networks [97]. Many computational methods have been developed for modeling or simulating GRNs.

CHAPTER III

IDENTIFY CLASSIFIER GENES USING ISML PIPELINE

From a regulatory standpoint, there is an increasing and continuous demand for more rapid, more accurate and more predictive assays due to the already large but still growing, number of man-made chemicals released into the environment [98]. Molecular endpoints such as gene expression that may reflect phenotypic disease symptoms manifested later at higher biological levels (e.g., cell, tissue, organ, or organism) are potentially biomarkers that meet such demands. As a high throughput tool, microarrays simultaneously measure thousands of biologically-relevant endpoints (gene expression). However, to apply this tool to animals under field conditions, one critical hurdle to overcome is the separation of toxicity-induced signals from background noise associated with environmental variation and other confounding factors such as animal age, genetic make-up, physiological state and exposure length and route [99, 100]. A common approach to biomarker discovery is to screen genome- or transcriptome-wide gene expression responses and identify a small subset of genes capable of discriminating animals that received different treatments, or predicting the class of unknown samples. It is relatively less challenging to identify differentially expressed genes from two or more classes of samples. However, the search for an optimal and small subset of genes that has a high discriminatory power in classifying field samples often having multiple classes is much more complicated.

We propose an integrated statistics and machine learning (ISML) pipeline to analyze the microarray dataset in order to construct classifier models that can separate samples into different chemical treatment groups. The results show that our approach can be used to identify and optimize a small subset of classifier/biomarker genes from high

dimensional datasets and generate classification models of acceptable precision from multiple classes.

Integrated Statistical and Machine Learning (ISML) Pipeline

Overview of ISML

A challenge in classifying or predicting the diagnostic categories using microarray data is the curse of dimensionality problem coupled with sparse sampling. That is, the number of examined genes per sample is much greater than the number of samples that are involved in classification [101]. The other crucial challenge is that the huge search space for an optimal combination of classifier genes renders high computational expenses [102]. To address these two issues, we developed the new ISML pipeline, which integrates statistical analysis with supervised and unsupervised machine learning techniques (Figure 3.1). The pipeline consists of four major components: (1) statistical analysis that reduces dimensionality through identification of the most differentially expressed genes; (2) tree-based algorithms that are used to further downsize the number of classifier genes with assigned weight and associated ranking; (3) MC-SVM and unsupervised clustering, each of which independently selects an optimal set of classifier genes using an iterative elimination process; and (4) the integration of the two independent gene sets to generate a final refined gene sets.

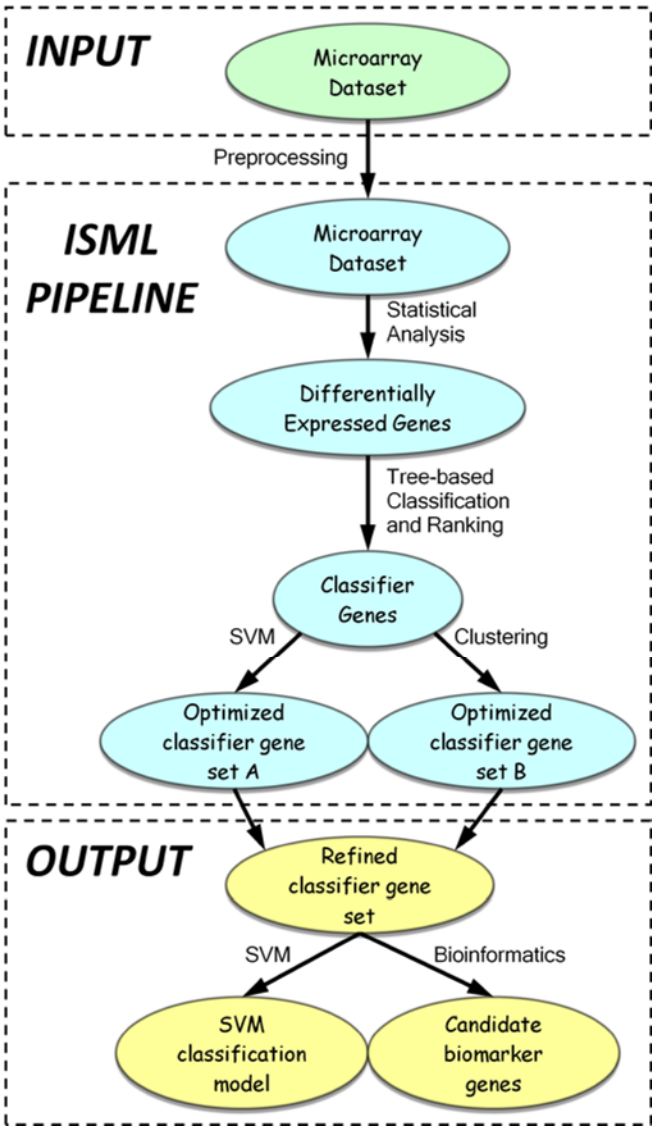

Figure 3.1. Overview of the ISML pipeline.

Feature Filtering by Statistical Analysis

Data Preprocessing

The following data pre-treatment steps were applied prior to further statistical and computational analyses: (1) feature filtering: flag out spots with signal intensity outside the linear range as well as non-uniform spots; (2) conversion: convert signal intensity into relative RNA concentration based on the linear standard curve of spike-in RNAs; (3)

normalization: normalize the relative RNA concentration to the median value on each array; and (4) gene filtering: filter out genes appearing in less than 50% of arrays.

Identification of Differentially Expressed Genes

The Class Comparison Between Groups of Arrays Tool in BRB-ArrayTools v.3.8 software package ([103]; linus.nci.nih.gov/BRB-ArrayTools.html) was used to identify significantly changed genes. The dataset was normalized and transformed previously, and then was imported into the BRB-ArrayTools application. The tool runs a random variance version of the t-test or F-test separately for each gene. It performs random permutations of the class labels and computes the proportion of the random permutations that give as many genes significant at the level set by the user as are found in comparing the true class labels. Differentially expressed genes were inferred by univariate statistical analysis. In general, we use a univariate test random variance model, multivariate permutation test with 10,000 random permutations, a confidence level of false discovery rate assessment = 99%, and a maximum allowed number of false-positive genes = 10.

Classifier Gene Selection and Ranking

Molecular endpoints such as gene expression that may reflect phenotypic disease symptoms manifested later at higher biological levels (e.g., cell, tissue, organ, or organism) are potentially biomarkers that meet such demands. As a high throughput tool, microarrays simultaneously measure thousands of biologically-relevant endpoints (gene expression). However, to apply this tool to animals under field conditions, one critical hurdle to overcome is the separation of toxicity-induced signals from background noise associated with environmental variation and other confounding factors such as animal age, genetic make-up, physiological state and exposure length and route [99, 100]. A common approach to biomarker discovery is to screen genome- or transcriptome-wide

gene expression responses and identify a small subset of genes capable of discriminating animals that received different treatments, or predicting the class of unknown samples. It is relatively less challenging to identify differentially expressed genes from two or more classes of samples. However, the search for an optimal and small subset of genes that has a high discriminatory power in classifying field samples often having multiple classes is much more complicated.

Classifier Gene Selection by Tree-Based Algorithms

A tree structure consists of a number of branches, one root, a number of internal nodes and a number of leaves. A decision tree is a decision support tool that uses a tree-like model of decisions and their possible consequences, where each internal node (non-leaf node) denotes a test on an attribute, each branch represents an outcome of the test, and each leaf node holds a class label. The topmost node in a tree is the root node. The occurrence of a node (feature/gene) in a tree provides the information about the importance of the associated feature/gene. At each decision node in a decision tree, one can select the most useful feature for classification using estimation criteria such as the concepts of entropy reduction and information gain. In a decision tree, the feature in the root is the best one for classification. The other features in the decision tree nodes appear in descending order of importance, which contribute to the classification, appear in the decision tree. The features that have less capability of discrimination are discarded during the tree construction. Thus, the decision tree algorithms could identify good features for the purpose of classification from the given training dataset.

Seven decision tree methods (SimpleCart, BFTree, FT, J48, LADTree, LMT and REPTree) were used for gene selection to avoid the biases and overcome limitations of each single algorithm [105, 106]. An ensemble strategy was also applied to increase

prediction accuracy using bagging (Bagging) and boosting (AdaBoostM1) [106]. These two well known methods are used to construct ensemble by re-sampling techniques. Bagging builds bags of the same size of the original data set by applying random sampling with replacement. While boosting resample original data set with replacement, but weights has been assigned to each training sample. The weights are updated iteratively to train subsequent classifier to pay more attention to misclassified samples. The last classifier combines the votes of each individual classifier.

All of these algorithms are implemented in the WEKA machine learning workbench v.3.6.0 ([108]; www.cs.waikato.ac.nz/ml/weka/). Table 3.1 summarizes the seven tree-based classification algorithms that were examined and the last two strategies were the ensemble ones. Each algorithm generated a set of classification rules and a selection of classifier genes. For each algorithm, a 10-fold cross validation method was used to calculate the accuracy of the classifiers.

The performance of the classification algorithms was evaluated based on three criteria: accuracy, Receiver Operating Characteristic (ROC) area, and size of the tree. Accuracy of a classifier M is the percentage of dataset that are correctly classified by the model M. ROC Area is the area under the ROC curve, which can be interpreted as the probability that the classifier ranks a randomly chosen positive instance above a randomly chosen negative one. Roughly speaking, the larger the area is, the better the model would be. The ROC can also be represented equivalently by plotting the fraction of true positives (TPR = true positive rate) versus the fraction of false positives (FPR = false positive rate). The ROC curve is a comparison of two operating characteristics (TPR & FPR) as the criterion changes [108].

Table 3.1

Tree-Based Classifier Algorithms in WEKA [17]

Classifier Name	Function
SimpleCart	Class implementing minimal cost-complexity pruning
BFTree	Class for building a best-first decision tree classifier
FT	Classifier for building "Functional trees" with logistic regression functions at inner nodes/leaves
J48	Class for generating a pruned or un-pruned C4.5 decision tree
LADTree	Class for generating a multi-class alternating decision tree using the LogitBoost strategy
LMT	Classifier for building 'logistic model trees' with logistic regression functions at the leaves
REPTree	Fast decision tree learner
Bagging (ensemble)	Class for bagging a classifier to reduce variance
AdaBoostM1 (ensemble)	Class for boosting a nominal class classifier using the Adaboost M1 method

ROC analysis provides tools to select optimal models and is related in a direct and natural way to cost/benefit analysis of diagnostic decision making. The size of the tree represents the number of selected genes in an assembled tree. Classification rules generated by algorithms with ensemble strategy included multiple trees and the total number of non-redundant classifier genes was counted as the tree size.

Ranking Classifier Genes by Weight of Significance

A weight of significance was assigned on a scale between 0 and 1 to every selected classifier gene based on its position/significance in an assembled decision tree according to Equation 3.1:

$$w_t(g) = \max_{p \in P}\{l_p\}\frac{1}{p\_max} \quad (3.1)$$

where $w_t(g)$ is the weight of gene g assigned by a tree model t, p_max is the longest path of the tree, and l_p is the height of the gene in path p. A "root" gene was awarded the largest weight whereas a "leaf" gene the smallest. The weight value was normalized to the longest leaf-to-root path, except for those genes selected by the LMT algorithm, whose weight had already been assigned by a logistic model. The overall weight for a classifier gene, i.e., the sum of its weight assigned in all the decision tree methods, was calculated in Equation 3.2:

$$W(g) = \sum_{t=1}^{N} A_t w_t(g) \quad (3.2)$$

where $W(g)$ is the overall weight of gene g, A_t is the accuracy of tree model t, and N is the total number of tree models. All of the classifier genes were ranked by their overall weight, i.e., the larger the weight it had, the higher it ranked. Let's look at an example. Suppose the following three classification trees are produced by one or more tree-based classification (see Figure 3.2).

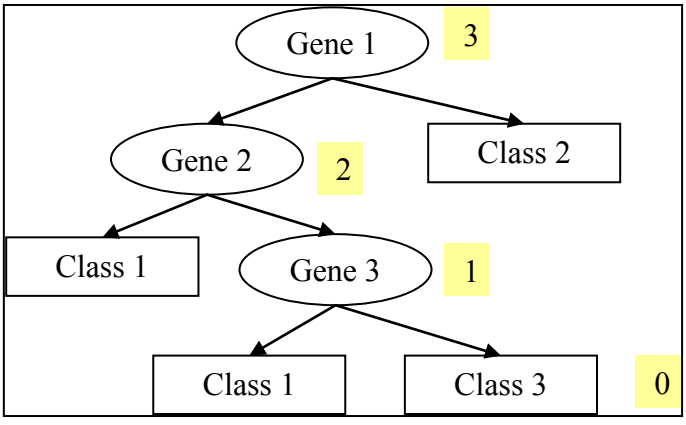

(a)

Figure 3.2. Classifier tree models with corresponding accuracy. The accuracy of each tree is (a) 90% (b) 85% and (c) 95%, respectively.

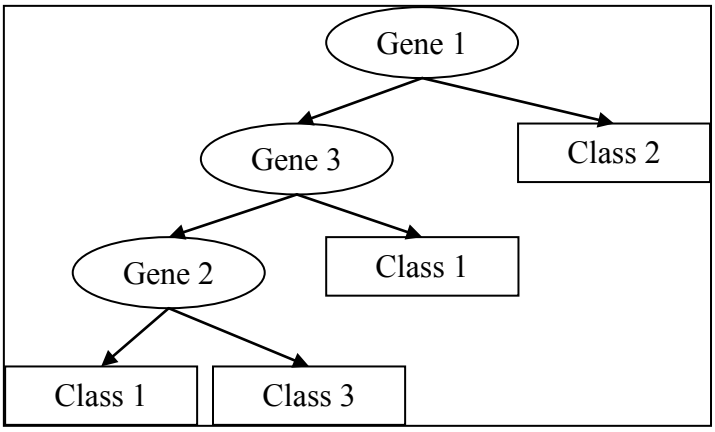

(b)

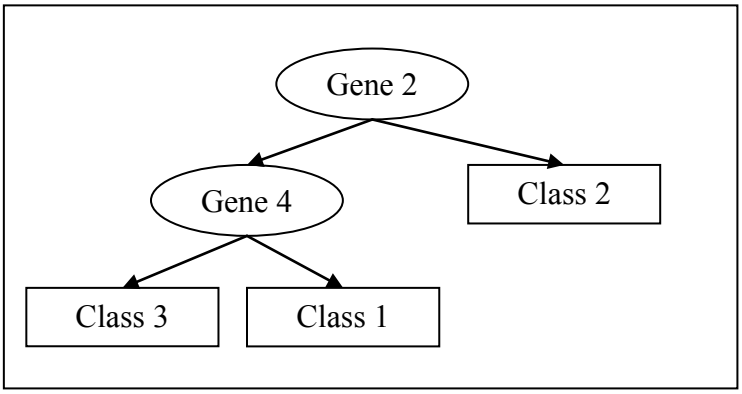

(c)

Figure 3.2. (continued).

Thus $w_1(gene2) = 2 \times \frac{1}{3} = 0.67$, $w_2(gene2) = 1 \times \frac{1}{3} = 0.33$, $w_3(gene2) = 2 \times \frac{1}{2} = 1$.

Summing up gives:

$$W(gene2) = 0.67 \times 0.90 + 0.33 \times 0.85 + 1 \times 0.95 = 1.8335.$$

Optimization by Machine Learning Approaches

Optimization of Classifier Genes by MC-SVM

Sequential minimum optimization (SMO), a fast algorithm for training SVM [109, 110], was used to build MC-SVM kernel function models, as implemented in WEKA. We designed the following steps to refine the classifier gene set:

(1) start with the highest ranking classifier gene to train the SVM using the training dataset and classify the testing dataset using the trained SVM;

(2) add one gene of immediately lower ranking in overall weight at a time to constitute a new gene set, and use the gene set to train and predict the samples; repeat this step until all the classifier genes have been included;

(3) calculate the classification accuracy of each class (control, TNT and RDX) and the weighted average accuracy of all three classes for each set of genes using results from the testing dataset;

(4) estimate the improvement or decline in classification accuracy as a result of adding one gene for each of the three classes plus the weighted average accuracy of all three classes;

(5) remove any gene(s) starting from the one ranking at the bottom that causes a decline in ALL four classification accuracies; and

(6) Iterate steps 1~5 until no more gene(s) can be removed. The remaining set of genes is considered the refined classifier gene set because of its small gene size and high accuracy.

Optimization of Classifier Genes by Clustering

Because both tree-based algorithms and SVM are supervised machine learning methods, an unsupervised clustering method was used to independently optimize the classifier genes. Clustering was performed using the K-mean clustering analysis as implemented in the WEKA toolbox. All the dendrogram trees were cut at a level so that all the 248 earthworm RNA samples were grouped into three clusters. The three pre-labelled clusters (control, RDX and TNT) served as the reference, and the three clusters derived from the dendrogram trees were compared to the reference clusters to determine

matching sample numbers. The optimization of classifier genes by clustering followed the same iterative steps as described above for MC-SVM.

Estimation of Classification Accuracy

Accuracy (also called true positive rate or recall) of a classifier was defined as the percentage of the dataset correctly classified by the method, i.e., number of correctly classified samples/total number of samples in the class. Due to the use of the whole dataset in feature selection, ten-fold stratified cross-validation with inner and outer loops was performed as described in [111] throughout this study to avoid sample selection bias and obtain unbiased estimates of prediction accuracies [112].

Identification of Significant Pathways

By using the ISML pipeline, we are able to reduce the dimensionality of microarray datasets, identify and rank classifier genes, and generate a small set of classifier genes. However, from the system biology point of view, networks/pathways of genetic regulation were able to discover the mechanisms of the modern biomedical research. Thus, having the list of classifier genes which are significant affected by treated chemical compounds, we are able to identify those relevant highly affected pathways. Combined with the reference network tool, which was introduced in the next chapter, all the pathways that includes the classifier genes were selected and ranked based on the number of classifier genes involved. The resulting ordered list of highly affected pathways are considered as the candidates for detailed analysis.

CHAPTER IV

REFNET: A TOOLBOX TO RETRIEVE REFERENCE NETWORK

Once a list of significant classifier genes has been obtained, the next consideration is the identification of the biological processes represented in the list. The information associated with a particular gene, such as the annotation and the relevant biological interactions, is available from many online resources [114, 115, 116, 117]. Many public databases contain genetic interactions retrieved from literature with wet-lab experimental validations. Unfortunately, only a few well-studied model organisms are curated and their GRN/Pathways are available in most of these public databases. A number of computational models also have been developed to infer gene regulatory network such as Boolean Network (BN [23, 26, 85]), Probabilistic Boolean Network (PBN [86, 87, 88]), Dynamic Bayesian Network (DBN [27, 28, 29, 30, 94, 95, 96]), etc. Such models are only assessed based on the evaluation criteria such as recall and precision tested on model organisms. However, researchers who work with non-model organisms also need to obtain genetic interaction information and use it to systematically analyze their own organisms. And they rely on these computational models to infer GRN and investigate the genetic interaction among thousands of genes for less-studied organisms. Due to the lack of "true" genetic interaction network as reference to assess the reconstructed GRNs, accuracy and reliability are the critical limitations of using the computational models which are only evaluated on model organisms for inference of GRNs for non-model organisms. Although some public network databases provide experimentally validated interactions among genes or proteins, limitations in accessibility and scalability make it difficult to extract relevant information for researchers.

Several bioinformatics toolkits have been developed to extract biological interactions from public databases for known interactions of well-studied organism. For example, BioNetBiulder [119, 120] and NetMatch [122] are Cytoscape [118] plug-ins for retrieving, integrating, visualization and analysis of known biology networks. However, their usage is very limited for species whose networks are unknown. Other tools such as BlastPath [124] and OmicViZ [121], also are Cytoscape [118] plug-ins, provide network mapping across species based on homology. But they only map query species to its related model organism; and have limited number of query genes / proteins. For less-studied organisms, their related species may not be well-annotated. Moreover, information from a single model organism is usually not enough to map network for query species. In addition, biological interactions among genes/proteins in an entire pathway may be more comprehensive than those among several random genes/proteins. To the best of our knowledge, currently no tools are available that provide an integrated environment for less-studied non-model organisms GRN. Thus, we propose to develop a cyber-based reference GRN analysis platform in order to (1) build reference GRNs/Pathways for non-model organisms; (2) provide biological prior knowledge of GRN which is useful for improving those computational models; (3) interpret and compare the GRNs built from computational models with wet-lab experiments; and (4) serve as a gene selection tool for GRN reconstruction. Figure 4.1 shows the overall workflow for the cyber-based RefNet analysis platform.

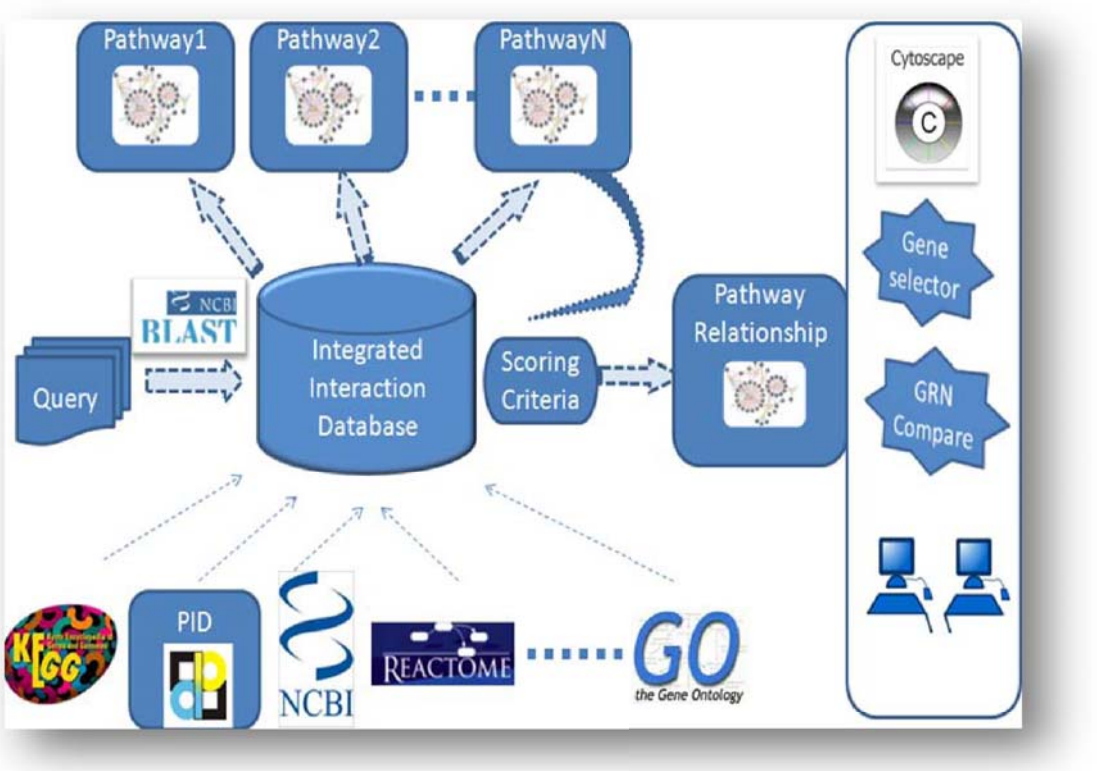

Figure 4.1. Overview of the RefNet analysis platform.

Basic Local Alignment Search Tool (BLAST)

Basic Local Alignment Search Tool

Functional annotation is based on the principle of sequence similarity with well-annotated sequences in public databases. This is accomplished by the sequence comparison methods such as the BLAST [128, 129], Smith-Waterman algorithm [125] and FASTA [126, 127]. Homology among proteins and DNA is often concluded on the basis of sequence similarity. In general, if two or more genes have highly similar DNA sequences, it is likely that they are homologous. But sequence similarity may also occur when the sequences are short, or sequences may be similar due to the binding to a particular protein, such as a transcription factor.

Basic Local Alignment Search Tool (BLAST) [128, 129] is one of the most popular and widely-used algorithm for comparing primary biological sequence information, such as the amino-acid sequences of different proteins or the nucleotides of DNA sequences. A BLAST search enables the comparison of a query sequence with a library or database of sequences. The library sequences that resemble the query sequence above a certain threshold will be identified. BLAST is implemented based on the Smith-Waterman Algorithm, but it emphasizes speed over sensitivity, which makes it more practical on the huge genome databases currently available. However, BLAST cannot guarantee the optimal alignments of a certain query sequence with database sequences.

Alignment Theory: Smith-Waterman Algorithm

Before BLAST, alignment programs used dynamic programming algorithms, such as the Needleman-Wunsch [130] and Smith-Waterman [125] algorithms, that required long processing times and the use of a supercomputer or parallel computer processors. Both algorithms are dynamic programming algorithms, but the main difference is that S-W algorithm sets the negative scoring matrix cells to zero, which renders the local alignments visible. Backtracking starts at the highest scoring matrix cell and proceeds until a cell with score zero is encountered, yielding the highest scoring local alignment.

Given a query sequence a_{m} and database B, where $b_n \in B$. Sequence a, b contains m and n nucleotides respectively. A matrix H is built as in Equation 4.1 and 4.2:

$$H(i,0) = 0, 0 \leq i \leq m \quad (4.1)$$

$$H(0,j) = 0, 0 \leq j \leq n \quad (4.2)$$

if $a_i = b_j$ $w(a_i,b_j) = w$(match) or if $a_i ! = b_j$ $w(a_i,b_j) = w$(mismatch)

$$H(i,j) = max\begin{Bmatrix} 0 & Otherwise \\ H(i-1,j-1+w(a_i,b_j) & \frac{Match}{Mismatch} \\ H(i-1,j)+w(a_i,-) & Deletion \\ H(i,j-1)+w(-,b_j) & Insertion \end{Bmatrix}, 1 \le i \le m, 1 \le j \le n \quad (4.3)$$

where:

- a,b = Strings over the Σ
- m = length(a)
- n = length(b)
- $H(i,j)$ - is the maximum Similarity-Score between a suffix of a[1...i] and a suffix of b[1...j]
- $w(c,d),\ c,d \in \sum \cup \{' - '\}$, *where '-' is the gap-scoring scheme*

For example, suppose we have sequence a = ACACACTA and sequence b = AGCACACA. We assign w (match) = +2, w (a, -) = w (-, b) = w (mismatch) = -1. The resulting matrix H will be obtained and by tracing back, sequence a and b was aligned as follows:

Sequence a = A-CACACTA
Sequence b = AGCACAC-A

Configurations of BLAST Program

BLAST increases the speed of alignment by decreasing the search space or number of comparisons it makes. A word list from the query sequence with words of a specific length is created and a short "word" (w) segments is used to create alignment "seeds." Once an alignment is seeded, BLAST extends the alignment according to a threshold (T) which is set by the user. When performing a BLAST query, the computer extends words with a neighborhood score greater than T. A cutoff score (S) is used to select alignments

over the cutoff, which means the sequences share significant homologies. If a hit is detected, then the algorithm checks whether *w* is contained within a longer aligned segment pair that has a cutoff score greater than or equal to *S*. When an alignment score starts to decrease past a lower threshold score (*X*), the alignment is terminated.

There are several different BLAST programs available for users to select the best one that suits their problem. These different programs vary in query sequence input, the database being searched, and what is being compared. Table 4.1 lists the program name and a short description.

Table 4.1

Different BLAST Programs

BLAST Program	Description
blastn	Search a nucleotide database using a nucleotide query
blastp	Search protein database using a protein query
blastx	Search protein database using a translated nucleotide query
tblastn	Search translated nucleotide database using a protein query
tblastx	Search translated nucleotide database using a translated nucleotide query

In RefNet, the program *blastx* is used after formatting the database of sequences to map gene fragments of our own organism (i.e., earthworm *Eisenia fetida*) to eight selected model organisms in the KEGG (Kyoto Encyclopedia of Genes and Genomes) database listed as following: *Anopheles gambiae* (mosquito), *Apis mellifera* (honey bee), *Caenorhabditis elegans* (nematode), *Drosophila melanogaster* (fruit fly), *Homo sapiens* (human), *Mus musculus* (mouse), *Rattus norvegicus* (rat) and *Schistosoma mansoni*

(flatworm). The default settings for the program are used and we limit the maximum target sequences to be 1 as the best hit for a query sequence is demanded. The cutoff for expected value is set to be 10 by default and the matching sequence which has a higher e-value (>10) are considered as statistically not similar. The e-value, together with the percentage of identity (*pident*) as well as the length of the identity (*nident*) is recorded.

KEGG Metabolic Pathways and GRN Database

Although many public databases contain information of genetic interactions associated with a particular pathway, pathway annotation is generally sparse for organisms other than human, mouse and rat. Many of the organisms that have had their genomes sequenced have very limited pathway annotation, usually in a dedicated database that is difficult to retrieve.

The primary causes of diseases can be associated with altered protein activities, altered biochemical composition of cells and tissues, or changes at the genetic level. Thus, identification of relationships between genes, transcripts, proteins, and metabolites is essential for understanding the underlying mechanisms for disease-associated pathways [123]. Pathway annotation has been attempted by a number of public databases, and the most notable ones are KEGG [123] and PANTHER [131]. Table 4.2 lists some of the commonly used public databases.

KEGG is a collection of online databases dealing with genomes, enzymatic pathways, and biological chemicals. The PATHWAY database records networks of molecular interactions in the cells, and variants of them specific to particular organisms. KEGG connects known information on molecular interaction networks, such as pathways and complexes, information about genes and proteins generated by genome projects and information about biochemical compounds and reactions. The gene expression data can

be superimposed onto relevant pathways, which is greatly helpful in identifying biological regulation through the co-expression of gene data obtained from microarrays.

Table 4.2

Commonly Used Public Databases of Genetic Interactions

Database Name	Database Type	Comments
DIP	Database of Interacting Proteins	Documents experimentally determined protein-protein interactions
BIND	Biomolecular Interaction Network Database	Archives biomolecular interaction, complex and pathway information
HPRD	Human Protein Reference Database	A database of curated proteomic information pertaining to human proteins
MINT	Molecular INTeraction database	Store data on functional interactions between proteins
KEGG	Kyoto Encyclopedia of Genes and Genomes	An integrated database resource consisting of systems information, genomic information, and chemical information
Reactome	Curated Knowledgebase of Biological Pathways	REACTOME is a curated pathway database encompassing human biology.
ENZYME	ENZYME database	A repository of information related to the nomenclature of enzymes.
BioGRID	Biological General Repository for Interaction Datasets	an online interaction repository of protein and genetic interactions

Table 4.3 summarizes the integrated resources included in the KEGG database.

In RefNet, all the systematic reference pathways/networks in the KEGG database are extracted and loaded into our own pathway annotation database. There are two major categories of reference pathways, namely metabolite pathway and non-metabolite pathway. We are only interested in most of the non-metabolite reference pathways since they capture the interaction networks for genetic information processing, environmental information processing and other cellular processes. Pathways in KEGG DISEASE

database also contains perturbed reaction/interaction networks for human diseases. The pathway knowledge from KEGG database is manually collected and summarized from literature and presented in computable forms. The molecular network shown in each pathway map is a graph consisting of nodes (e.g., genes, proteins, small molecules, etc.) and edges (reaction, interactions and relations). In general, if two genes in the pathway map are connected with an edge, they are considered to have regulatory relationship.

Table 4.3

KEGG Databases [123]

Category	Database	Content
Systems Information	KEGG PATHWAY	Pathway maps
	KEGG BRITE	Functional hierarchies
	KEGG MODULE	Pathway modules
	KEGG DISEASE	Human diseases
	KEGG DRUG	Drugs
	KEGG ORTHOLOGY	KEGG orthology (KO) groups
Genomic Information	KEGG GENOME	KEGG organisms
	KEGG GENES	Genes in high-quality genomes
	KEGG SSDB	Sequence similarities and best hit
	KEGG DGENES	Genes in draft genomes
	KEGG EGENES	Genes as EST contigs
Chemical Information	KEGG COMPOUNDS	Metabolites and other small molecules
	KEGG GLYCAN	Glycans
	KEGG REACTION	Biochemical reactions
	KEGG RPAIR	Reactant pair chemical transformation
	KEGG ENZYME	Enzyme nomenclature

Each gene extracted from the KEGG Gene database can be uniquely mapped to a KEGG Orthology (KO) identification. The KO entry represents an ortholog group that is linked to a gene product in the KEGG pathway diagram. Thus, the BLAST scores

between a query sequence and the reference sequence set from the KEGG GENES database are computed, and homologs are found in the reference set.

RefNet: Reference Network for Non-Model Organisms

After BLAST between query gene and the reference gene set from KEGG GENES database, homologs are found for each query sequence. Then, homologs ranked above the threshold are selected as ortholog candidates based on the BLAST score. Ortholog candidates are divided into KO groups according to the annotation of the KEGG GENES database and each query sequence was mapped with the corresponding KO group. Figure 4.2 shows the flow chart of RefNet pipeline.

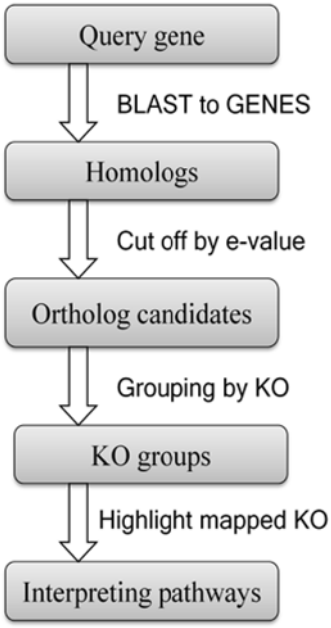

Figure 4.2. Overall procedure of RefNet.

Interpretation of Retrieved Reference Network

The KEGG represents the metabolic and regulatory processes in the form of wiring diagrams, which can be used for browsing and information retrieval as well as a base for modeling and simulation. And it helps in understanding biological processes and higher-order functions of biological systems. Currently the KEGG website uses semi-static

visualizations for the presentation and navigation of its pathway information. However, it does not provide the possibilities of dynamic visualizations or customized visualization of user-specific pathways. The KEGG system provides a XML representation of its pathway information called KGML (KEGG Markup Language). Several applications that support KGML are available for the visualization, analysis and modeling of the biological networks such as KGML-ED [132], VisANT [133, 134], kegg2sbml, Biopathways Workbench etc. Not only interactive visualization and exploration of pathways is desirable to study biological processes, but scientists would also like to change the pathway structure as to customize interpretation of the pathway. The KGML visualization and editing tool (KGML-ED) application is a visual exploration method in a Java based graphical editor. It is based on Gravisto [135], a graph editor and visualization system, and supports KGML file import and export, visualization and editing of pathway structures and attributes consistent to the KGML pathway model.

Based on the results of mapping between query sequence and KO reference genes from the KEGG GENE database, all the reference pathways that are extracted from the KEGG database were interpreted as highlighting those KO reference genes if they could be mapped to a query sequence from our own organism. That is, for each pathway map, the node (representation of ortholog gene) is marked “red” if it is the best hit of a query sequence from our organism and the gene names are replaced by its corresponding KO group identification. The rest of the structure on the map remains the same as the original map from KEGG database. By using the KGML-ED tool, the customized interpretation of pathway maps, which include mapping information of query gene and KO reference gene, are generated and can be used as graphical representation of reference network for reconstruction of GRNs/Pathways for our own non-model organism.

CHAPTER V

GENE REGULATORY NETWORK RECONSTRUCTION

Inference of gene regulatory network is yet another major application of analysis of gene expression data. Such study is also known as reverse engineering problem, specifically, reverse engineering of gene regulatory networks. Previous studies [78, 79] indicate that microarray expression data can be used to make predictions about the genetic transcriptional regulation relationships. In a gene regulatory network, the nodes of this network could be protein products, their coded genes/mRNAs, and complexes of groups of proteins. While the edges between nodes represent protein-to-protein interactions, protein-to mRNA interactions, or molecular reactions. The structure of gene regulatory network is an abstraction of the system's chemical dynamics, describing the mechanisms how one substance affects all the others to which it is connected. Such gene regulatory networks are inferred from the biological knowledgebase for a certain system and represent a distillation of the collective knowledge regarding a set of related biochemical reactions.

Mathematical models of GRN have been developed to capture the behavior of the modeled system, and generate predictions corresponding with experimental observations in some cases. In some other cases, models could make accurate novel predictions, which can be tested experimentally. Several approaches are used for reconstruction or inference of gene regulatory networks from gene expression data such as clustering, classification, and visualization, etc. These methods generally group genes based on the similarity of expression patterns. In addition, many computational approaches have been proposed to reconstruct gene regulatory networks based on large-scale microarray data retrieved from biological experiments such as information theory [80, 81, 82, 83, 84], Boolean networks

[23, 26, 85, 86, 87, 88], differential equations [89, 90, 91, 92, 93], Bayesian networks [27, 28, 29, 30, 94, 95, 96] and neural networks [97]. Many computational methods have been developed for modeling or simulating GRNs. In this chapter, we reviewed several widely-used gene regulatory network reconstruction methods, which provide a guideline to choosing the most appropriate methods to infer the GRNS in a case study described in Chapter VI.

Information Theory

Information theoretic approaches use a generalization of pairwise correlation coefficient in Equation 5.1, called Mutual Information (MI), to compare expression profiles from a set of microarrays. For each pair of genes, their MI_{ij} is computed and the edge $a_{ij}=a_{ji}$ is set to *0* or *1* depending on a significance threshold to which MI_{ij} is compared. MI can be used to measure the degree of independence between two genes.

$$r_{ij} = \frac{\sum_{k=1}^{M}(x_i(k)\, x_j(k))}{\sqrt{(\sum_{k=1}^{M} x_i{}^2(k) \sum_{\mathrm{k=1}}^{\mathrm{M}} \mathrm{x_j}{}^2(\mathrm{k}))}} \quad (5.1)$$

Mutual information, MI_{ij}, between gene *i* and gene *j* is computed as in Equation 5.2:

$$\mathrm{MI_{ij}} = H_i + H_j - H_{ij} \quad (5.2)$$

where *H*, the entropy, is defined as in Equation 5.3:

$$\mathrm{H_i} = \sum_{k=1}^{n} p(\mathrm{x_k}) \log\big(p(\mathrm{x_k})\big) \qquad (5.3)$$

The entropy H_i has many interesting properties; specifically, it reaches a maximum for uniformly distributed variables, that is, the higher the entropy, the more randomly distributed are gene expression levels across the experiments. From the definition, it follows that MI becomes zero if the two variables x_i and x_j are statistically independent

($P(x_i x_j)=P(x_i)P(x_j)$), as their joint entropy $H_{ij}=H_i+H_j$ [80, 81, 82]. A higher MI indicates that the two genes are non-randomly associated to each other. It can be easily shown that MI is symmetric, $M_{ij}=M_{ji}$, therefore the network is described by an undirected graph G, thus differing from Bayesian networks which is a directed acyclic graph. The relationship between entropy and mutual information is described in Figure 5.1.

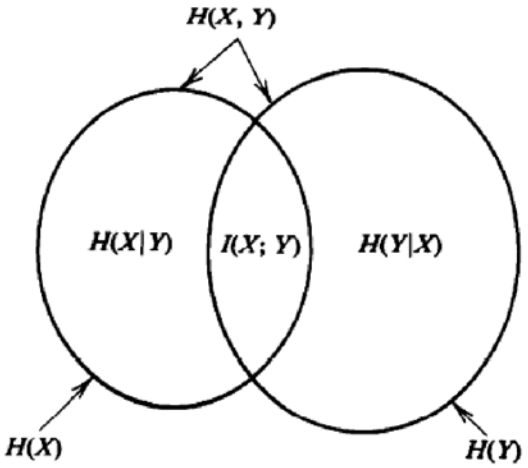

Figure 5.1. Relationship between entropy and mutual information [80].

MI is more general than the Pearson correlation coefficient. This quantifies only linear dependencies between variables, and a vanishing Pearson correlation does not imply that two variables are statistically independent. In practical application, however, MI and Pearson correlation may yield almost identical results [82].

The definition of MI in Equation 5.2 requires each data point to be statistically independent from the others. Therefore information-theoretic approaches can deal with steady-state gene expression data set or with time-series data as long as the sampling time is long enough to assume that each time point is independent of the previous points. Edges in networks derived by information theory approaches represent statistical dependences among gene expression profiles. As in the case of Bayesian network, the edge does not represent a direct causal interaction between two genes, but only a

statistical dependency. It is possible to derive the information theory approaches a method to approximate the joint probability distribution of gene expression profiles, as it is performed for Bayesian networks.

The network inference algorithms RELNET (RELevance NETworks, [81]), ARACNE (Algorithm for the Reverse engineering of Accurate Cellular Networks, [82, 83]) and CLR (Context Likelihood of Relatedness, [84]) apply network schemes in which edges are assigned by statistically weighted scores derived from the mutual information. In [85], an asymmetric mutual information measurement was proposed to obtain directed networks. Similarly, the use of partial correlations to detect conditionally dependent genes in GGMs (Graphical Gaussian Models) also allows us to distinguish direct from indirect associations [136].

Boolean Network and Probabilistic Boolean Network (PBN)

The Boolean Network [137, 138, 139] is useful in inference of gene regulatory networks due to its ability in monitoring the dynamic behavior in complicated systems which are based on large quantities of gene expression data [85, 86, 140]. To learn and reverse engineer the genetic interactions with no prior knowledge is the main objective of Boolean Network [86, 140]. The Boolean function is used to predict the relationship of co-express by other correlated genes in a Boolean Network. A Probabilistic Boolean Network (PBN) [22] is the stochastic extension of Boolean Network. PBN is formed by a group of Boolean Network and each network in PBN corresponds to a contextual condition determined by variables outside the model. PBN is widely used in many applications in the area of GRN inference. For instance, [23] proposed a model to generate an explicit formula for the transition probabilities for random gene perturbations. Some learning methods [24, 25, 26] are also investigated for Probabilistic

Boolean Network. PBN and DBN are studied in terms of fundamental relationships [96] considering the same joint probability distribution over common variables.

In a Boolean Network, by using the logical rules target gene's expression level is functionally related to other genes' expression states. In addition, the target gene is updated by other genes through a Boolean function. In a Boolean network, the gene expression values need to be discretized into two states: namely on and off, which corresponds to "activated" and "inhibited" respectively. A probabilistic Boolean network consists of a family of Boolean networks and incorporates rule-based dependencies between variables. In a PBN model, BNs are allowed to switch from one to another with certain probabilities during state transitions.

Boolean Network

A Boolean network $G(V,F)$ [87, 181] is defined by a set of variables representing genes $V=\{x_1,x_2,\ldots,x_n\}$ (where $x_i \in \{0,1\}$ is a binary variable) and a set of Boolean functions $F=\{f_1,f_2,\ldots,f_n\}$ which represents the transitional relationships between different time points. A Boolean function $f(x_{j_1(i)}, x_{j_2(i)}, \ldots, x_{j_{k(i)}(i)})$ with $k(i)$ specified input nodes is assigned to node x_i. The gene status (state) at time point $t+1$ is determined by the values of some other genes at previous time point t using one Boolean function f_i taken from a set of Boolean functions F . So we can define the transitions as in Equation 5.4:

$$x_i(t+1) = f\left(x_{j_1(i)}(t), x_{j_2(i)}(t), \ldots, x_{j_{k(i)}(i)}(t)\right) \quad (5.4)$$

where each x_i is the expression value of gene i, if $x_i = 1$, it is activated; if $x_i = 0$, gene i is inhibited. The variable $j_{k(i)}$ is the mapping between gene networks at different time points. Boolean function F is the rules of regulatory interactions between different genes.

Figure 5.2 shows an example of a Boolean network. The connected graph is represented by (a), and the transition function is defined by (b).

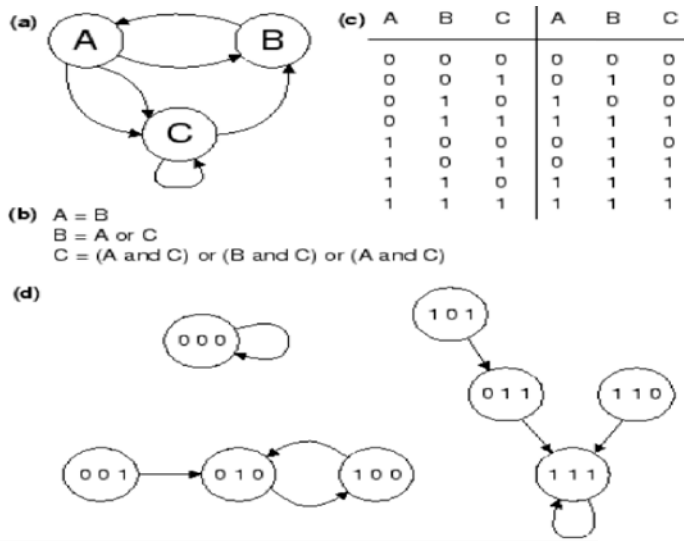

Figure 5.2. An example of a Boolean network. (a) the wiring diagram; (b) the updating rules; (c) a state transition table; and (d) the state space of the network.

Probabilistic Boolean Network

By combining one or more possible transition Boolean functions, the extension of BN becomes PBN. Each network in PBN can be randomly selected to update the target gene based on the selection probability. It is proportional to the coefficient of determination (COD) of each Boolean function. The same set of nodes $V=\{x_1,x_2,...,x_n\}$ as in Boolean network is used in a PBN $G(V,F)$ [22], but the list of function sets $F=\{f_1,f_2,\ldots,f_n\}$ is replaced by $F=\{F_1,F_2,\ldots,F_n\}$, where each function set $F_i=\{f_j^{(i)}\}_{j=1,2,\ldots,l(i)}$ composed of $l(i)$ possible Boolean functions corresponds to each node x_i. A realization of the PBN at a given time point is determined by a vector of Boolean functions. Each realization of the PBN corresponds to one of the vector functions$f_k = f_{k(1),}^{(1)} f_{k(2),}^{(2)} \ldots f_{k(n)}^{(n)}$), $1 \le k \le N$, $1 \le k(i) \le l(i)$, where $f_{k(i)}^{(i)} \in F_i$ and N is the number of possible realizations. Given the values

of all genes in network at time point t and a realization f_k, the state of the genes after one updating step is expressed as in Equation 5.5:

$$(x_1(t+1), x_2(t+1), \dots x_n(t+1)) = f_k(x_1(t), x_2(t), \dots x_n(t)) \quad (5.5)$$

Given genes $V = \{x_1, x_2, \dots, x_n\}$, each x_i is assigned to a set of Boolean functions $F_i = \{f_j^{(i)}\}_{j=1,2,\dots,l(i)}$ to update target gene. The PBN will reduce to a standard Boolean network if $l(i)=1$ for all genes. A basic building block of a PBN describing the updating mechanism is shown in Figure 5.3.

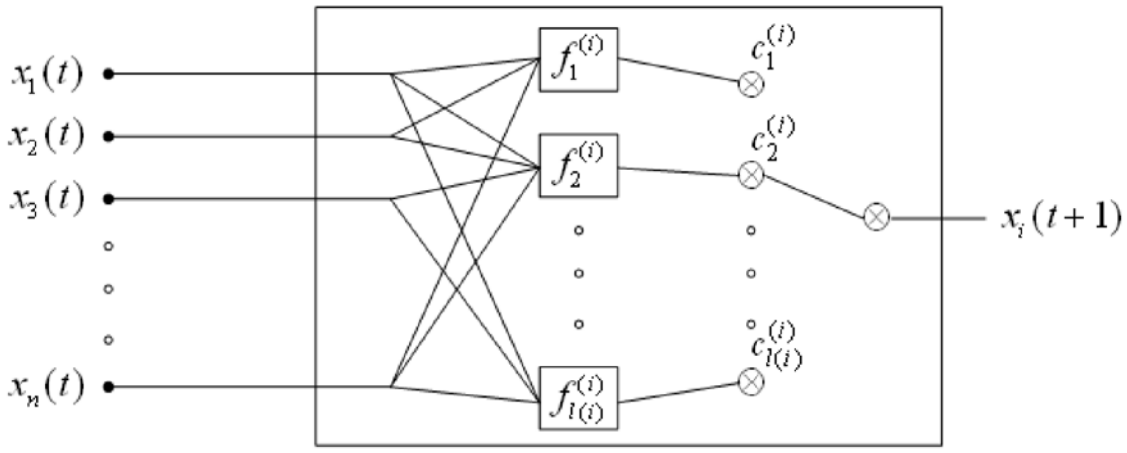

Figure 5.3. A basic building block of a PBN.

Inference of Probabilistic Boolean Network

For each target gene, Coefficient of Determination (COD) is used to select a set of predictors [22, 25] at any time point t. Previously, the COD is used for the steady state data sets and then Monte Carlo approaches combined with PBN are used to approximate dynamics [86] and some theoretical results are given in [182]. Here we use upper case letters to represent random variables: Let X_i be the target gene, $X_1^{(i)}, X_2^{(i)}, \dots, X_{l(i)}^{(i)}$ be sets of genes and $f_1^{(i)}, f_2^{(i)}, \dots, f_{l(i)}^{(i)}$ be available Boolean functions. Thus, the optimal predictors of X_i can be defined by $f_1^{(i)}(X_1^{(i)}), f_2^{(i)}(X_2^{(i)}), \dots, f_{l(i)}^{(i)}(X_{l(i)}^{(i)})$ and the probabilistic error

measure can be represented as $\varepsilon(X_i, f_k^{(i)}(X_k^{(i)}))$. For each k, the COD for X_i relative to the conditioning set $X_k^{(i)}$ is defined by Equation 5.6:

$$\omega_k^i = \frac{\varepsilon_i - \varepsilon(X_i, f_k{}^{(i)}(X_k{}^{(i)}))}{\varepsilon_i} \quad (5.6)$$

where ε_i is the error of the best estimate of X_i [25].

Based on the above equations [22, 25], the Boolean functions which are corresponding to the highest CODs will be chosen in the probabilistic network. The selected Boolean functions will be used to predict the state of gene (gene expression status) on the subsequent time point as well as to infer gene regulatory networks.

Bayesian Network and Dynamic Bayesian Network (DBN)

Due to the probabilistic nature of Bayesian network, it is widely used in reconstruction of gene regulatory network from time series dataset. Dynamic Bayesian network is the temporal extension of Bayesian network. DBN can be used to model complex temporal stochastic processes as it captures several other often used modeling frameworks such as hidden Markov models (and its variants) and Kalman filter models. The drawbacks of Bayesian network approach makes it fail to capture temporal information and unable to model cyclic networks. The Dynamic Bayesian network approaches solved such problems as it is better suited for characterizing time series gene expression dataset. A lot of researches have been conducted to infer GRNs from gene expression data using BN and DBN. For example, the stochastic machine learning algorithm is used to model genetic interactions are capable of handling dataset with missing variables [29]. In addition, *Min Zou et al.* [28] proposed a new DBN-based approach, in which the number of potential regulators is limited in order to reduce search space. *Yu, J. et al.* [27] developed a simulation approach to take advantage of DBN algorithm, especially in the

case of limited biological dataset. In [30], a higher order Markov DBN approach is proposed in order to model multiple time units in a delayed GRN. Also, likelihood maximization algorithms have been used to predict hidden parameters and impute missing gene expression values [31].

Bayesian Network

A Bayesian network is a graphical model for probabilistic relationships among a set of random variables X_i, where $i=1…n$. Such relationships are represented in a structure of directed acyclic graph G, in which the vertices are random variables X_i. The relationship between the variables are indicated as a joint probability distribution $P(X_1, …, X_n)$ which is consistent with the independence assertions embedded in the graph G and has the form as in Equation 5.7:

$$P(X_1, \dots, X_n) = \prod_{i=1}^{N} P(X_i = x_i \big| X_j = x_j, \dots, X_{j+p} = x_{j+p}) \quad (5.7)$$

where the $p+1$ genes, on which the probability is conditioned, are called the parents of gene i and represent its regulators, and the joint probability density is expressed as a product of conditional probabilities by applying the chain rule of probabilities and independence. This rule is based on the Bayes' theorem: $P(A,B)=P(B||A)*P(A)=P(A||B)*P(B)$. The joint probability distribution can be decomposed as the product of conditional probabilities [26, 94]. A simple example of Bayesian network is shown in Figure 5.4.

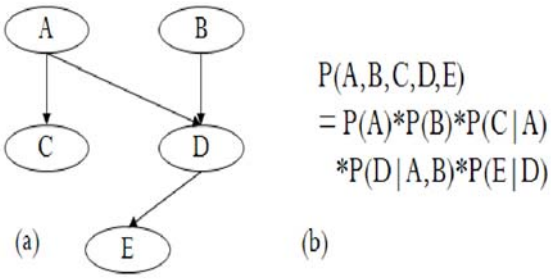

Figure 5.4. A simple example of Bayesian network. (a) Graph representation of a Bayesian network. (b) Probability representation corresponding to network in (a).

The computational cost of DBN approach is expensive since the probability of every possible event as defined by the values of all variables needs to be stored in order to describe the joint distribution over *n* variables (genes). Thus, there are exponentially many such events and gives the search space complexity of $O(2^n)$. In Bayesian network, if the maximum number of parents is denoted as *p*, we have the space complexity of Bayesian network is $\Theta(2^p \cdot n)$. Since *p* is usually much smaller than *n*, the search space of BN is much lower than the method that exhaustively enumerates all the possible events.

Bayesian networks reflect the stochastic nature of gene regulation and are based on the Bayes' rule. We assume that the gene expression values are random variables which follow a probability distribution. Since probability is used to represent their regulatory relationships, Bayesian networks are considered to capture randomness and noise as inherent features of genetic regulation processes [94]. In the process of gene regulatory network inference to derive a valid network structure [183], Bayesian networks combine different types of data and prior knowledge. In addition, the ability to avoid over-fitting a model to training data and to handle incomplete noisy data as well as hidden variables such as transcription factors have made BNs good models to infer gene regulatory networks.

Three essential elements in the process of learning a BN: model selection, parameter learning as well as model scoring [184]. In model selection, instead of using brute-force search algorithm, heuristics methods are usually used to learn a BN efficiently since the brute-force search will grow exponentially as the number of genes increase in a directed acyclic graph. In parameter learning, the goal is to find the best conditional probabilities (CP) for each node in a graph and experimental dataset. In model scoring, each candidate model will be scored and higher score indicates the network model (the DAG and the learned CP distribution) better fits to the data. The inferred GRN will be the model with the highest score.

Dynamic Bayesian Network

The drawbacks of Bayesian network approach makes it fail to capture temporal information and unable to model cyclic networks. The Dynamic Bayesian network (DBN) [185] approaches solved such problems as it is better suited for characterizing time series gene expression dataset. DBN can be used to model complex temporal and cyclic relationships of genes by incorporating time course (or time slice) information. Here we are modeling a dynamic system while the gene regulatory network does not change over time. By incorporating time series information, DBN represents the cyclic relations among genes in Figure 5.5.

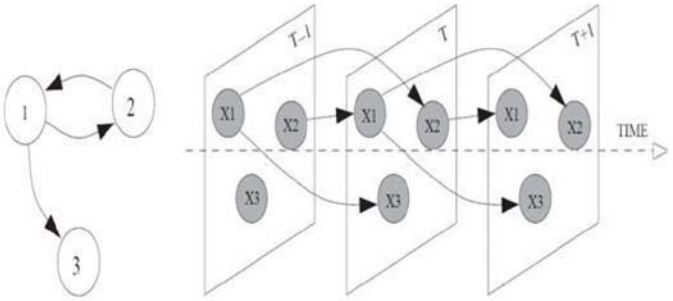

Figure 5.5. Static Bayesian network and DBN.

A DBN is defined by a pair (B_0, B_1) means the joint probability distribution over all possible time series of variables $X=\{X_1,X_2,\ldots,X_n\}$, where $X_i(1\leq i\leq n)$ represents the binary-valued random variables in the network. Besides, we use lower case $x_i(1\leq i\leq n)$ to denote the values of variable X_i. It is composed of an initial state of BN and a transition two-slice temporal Bayesian network (2TBN). An example of DBN is shown in Figure 5.6.

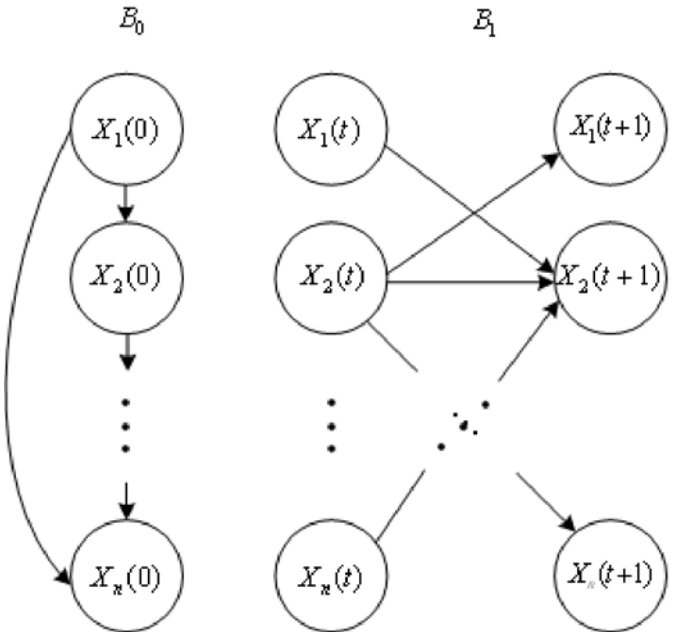

Figure 5.6. A basic building block of DBN.

As we transit from one time slice to the next, the system is updated by Dynamic Bayesian network and its behaviors are predicted for future state. By changing the nature of the static BN, it has been adapted to a dynamic model. There are two categories of temporal approaches based on the way to represent time: time-points representation and time-intervals representation. We could also treat time intervals as a group of consecutive time points and thus it is more appropriate and expressive to use time-points representation.

Leaning Bayesian Network

In general, it is difficult or hardly to manually capture the complete structure and parameters of Bayesian network. Therefore, the task of learning BN from gene expression data becomes very important. Estimating the parameters of the model and inferring the structure of the GRN are two key elements to learn a Bayesian network from a given gene expression data.

Parameter Learning

For a given graph G, maximizing the joint likelihood of gene expression data is generally used to estimate the parameters (also known as generative parameter learning [186]). Recently, the algorithms of maximizing conditional likelihood of the class variables given the observed evidence variables have been proposed in order to learn the parameters since BNs are widely used as classifiers. Such algorithms are called discriminative parameter learning [187, 188, 189].

Generative Parameter Learning

Given a set of training data , which is composed of a set of independent and identically distributed instances $[x^1,\ldots,x^N]$, where all components are observed, generative parameter learning methods estimate the parameters of a BN either by directly maximizing the joint likelihood of training data, or by computing the posterior over parameters θ given a prior distribution $P(\theta)$.

The method of maximum likelihood estimation uses the conditional independence assumptions encoded in the structure. The joint log likelihood of training data can be factored in Equation 5.8:

$$\log P(D|\theta) = \sum_{i=1}^{N} \sum_{j=1}^{n} \log P(x_j^i | x_{\pi(j)}^i, \theta) \quad (5.8)$$

The second generative method is called maximum a posteriori estimation (MAP). Bayesian networks allow us to incorporate prior domain knowledge and use it to effectively avoid the problem of over-fitting, especially when limited number of training datasets is given. Given a prior density *P(θ)*, we can learn the parameters to maximize the posterior as in Equation 5.9:

$$\log P(\theta|D) = \log \frac{P(\theta)P(D|\theta)}{P(D)} \quad (5.9)$$

This is equivalent to maximizing $P(\theta)\, P(D|\theta)$ because $P(D)$ is invariant with respect to θ. A commonly used algorithm to learn BN from incomplete data is the Expectation Maximization (EM) method.

Discriminative Parameter Learning

Due to the shortcoming of inconsistency with its performance when optimizing a criterion such as maximum likelihood or MAP, the generative parameter learning method is not the best way to train classification models. Recently, an improved discriminative approach for supervised parameter learning that takes conditional likelihood as the optimization criterion is proposed in [187, 188, 189, 190].

Although it is easy to learn parameters given complete dataset, to find the global maximum is still difficult when using the discriminative conditional likelihood criterion for general Bayesian networks. To find the parameters for a fixed BN structure that maximize the conditional likelihood of a given sample of incomplete data is a NP-hard problem as in [187].

Structural Learning

If the topology of the target Bayesian network is fixed, the task is to estimate the CPTs or CPDs for every node in the network. Or else, if the topology is unknown, structure

learning is required to learn the graph topology of the target BN before the parameters could be determined. In addition, the dataset could be either complete or incomplete for BN learning. Thus, four cases of learning structure of BNs are summarized based on the above varieties [191]. Table 5.1 shows the four cases for learning Bayesian network structure.

Table 5.1

Methods for Learning Bayesian Network Structure and Parameter Determination

Structure/Observability	Method
Known, full	Sample statistics
Known, partial	EM or gradient ascent
Unknown, full	Search through model space
Unknown, partial	Structural EM

Full observability means that the values of all variables are known; partial observability means that we do not know the values of some of the variables. This might be because they cannot be measured (in which case they are usually called hidden variables), or because they just happen to be unmeasured in the training data (in which case they are called missing variables). Unknown structure means we do not know the complete topology of the gene regulatory network. Usually we know some parts of it, or at least know some properties of the graph, for instance, the maximum number of parents (fan-in) that a node can take in, and we may know that nodes of a certain "type" only connect to other nodes of the same type. Such constraints are called prior knowledge. Therefore, the learning task becomes parameter estimation when we know the structure of the model.

DBN Implementation

Kevin Murphy [185, 191] implemented a Dynamic Bayesian Network toolbox using the mathematical programming language (MATLAB), namely Bayes Net toolbox (BNT). It is an open-source package for directed graphical models and supports many types of nodes (probability distributions), exact and approximate inference, parameter and structure learning, and static as well as dynamic models. BNT can be freely downloaded from [192]. In Murphy's method, the gene expression data was first discretized from continuous form and the number of discrete steps is kept as low as possible. In general, three discrete steps were used: one for unchanged, one for up-regulated and one for down-regulated expression values. Then the BNT function *learn_struct_dbn_reveal* is called to conduct structural learning, which employs the REVEAL algorithm [193]. The BNT function called *draw_layout* is used to visualize the generated inter-slice adjacency matrix that represents the transition network. A number of other implementations of DBN method using time series gene expression data are proposed in [27, 28, 29, 30].

Time-Delayed Dynamic Bayesian Network

There are two major problems with Murphy's DBN method which greatly reduce their effectiveness. The first is the lack of a systematic way to determine the time lag of biological relevance. Such problem results in a relatively low accuracy of inferring gene regulatory networks. The second is the excessive computational cost of huge searching space. Only limited number of genes can be modeled and reconstructing GRN. Thus, *Min Zou et al.* [28] introduces a DBN-based analysis that can predict gene regulatory networks from time course expression data with significantly increased accuracy and reduced computational time. Based on the characteristics of our microarray dataset, Zou's implementation is used to reconstruct gene regulatory network. Figure 5.7 shows the process of approach in [28]: (1) Identification of the initial expression changes; (2)

Potential regulators; (3) Estimation of the transcriptional time lag; (4) DBN: statistical analysis of the expression relationship between the potential regulator and its target gene in time slices; and (5) Predicted gene regulatory network.

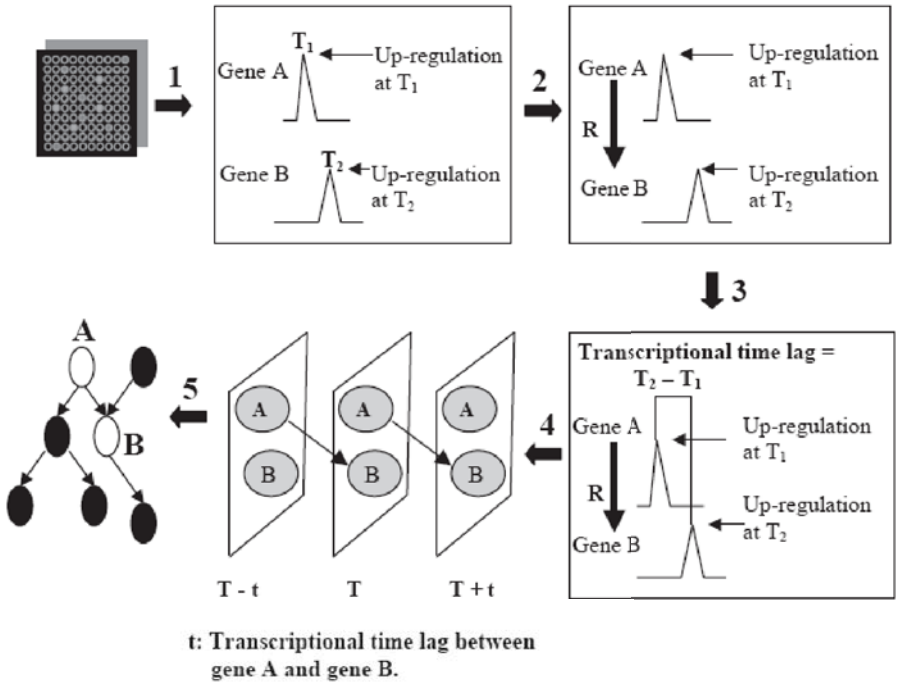

Figure 5.7. Process of time lag DBN.

All the genes in the data are treated as potential regulators of certain target gene in Murphy's method, which brings the challenge of inferring large-scale GRN due to the exponentially increasing of computational time. However, most transcriptional regulators present either an earlier or simultaneous change in the expression level when compared to the target genes [194]. Therefore, we can significantly reduce the computational overhead by limiting the number of potential regulators for each target gene. Also, in Zou's method, an estimation of the transcriptional time lag between potential regulators and their target genes are conducted and is expected to be more accurate because it takes into account variable expression relationships of different regulator–target pairs.

CHAPTER VI

MICROARRAY DATA MINING: CASE STUDY

Military-related activities produce many different chemicals, a portion of which inevitably contaminate soil. Neurotoxicity has been associated with energetic compounds, TNT and RDX as well as their degradation products. Monitoring, assessing and predicting the risks these chemicals pose when released require fundamental knowledge on how neurotoxicity occurs. A major barrier to development of predictive risk tools is the lack of an appropriate and detailed model of the molecular events leading to neurotoxicity when organisms are exposed to contaminated soils. We are interested to identify and discover how components involved in neurotransmission within the soil organism *Eisenia fetida* interact and are affected by neurotoxicants. Understanding this network of interactions is essential for development of predictive risk models in the future.

As a terrestrial toxicological model organism, *E. fetida* has a simple but efficient nervous system that is an excellent model to study the major neurotransmitters and synaptic pathways. Many neurotransmission pathways are conserved between *E. fetida* and vertebrates. Previously, we discovered that at sub-lethal doses, TNT affected genes involved in neurological processes. At appropriate dosages RDX both exhibit reversible neurotoxicity in *E. fetida*. However, it is unclear whether RDX has affected other neurotransmission pathways and how genes involved in these pathways interact in a broader network context to compensate for or to cope with the perturbation caused by exposure to a neurotoxicant. Therefore, a system biology approach is used to discover effects of neurotoxicants on neurotransmitter pathways related gene expression in a gene regulatory network (GRN). First, the data set of gene expression values are preprocessed and analyzed by ISML pipeline to discover classifier genes that significantly affected by

the chemical and identify relevant pathways/GRNs for further study. Then, reference networks of user-selected pathways in the organism of interest were built by RefNet toolbox. Last, a set of genes in a certain pathway were selected and used to reconstruct gene regulatory networks in order to discover the mechanisms of perturbations of the network after being exposed to the chemical. Two case studies will be described in the following section to walk through the procedure.

Multi-Class Earthworm Microarray Dataset

DNA microarray, a maturing genomic technology, has been used extensively as a diagnostic tool to complement traditional approaches such as histopathological examination for various diseases (particularly cancers) because microscopic appearances sometimes can be deceiving [141, 142, 143, 144]. Microarrays have also successfully served as a research tool in discovering novel drug targets [145] and disease- or toxicity-related biomarker genes for cancer classification [146]. In ecological risk assessment, indigenous species such as fish and earthworms are often used as bioindicators for adverse effects caused by environmental contaminants. Previously, we developed an earthworm (*Eisenia fetida*) cDNA microarray to analyze toxicological mechanisms for two military-unique explosive compounds 2,4,6-trinitrotolune (TNT) and 1,3,5-trinitro-1,3,5-triazacyclohexane (also known as Royal Demolition eXplosive or RDX) [147, 148]. These two compounds exhibit distinctive toxicological properties that are accompanied by significantly different gene expression profiles in the earthworm *E. fetida* [147, 148, 149], which has motivated us to look further into toxicant- or toxicity-specific signature genes/biomarkers. The second motivation comes from the fact that many diagnostic assays exist for human diseases while very few are available for evaluating impacts on environmentally-relevant organisms. Gross survival, growth and reproduction rates are

often used as assessment endpoints without reflecting the diseased population of affected animals that is an important part of long-term impact assessment. The last motivation is that computational tools such as machine learning techniques have been widely used in cancer and toxicant classification with microarray data but rarely applied in microarray data analysis of environmentally relevant organisms [150, 151, 152].

From a regulatory standpoint, there is an increasing and continuous demand for more rapid, more accurate and more predictive assays due to the already large, but still growing, number of man-made chemicals released into the environment [153]. Molecular endpoints such as gene expression that may reflect phenotypic disease symptoms manifested later at higher biological levels (e.g., cell, tissue, organ, or organism) are potentially biomarkers that meet such demands. As a high throughput tool, microarrays simultaneously measure thousands of biologically-relevant endpoints (gene expression). However, to apply this tool to animals under field conditions, one critical hurdle to overcome is the separation of toxicity-induced signals from background noise associated with environmental variation and other confounding factors such as animal age, genetic make-up, physiological state and exposure length and route [150,151]. A common approach to biomarker discovery is to screen genome- or transcriptome-wide gene expression responses and identify a small subset of genes capable of discriminating animals that received different treatments, or predicting the class of unknown samples. It is relatively less challenging to identify differentially expressed genes from two or more classes of samples. However, the search for an optimal and small subset of genes that has a high discriminatory power in classifying field samples often having multiple classes is much more complicated.

For instance, *Falciani* and colleagues profiled gene expression of 77 hepatic samples of European flounder (*Platichthys flesus*) collected from six different environmental sites [150]. Using a multivariate variable selection coupled with a statistical modelling procedure they demonstrated that the accuracy of predicting the geographical site of origin based on gene expression signatures in flounder livers was limited to specific sites. After incorporating prior knowledge and data from laboratory exposures to individual toxicants, they were able to limit the search space for a combination of effective classifier genes and built a very accurate model consisting of only 17 genes for classification of all the different environmental sites. Similarly, Nota and co-workers recently identified a set of 188 genes from expression profiles of the springtail (*Folsomia candida*) exposed to a soil spiked with six different metals using the uncorrelated shrunken centroid method, and predicted an independent test soils set with an accuracy of 83% but failed on field soils collected from two cobalt-contaminated sites using this gene set [151]. Several other studies also reported a varying degree of success in the identification of classifier genes in both aquatic species like the zebrafish (*Danio rerio*) [152], the common carp *Cyprinus carpio* [154] and the water flea *Daphnia magna* [155], and terrestrial organisms such as the earthworm *Lumbricus rubellus* [156].

As part of a larger effort towards discovering novel biomarkers for ecological risk assessment of military lands, researchers at the Environmental Laboratory of U.S. Army Engineer Research and Development Center have developed a 15208-oligonucleotide *E. fetida* array, and generated a large-scale microarray dataset from a laboratory study where earthworms (*E. fetida*) were exposed to various concentrations of TNT or RDX for various lengths of time in soil, mimicking field exposure scenarios (see below for details). The objective of the current study was to identify a small set of classifier genes

that could be used to build a predictive model capable of accurately separating all exposed earthworm samples into three categories: control, TNT-treated and RDX-treated. We focused on identifying and optimizing classifier genes from the earthworm dataset using a machine learning approach.

Experimental Design and Dataset Generation

The following experiment id designed and conducted by Dr. Ping Gong at the Environmental Laboratory of U.S. Army Engineer Research and Development Center. Adult earthworms (*E. fetida*) were exposed in a field collected pristine silty loam soil (3% sand, 72% silt, 26% clay, pH 6.7, total organic C 0.7%, and CEC 10.8 mEq/100 g) spiked with TNT (0, 6, 12, 24, 48, or 96 mg/kg) or RDX (8, 16, 32, 64, or 128 mg/kg) for 4 or 14 days. The 4-day treatment was repeated a second time with the same TNT concentrations; however RDX concentrations were 2, 4, 8, 16 or 32 mg/kg soil. Each treatment originally had 10 replicate worms with 8~10 survivors at the end of exposure, except the two highest TNT concentrations. At 96 mg TNT/kg, no worms survived in the original 4-day and 14-day exposures, whereas at 48 mg TNT/kg, all 10 worms died in the original 4-day exposure. Total RNA was isolated from the surviving worms as well as the Day 0 worms (worms sampled immediately before experiments). A total of 248 worm RNA samples (= 8 replicate worms × 31 treatments) were hybridized to a custom-designed oligo array using Agilent's one-color Low RNA Input Linear Amplification Kit. The array contained 15,208 non-redundant 60-mer probes (GEO platform accession number GPL9420), each targeting a unique *E. fetida* transcript [157]. After hybridization and scanning, gene expression data were acquired using Agilent's Feature Extraction Software (v.9.1.3). In the current study, the 248-array dataset was divided into three worm groups regardless of exposure length and concentration: 32 untreated controls, 96

TNT-treated, and 120 RDX-treated. This MIAME compliant dataset has been deposited in NCBI's Gene Expression Omnibus [158] and is accessible through GEO Series accession number GSE18495.

Data Preprocessing

The following data pre-treatment steps were applied prior to further statistical and computational analyses: (1) feature filtering: flag out spots with signal intensity outside the linear range as well as non-uniform spots; (2) conversion: convert signal intensity into relative RNA concentration based on the linear standard curve of spike-in RNAs; (3) normalization: normalize the relative RNA concentration to the median value on each array; and (4) gene filtering: filter out genes appearing in less than 50% of arrays (i.e., present on at least 124 arrays). There were more than 14,000 genes remaining after this procedure.

Feature Filtering by Univariate Statistical Analysis

The Class Comparison Between Groups of Arrays Tool in BRB-ArrayTools v.3.8 software package ([21]; linus.nci.nih.gov/BRB-ArrayTools.html) was used to identify significantly changed genes. The collated earthworm array dataset was imported without any further normalization or transformation. The tool runs a random variance version of the t-test or F-test separately for each gene. It performs random permutations of the class labels and computes the proportion of the random permutations that give as many genes significant at the level set by the user as are found in comparing the true class labels. The following eight class-comparison analyses were conducted to infer genes differentially expressed in response to TNT or RDX: (1) two 2-class comparisons: pooled controls vs. pooled TNT or RDX treatments; and (2) six multiple-class comparisons: 4-day TNT or RDX multiple concentrations, 4-day repeat TNT or RDX multiple concentrations, and

14-day TNT or RDX multiple concentrations. The following settings were employed: a univariate test random variance model, multivariate permutation tests with 10,000 random permutations, a confidence level of false discovery rate assessment = 99%, and a maximum allowed number of false-positive genes = 10.

Differentially expressed genes were inferred by univariate statistical analysis. At the same level of statistical stringency, the significant gene lists derived from four different comparisons for either TNT or RDX shared very few common genes (Figure 6.1), suggesting different genes may be significantly altered under different conditions. In Figure 6.1, both Venn diagrams are produced as follows: TNT/RDX-Control: two-class comparison between pooled controls and pooled TNT/RDX treatments; TNT/RDX-D4orig: multiple-class comparison of 4-day TNT/RDX treatments including the control group; TNT/RDX-D4Rpt: multiple-class comparison of 4-day repeat TNT/RDX treatments including the control group; TNT/RDX-D14: multiple-class comparison of 14-day TNT/RDX treatments including the control group.

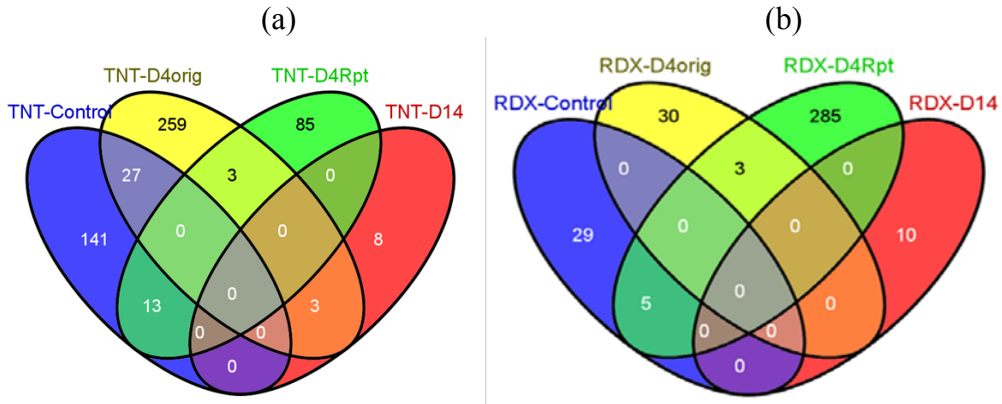

Figure 6.1. Summary of DEGs in multi-class earthworm microarray dataset. The number and overlapping of significant genes statistically inferred from class comparisons for (a) TNT and (b) RDX treatments.

To validate these results, we used ANOVA in GeneSpring GX 10 to analyze the same dataset by applying the Benjamini-Hochberg method for multiple testing corrections and

a cut-off of 1.5-fold change. By allowing a variable threshold of cut-off p-value, the same amount of top significant genes can be derived from the same comparisons as we did using BRB-ArrayTools. The two sets of significant gene lists share 85~95% common genes (data not shown), indicating a high level of statistical reproducibility. The difference in the resulting gene lists may be primarily attributed to the use of a 1.5-fold change as the cut-off level by GeneSpring. A total of 869 unique genes were obtained after combining all significantly changed gene lists from TNT- and RDX-exposures. A screenshot of the table containing the expression information of these 869 transcripts in all 248 earthworm samples is provided in Figure 6.2.

Sample name	D0 C-1	D0 C-10	D0 C-2	D0 C-3	D0 C-4	D0 C-6	D0 C-7	D0 C-9	D14 C-1	D14 C-2	D14 C-3	D14 C-4	D14 C-5	D14 C-6	D14 C-7	D14 C-8
Treatment	Control	Control	Control	Control	Control	Control	Control	Control	Control	Control	Control	Control	Control	Control	Control	Control
Exposure length (day)	0	0	0	0	0	0	0	0	14	14	14	14	14	14	14	
Exposure concentration (mg/kg soil)	0	0	0	0	0	0	0	0	0	0	0	0	0	0	0	
Replicate number (1~10)	1	10	2	3	4	6	7	9	1	2	3	4	5	6	7	
Original/Repeat (4-day only)																
ProbeName	D0 C-1	D0 C-10	D0 C-2	D0 C-3	D0 C-4	D0 C-6	D0 C-7	D0 C-9	D14 C-1	D14 C-2	D14 C-3	D14 C-4	D14 C-5	D14 C-6	D14 C-7	D14 C-8
TA1-000100	1.544784	1.077037	0.688884	1.05738	1.332549	1.57862	1.611328	1.245391	1.747124	2.157616	1.829691	2.920179	1.167503	1.855323	1.340083	1.6671
TA1-000275	0.14782	0.314516	0.14761	0.249146	0.165994	0.150551	0.390794	0.356923	0.159595	0.170184	0.150436	0.204587	0.173562	0.192852	0.307359	0.2282
TA1-000564	0.359075	0.475052	0.388038	0.475644	0.382291	0.276957	0.430003	0.348014	0.333625	0.61265	0.456999	0.515717	0.444997	0.320232	0.387434	0.5392
TA1-000769	38.30267	26.95064	9.274611	17.74399	19.20062	25.12587	16.51482	25.18786	27.72135	10.11865			46.64916	37.3908	27.02624	23.662
TA1-000891	0.716841	0.68717	0.385697	0.828677	1.328373	0.901697	0.475308	0.723583	1.044579	0.435081	1.265013	1.09192	1.1403	2.472947	1.28626	1.0618
TA1-000950	1.162251	1.179841	0.651138	0.974386	1.101545	0.684706	0.717452	0.414236	0.81644	3.421419	2.530951	4.485153	1.094641	1.183803	0.569419	1.8788
TA1-001156	1.774544	2.042302	0.772284	1.571739	1.488568	2.333164	1.107841	0.660244	1.198035	1.513243	1.343693	2.406861	1.967941	1.463943	1.390551	1.4776
TA1-001307	3.797535	2.938382	1.834077	2.916957	2.303589	3.895747	2.336985	3.214723	1.701517	3.076681	4.601008	2.802051	2.680372	5.02588	2.904013	3.540
TA1-001540	1.919337	2.1194	2.919001	1.470989	2.875442	2.423691	2.63847	2.682649	2.054468		4.218672	2.523373	1.311972	2.151566	2.012633	2.3346
TA1-001740	1.411449	1.654132	1.50774	1.172897	1.59301	1.30633	1.45087	1.436459	1.570249	1.925078	2.244129	2.323274	1.561058	2.860336	1.750776	1.685
TA1-001926	0.588648	0.356612	0.222095	0.441178	0.280621	0.43888	0.425447	0.224052	0.476928	0.850978	0.949609	1.076174	0.724102	0.68727	0.481688	0.4324
TA1-002058	1.786619	1.483087	1.271286	1.376737	1.647871	1.631845	1.681641	1.545831	1.788568	2.397994	1.827378	2.522547	1.649183	2.289576	1.702058	1.4553
TA1-002129	0.71438	0.886693	0.94346	0.687495	0.637048	0.642812	0.949783	0.947267	0.788916	0.891019	0.871243	0.690266	0.933609	0.693013	0.8663	0.8042
TA1-002164	2.700121	3.722432	4.030156	3.484329	2.346676	1.93343	2.386889	5.083236	2.468901	2.021314	1.713614	1.845082	3.034879	2.598145	3.288251	1.9769
TA1-002326	11.60917	7.775463	4.223958	8.809794	11.95399	13.18617	7.771365	7.224754	11.83092	15.53429	13.24257	14.57046	22.90601	16.69056	13.06242	8.1503
TA1-003377	0.505765	0.385217	0.589033	0.31383	0.2372	0.384667	0.367004	0.325013	0.689097	0.691483	0.777047	0.809404	0.773684	0.52471	0.510341	0.6878
TA1-003668	1.362902	0.988556	1.209048	1.606816	0.901654	1.382339	2.272725	0.930765	1.489156		1.272201	2.046709	1.995231	1.079373	1.641666	1.2461
TA1-003758	9.770025	8.031266	8.789311	7.809334	10.74012	10.19207	10.29742	9.56411	8.353381	10.60459	22.34594	31.29189	9.242507	19.54583	5.532934	11.50
TA1-003867	0.38152	0.279408	0.329279	0.240491	0.295531	0.420889	0.380998	0.261468	0.437766	0.864935	0.601401	0.675228	0.432655	0.427863	0.332577	0.6084
TA1-003891	0.577529	0.760452	0.53521	0.803309	0.930456	0.778426	0.518406	0.375806	0.284242	0.400928	0.444327	0.663483	0.390437	0.321888	0.423074	0.3455
TA1-003991	2.47244	2.25811	2.151531	1.738275	3.016575	2.490514	1.847488	2.52728	1.933712	2.777173	4.707392	9.466824	2.136787	4.72644	0.999485	2.7540
TA1-004779	0.549094	0.468816	0.375165	0.710748	0.568055	0.538746	0.431093	0.850794	0.503225	0.285483	2.127162	0.56611	0.889369	1.782117	2.50519	0.5893
TA1-005582	0.642947	0.514529	0.45564	0.416561	0.522434	0.566433	0.696677	0.476993	0.753838	0.910153	0.789311	1.029308	0.696862	0.683665	0.722561	0.8158
TA1-006771	1.157378	1.109421	1.665206	0.881498	1.230351	1.316628	0.82265	1.087407	1.910959	2.235027	2.452328	1.781063	1.58624	1.45182	1.486406	1.6790
TA1-007089	0.938868	0.619251	0.508233	0.596224	0.8898	0.559613	1.089413	0.566473	1.56374	2.100168	1.509102	2.334239	1.541933	0.983092	1.425668	0.9607
TA1-007182	0.444974	0.97537	0.248752	0.455094	0.86561	0.469695	0.338176	0.068475	0.454283	0.893971	0.853802	0.969706	0.26842	0.483395	0.295316	0.5256
TA1-007521	1.158596	0.841021	0.741834	2.089004	0.775725	1.220261	0.731894	0.511144	2.440875	3.389111	1.242686	7.409944	5.641703	3.194938	1.210107	2.5187
TA1-008216	1.423581	1.244242	0.98828	1.391971	1.080971	1.432107	1.643926	1.045123	1.425685	1.570316	1.469748	1.696198	1.26052	1.173362	1.046654	1.336
TA1-008229	0.49833	0.365725	0.233791	0.455182	0.572644	0.396296	0.484982	0.227582	0.470513	0.50234	0.442675	0.914685	0.434867	0.720749	0.539636	0.416
TA1-008487	1.059835	1.017572	1.131253	0.926451	0.711972	1.028531	1.129205	0.839929	1.464178	2.1053	2.307273	1.879249	2.329613	1.648815	0.868814	1.6830
TA1-008507	0.647878	0.637106	0.749585	0.483717	0.863851	0.715925	0.650253	0.351455	0.794174	1.635238	1.099535	2.13429	0.868841	1.180892	0.975908	1.0132

Figure 6.2. Screenshots of gene expression data of multi-class earthworm dataset.

Identification and Optimization of Classifier Genes

Integrated Statistical and Machine Learning (ISML) Approach

An integrated statistical and machine learning (ISML) pipeline was applied to the 15K earthworm dataset which are exposed to chemical compounds such as TNT and RDX. Figure 6.3 shows the overall process of identifying 58 classifier genes from 15K genes. The pipeline illustrates the analytical procedure that integrates statistical analysis with supervised machine learning and unsupervised clustering. Numbers in brackets indicate the amount of genes remaining.

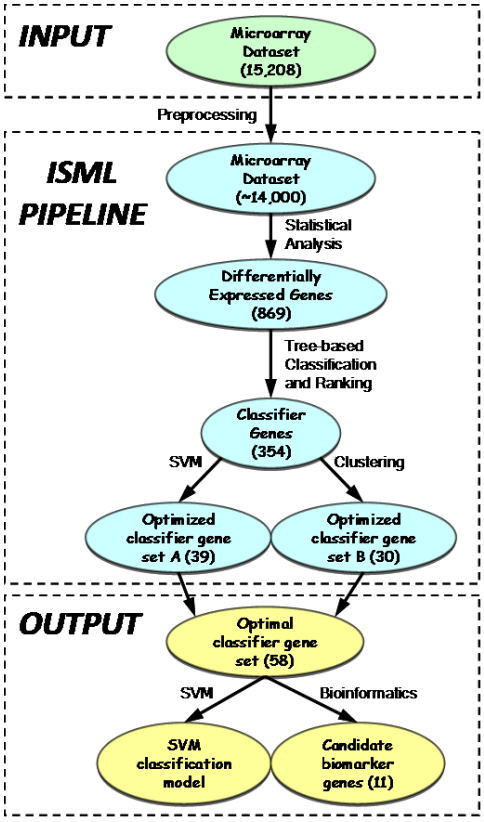

*Figure 6.3.*Application of ISML pipeline in multi-class earthworm dataset.

Classifier Gene Selection and Ranking

Seven decision tree methods (SimpleCart, BFTree, FT, J48, LADTree, LMT and REPTree) were used for gene selection to avoid the biases and overcome limitations of

each single algorithm [105, 106]. An ensemble strategy was also applied to increase prediction accuracy using bagging (Bagging) and boosting (AdaBoostM1) [106]. All of these algorithms are implemented in the WEKA machine learning workbench v.3.6.0 ([108]; www.cs.waikato.ac.nz/ml/weka/). The resulting tree structure each generated a set of classifier genes. The performance of a classifier was evaluated using three criteria: accuracy (see below for definition), precision (or sensitivity = number of correctly classified samples / total number of samples classified into this class), and the area under the ROC (Receiver Operating Characteristic) curve.

We used seven different tree-based machine learning algorithms to select classifier genes from the 869 statistically significant genes. Each algorithm in combination with bagging or boosting generated decision trees, separating earthworm samples into three pre-defined classes based on the expression of classifier genes. A different set of classifier genes was selected by each algorithm (Table 6.1). The classification accuracy varied from 75.0% for SimpleCart with boosting to 84.7% for LMT with bagging. There is a significant correlation between ROC area and accuracy (correlation coefficient = 0.94).

A total of 354 unique classifier genes were obtained after pooling classifier genes from all decision trees. Each classifier gene was then ranked by an overall weight of significance. The distribution and histogram of overall weights of these genes are shown in Figure 6.4. The overall weight of 127 (or 36%) of classifier genes are below 0.1 (Figure 6.4a). Only the top 43 or 14 genes had an overall weight larger than 0.5 or 1.0 (Figure 6.4b), respectively. Over 90% of these genes have one or more strings of annotation information obtained using such bioinformatics programs as BLASTX, BLASTN, InterProScan and PIPA [159].

Table 6.1

Summary of Classification Results Using Tree-Based Classification Algorithms

Ensemble Method	Tree-Based Algorithm	Accuracy (%)	ROC Area
Boosting	BFTree	75.8	0.878
Boosting	J48	79.8	0.882
Boosting	LADTree	77.4	0.881
Boosting	SimpleCart	75.0	0.868
Boosting	FT	83.5	0.930
Boosting	LMT	81.8	0.936
Bagging	J48	75.4	0.868
Bagging	LADTree	75.0	0.876
Bagging	REPTree	75.0	0.870
Bagging	SimpleCart	76.2	0.855
Bagging	FT	82.7	0.937
Bagging	LMT	84.7	0.944

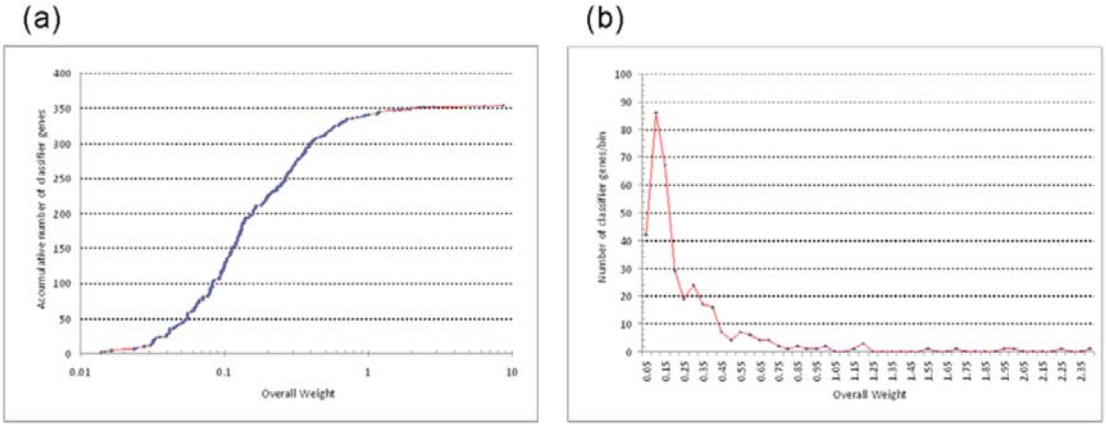

Figure 6.4. The accumulative distribution (a) and histogram (b) of weights of 354 classifier genes. In the histogram, the bin size is set at 0.05, and three genes with the highest overall weight of 2.81, 6.38 and 8.70, respectively, are not shown.

Refinement of the Classifier Gene Set Using MC-SVM or Clustering

Two different algorithms, SMO and K-mean clustering, were employed to optimize the number and set of genes from the 354 ranked classifier genes. Composition of the

classifier gene set had a significant influence on classification accuracy (Figure 6.5). Using SMO, as few as 16 top ranked genes classified 81% of the 248 samples into correct classes (Figure 6.5a). Starting at the 250th gene, the inclusion of additional classifier genes not only did not improve the classification accuracy for the TNT and the RDX classes as well as the weighted average accuracy, but deteriorated the accuracy for the control class (Figure 6.5a). Similarly, with the clustering approach, the top ranked 31 genes correctly clustered 66% of the samples, while addition of other genes did little, if any, to improve the accuracy of either individual classes or the weighted average (Figure 6.5b). Clearly, individual classifier genes vary remarkably in its contribution to the change of classification accuracy, which also depends on the choice of machine learning algorithms. The iterative optimization process effectively removed many genes that made no or negative contribution to the classification performance. As a result, this process produced a SVM- and a clustering-optimized subset consisting of 39 and 30 genes, respectively (Figure 6.6).

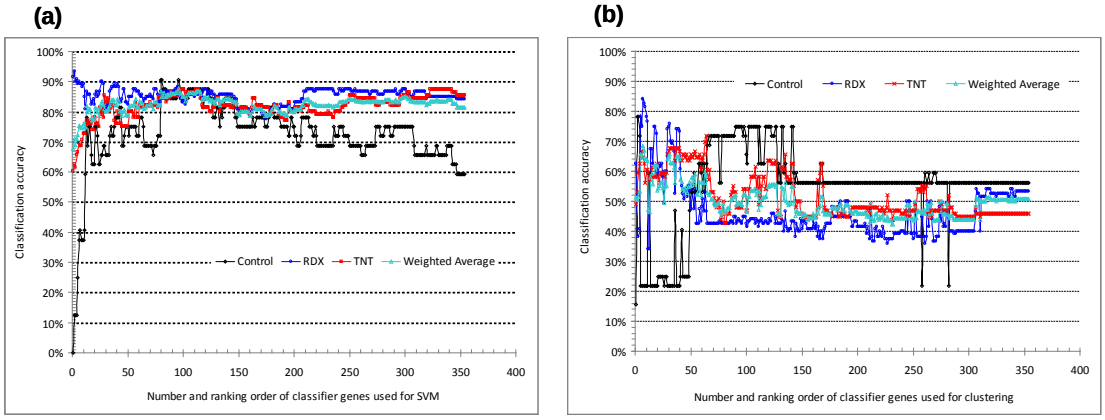

Figure 6.5. Classification accuracy using 354 classifier genes by SVM and clustering. Classification accuracy of 248 earthworm samples using SVM (a) or clustering (b) with an increasing number of top ranked classifier genes. The weighted average accuracy and the accuracy for each of the three classes (control, RDX and TNT) are shown for each set of genes (1~354 genes). Genes were added to the increasing gene set one at a time in the order of decreasing overall weight (see also Figure 6.4a).

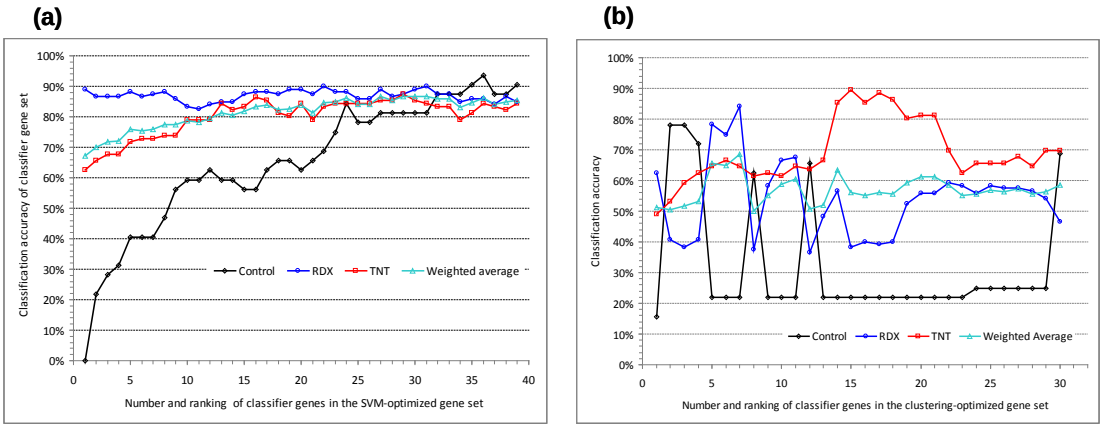

Figure 6.6. Classification accuracy using 39 or 30 classifier genes by SVM or clustering, respectively. Classification accuracy of 248 earthworm samples using an increasing number of classifier genes optimized by SVM (a) or clustering (b). The weighted average accuracy and the accuracy for each of the three classes (control, RDX and TNT) are shown for each set of genes (1~39 genes in 6.6(a) or 1~30 genes in 6.6(b)). One gene (the next highest ranked gene) at a time was added to the previous gene set to generate a new gene set (see also Figure 6.4(a)).

The first 24 genes of the SVM-optimized subset clearly played more important roles than the remaining 15 genes that only slightly improved the accuracy for the control class and changed very little the accuracy for the TNT and the RDX classes (Figure 6.5a). The subset of 39 genes performed well in terms of accuracy, ROC area, and precision, with 83~91% in accuracy and precision except for the 76% precision of the control class (Table 6.2). The case for the clustering-optimized subset is a bit perplexing as the accuracy of the control and the RDX classes changed in opposite directions after adding the 2^{nd}, 5^{th}, 7^{th}, 9^{th}, 11^{th} and 13^{th} genes (Figure 6.5b). Nevertheless, the whole subset of 30 genes evened up the accuracy for all classes (Figure 6.6b and Table 6.3) and gave an average of 72.5% precision for the three classes (Table 6.3). The sensitivity for the control class was relatively lower, especially in classification by clustering, when compared with that for the other two classes. An examination of the samples that were incorrectly clustered into the control class showed that they were mostly exposed for 4

Table 6.2

Confusion Matrix Showing Classification Results Using 39 Classifier Genes by SVM

True Class (No. Samples)	No. Samples Classified as			Accuracy (%)	ROC Area
	Control	RDX	TNT		
Control (32)	29	2	1	90.6	0.938
RDX (120)	7	106	7	88.3	0.887
TNT (96)	2	14	80	83.3	0.913
Precision (%)	76.3	86.9	90.9		
Weighted average (248)	87.1 (precision)			86.7	0.904

Note. The confusion matrix showing classification results for testing datasets obtained by MC-SVM using the optimized set of 39 classifier genes.

Table 6.3

Confusion Matrix Showing Classification Results Using 30 Classifier Genes by Clustering [a]

True Class (No. Samples)	No. Samples Classified as			Accuracy (%)
	Control	RDX	TNT	
Control (32)	22	1	9	68.8
RDX (120)	46	56	18	46.7
TNT (96)	21	8	67	69.8
Precision (%)	24.7	86.2	71.3	
Weighted average(248)	72.5 (precision)			58.5

Note. The confusion matrix showing classification results for testing datasets obtained by clustering using the optimized set of 39 classifier genes. [a] The optimized set of 30 classifier genes were used. ROC area was not computable for clustering.

days to the lowest three concentrations of RDX or TNT (data not shown). A plausible reason for this misclassification is that gene expression in these samples may not be significantly different from that in the controls due to low levels of contaminant. The uneven sample size might explain why the SVM precision for the control class (32 samples) is relatively lower than that for the other two classes (96 and 120).

Optimized Gene Subset for Classification

The two subsets of classifier genes optimized by SVM and clustering share 11 common genes, and the combination of these two resulted in a set of 58 unique genes that represents a refined gene set for the three-class classification. Using this gene set, we were able to build a SVM model with high performance parameters including accuracy, sensitivity and ROC area (Table 6.4). The classification results for both supervised SVM and unsupervised clustering are slightly less superior with the 58-gene set (Table 6.4) than with the 39- or the 30-gene set (Tables 6.2 and 6.3). As summarized in Table 6.5, 38 genes or 65.5% of the optimal gene set are among the 70 highest ranked classifier genes, 15 or 75% of the top 20 ranked genes are included in the optimal gene set, and 7 or 63.6% of the 11 genes picked by both SVM and clustering come from the top 12 ranked classifiers. These results reinforce the merit of our weight-of-significance ranking system.

Discussion

Microarray datasets possess an exceptionally high complexity distinguished by high feature dimension and low sample size. Like other microarray studies, the primary objective of this study was to search for an optimal or near optimal subset of genes that could be used to predict the exposure history of unknown samples. It has been proven in both theory and practice that feature selection can effectively enhance learning efficiency, increase predictive accuracy, reduce complexity of learned results, and improve the

Table 6.4

Confusion Matrix Showing Classification Results Using 58 Classifier Genes by SVM or Clustering [a]

True Class (No. Samples)	No. Samples Classified as			Accuracy (%)	ROC Area
	Control	RDX	TNT		
SVM					
Control (32)	26	6	0	81.3	0.936
RDX (120)	9	100	11	83.3	0.856
TNT (96)	2	13	81	84.4	0.913
Precision (%)	70.3	84.0	88.0		
Weighted average (248)	83.8 (precision)			83.5	0.904
Clustering [a]					
Control (32)	22	1	9	68.8	NA
RDX (120)	48	55	17	45.8	NA
TNT (96)	22	10	64	66.7	NA
Precision (%)	23.9	83.3	71.1		
Weighted average (248)	70.9 (precision)			56.9	NA

Note. Confusion matrix of classification results obtained using the refined set of 58 classifier genes combined from the SVM- and the clustering-optimized gene sets. [a] ROC area was not computable with clustering.

accuracy of classification models [156, 160, 161]. Although numerous supervised or unsupervised machine learning techniques have been used for feature selection and sample classification of microarray data (for reviews see [162, 163, 164]), classification performance appears to depend strongly on the dataset and less on the variable selection and classification methods [165]. Meanwhile, it has been demonstrated that a combined

Table 6.5

Optimized Set of 58 Classifier Genes

Gene Order	Probe Name	Overall Weight	Rank [a]	Picked By	Expression Altered By	Target Gene Annotation
1	TA2-091233	8.70	1	Both	RDX	Polypyrimidine tract binding (PTB) protein
2	TA1-023824	6.38	2	Both	TNT	NADH-coenzyme Q reductase
3	TA1-204280	2.81	3	Clustering	RDX	DEAD box polypeptide 46 (DDX46)
4	TA1-012917	2.40	4	Both	TNT	Unavailable
5	TA2-092252	2.21	5	Both	RDX	Diazepam binding inhibitor (DBI)-like protein
6	TA1-022179	1.96	6	Both	RDX	Signal-peptide
7	TA1-200771	1.94	7	Both	TNT	Superoxide dismutase (SOD)
8	TA1-003377	1.50	9	SVM	RDX	Unavailable
9	TA2-113782	1.20	10	SVM	Both	Signal-peptide
10	TA2-139945	1.17	12	Both	TNT	Earthworm valosine containing peptide-2 (evcp-2)
11	TA2-210040	1.14	13	SVM	TNT	Unavailable
12	TA1-173733	1.00	14	Clustering	RDX	Signal recognition particle
13	TA2-206312	0.96	15	Clustering	TNT	Heat shock protein 70 (HSP70)
14	TA1-200094	0.84	19	Clustering	RDX	Serine/Threonine protein phosphatise
15	TA1-084360	0.78	20	SVM	TNT	Translational elongation factor 2 (EF2)
16	TA2-056405	0.70	21	SVM	TNT	Heterogeneous nuclear ribonucleoprotein (hnRNP) K
17	TA2-029918	0.66	25	SVM	Both	Unknown
18	TA1-189015	0.65	26	SVM	RDX	60S acidic ribosomal protein P2
19	TA2-153080	0.62	29	SVM	RDX	Electron transfer flavoprotein (ETF) β-subunit
20	TA2-135639	0.58	32	SVM	Both	Unavailable
21	TA1-056351	0.56	34	Clustering	TNT	Unavailable
22	TA1-167854	0.55	35	SVM	RDX	Unknown
23	TA2-099898	0.55	36	Clustering	TNT	Presenilin
24	TA2-005815	0.53	38	SVM	TNT	Unknown
25	TA1-065695	0.52	39	SVM	TNT	Unknown
26	TA2-088504	0.51	41	SVM	TNT	Eukaryotic release factor 1 (eRF1)
27	TA1-020439	0.50	42	Clustering	RDX	Unknown

Table 6.5 (continued).

Gene Order	Probe Name	Overall Weight	Rank [a]	Picked By	Expression Altered By	Target Gene Annotation
28	TA1-194525	0.50	43	Both	Both	Valosine containing peptide-2 (evcp-2)
29	TA2-146992	0.45	47	SVM	RDX	ATP synthase 9 mitochondrial
30	TA2-058573	0.44	48	Clustering	TNT	Arginine/Serine-rich splicing factor
31	TA1-086892	0.42	50	Clustering	TNT	Unavailable
32	TA1-030037	0.42	51	SVM	RDX	S10_Plectin
33	TA2-058673	0.41	52	SVM	TNT	Unavailable
34	TA2-006089	0.40	55	SVM	TNT	Translational elongation factor 2 (EF2)
35	TA1-213621	0.37	63	Both	TNT	Vacuolar ATP synthase proteolipid subunit
36	TA1-058331	0.36	67	SVM	TNT	Titin
37	TA1-095832	0.36	68	Clustering	RDX	Unknown
38	TA2-144740	0.35	70	SVM	RDX	26S proteasome complex subunit DSS1
39	TA1-183759	0.32	78	Both	RDX	26S proteasome regulatory subunit RPN1
40	TA1-058194	0.32	80	SVM	TNT	Unknown
41	TA1-026013	0.31	83	SVM	TNT	Heat shock protein 70 (HSP70)
42	TA1-017276	0.31	85	SVM	TNT	RNA-binding domain, RBD
43	TA2-203946	0.31	86	SVM	TNT	Peptidase (mitochondrial processing) β isoform 2
44	TA1-153822	0.30	88	Clustering	TNT	Pyruvate kinase
45	TA1-184000	0.30	89	Clustering	TNT	NADPH FAD oxidoreductase
46	TA1-193191	0.27	102	Clustering	RDX	Cytochrome c oxidase subunit IV (COX4)
47	TA1-118706	0.27	104	SVM	TNT	Oxidoreductase
48	TA2-119638	0.25	116	SVM	TNT	Unavailable
49	TA2-118209	0.23	121	Clustering	TNT	Unavailable
50	TA2-081772	0.20	132	Clustering	TNT	NADH-coenzyme Q reductase
51	TA1-208104	0.14	163	SVM	TNT	Lipocalins
52	TA1-118589	0.11	207	SVM	RDX	40S ribosomal protein S10
53	TA2-031808	0.10	225	Clustering	RDX	Biogenesis of lysosome-related organelles complex-1 subunit
54	TA1-123240	0.09	246	Clustering	RDX	RNA-binding protein
55	TA2-090604	0.08	254	Clustering	TNT	Arginine/Serine-rich coiled-coil 2 isoform 2

Table 6.5 (continued).

Gene order	Probe name	Overall weight	Rank [a]	Picked By	Expression altered by	Target gene annotation
56	TA1-008487	0.08	265	Clustering	TNT	Cytochrome C1
57	TA2-118601	0.08	266	Both	RDX	Translationally-controlled tumor protein homolog (TCTP)
58	TA2-095503	0.04	319	SVM	RDX	60S ribosomal protein RPL36A

Note. Optimized set of 58 classifier genes as an output of the ISML pipeline. [a] Rank indicates the weight-of-significance ranking among the 354 classifier genes.

use of different classification and feature selection approaches can enhance confidence in selecting relevant genes [156, 164] and that ensemble methods such as bagging and boosting can improve classification performances [106]. These two strategies are both reflected in our ISML pipeline (Figure 6.3, Table 6.1).

We first used the univariate statistical analysis [166] that selected 869 features/genes. These genes may represent a wide variety of transcripts that responded not only to toxicants TNT or RDX, but also likely to other environmental stresses. To further down select the features, we employed several decision-tree algorithms. A decision tree is constructed by selecting the most discriminative features / nodes for classification [164] and biomarker genes discovery [103] from microarray data. In a decision tree, the occurrence of a node (feature / gene) provides the information about the importance of the associated feature / gene [103]. The root gene has the most information gain for classification, and the other nodes genes appear in descending order of power in discrimination [38]. During the decision learning, the genes that have no discrimination capability are discarded. A total of 515 genes were eliminated from the 869 differentially expressed genes by tree-based algorithms, leaving 354 classifier genes. This represents a 59% feature reduction.

As our goal was to scale down the size of potential classifier gene set while maintaining a high discriminative power, we introduced in the ISML pipeline a new algorithm to compute and rank the overall weight of the 354 individual classifier genes based on their contribution/significance to classification. We also developed a novel optimization algorithm for iteratively removing classifier genes that had little or a negative impact on classification performance. This bottom-up removal process began with the least important gene having the lowest overall weight. We chose to eliminate those genes that only reduced the classification accuracies of all classes as well as the weighted average. This conservative approach was adopted to preserve genes that might increase the accuracy of one class but decrease that of another, like the 2^{nd}, 5^{th}, 7^{th}, 9^{th}, 11^{th} and 13^{th} genes in the clustering-optimized gene set (Figure 6.6b). These genes are usually important for discriminating one particular class while confounding other classes.

SVMs are powerful classification models that have shown state-of-the-art performance on several diagnosis and prognosis tasks on biological data [106, 167]. SVM-based classification can usually achieve higher accuracy/precision on a given dataset than unsupervised algorithms. Ideally, an SVM analysis should produce a hyper-plane that completely separates the feature vectors into non-overlapping groups. However, perfect separation may not be possible, or it may result in a model with so many feature vector dimensions that the model does not generalize well to other data, which is a problem commonly known as over-fitting [168]. The risk of over-fitting to the specific dataset in compensation for high accuracy/precision may render a high probability of misclassification when the trained SVM model is applied to predict unknown samples of other independent datasets. Unlike SVM, unsupervised learning algorithms can overcome this shortfall with a trade-off of less superior

accuracy/precision. Our ISML pipeline adopted a compromise between these two approaches. Although the effectiveness, efficiency and superiority of this approach has to go through more stringent validation and testing, our results indicate that the final combined gene set produced nearly as good classification outcome as the two separately optimized gene subsets. This combined gene set need to be tested in field samples where exposure history including species and concentration of contaminants as well as exposure length is often unknown. Currently, a field soil study is undertaken to validate this optimal gene set, where lab-cultured mature earthworms are exposed in field soils primarily contaminated with TNT or RDX.

Classification accuracy was evaluated in this study on a sole basis of the pre-defined exposure history, that is, each sample was labelled with *a priori* class corresponding to the chemical it had been exposed to, disregarding the differences in soil concentration of TNT or RDX. The accuracy of biological classification can be impaired for soils containing low toxicant concentrations which may not induce gene expression effects significant enough to distinguish exposed animals from the controls. This might contribute partly to the lower accuracy obtained from clustering than from SVM. It is desirable to define a threshold such as the lowest observable effect concentration expressed as the toxicant concentration in soil or animals (body burden). We prefer body burden as an exposure measure over soil concentration due to the often heterogeneous distribution of toxicants in soil. This way, animals with a tissue concentration below the threshold can be grouped/pre-defined together with unexposed control animals, which potentially benefits clustering more than SVM.

To define a sensitive threshold, one can measure disease-related biological endpoints that are presumably more sensitive than the mortality and growth endpoints in short-term

exposures of 4 or 14 days. Alternatively, one can measure toxicity-related phenotypic (e.g., biochemical, physiological, or pathological) endpoints if a more toxicological meaningful discrimination is desired. The SVM classification model for exposure classification in the output of the ISML pipeline can be conveniently converted into a disease or toxicity diagnosis model.

Another confounding factor that affects classification accuracy is that vulnerability and susceptibility vary from one animal to another, which may be caused by many factors such as genetic make-up, age, and physiological status. We believe that the diagnosis or prediction accuracy of unknown samples can be greatly improved if gene expression profiles of biologically well-characterized, pre-defined animals are used as the training dataset, just like in cancer microarray studies.

Among the 58 optimized genes, 93% genes exhibited toxicant-specific gene expression alterations, that is, 32 genes responded specifically to TNT, 22 to RDX, and only 4 to both chemicals (Table 6.5). Forty-two genes (72%) have meaningful annotation with a wide range of biological functions spanning from antioxidant response (COX4 and NADH-coenzyme Q reductase) to spermatogenesis (evcp-2) and GABA receptor modulator (DBI, also known as Acyl-CoA-binding protein or ACBP). Three of the top 10 ranked genes, PTB, DBI and SOD, have previously been shown being altered by TNT [157] or RDX [158]. Two probes targeting two highly similar transcripts coding for evcp-2, a gene expressed specifically in the anterior segments of sexually mature earthworms [169], take the 10^{th} and the 28^{th} positions on the optimal gene list, suggesting that both TNT and RDX may affect spermatogenesis. On the list, there are also several stress-responding genes such as HSP70 (#13 & #41) [170] as well as cancer-related genes such as TCTP (#57) [171]. It is worth noting that six genes, PTB (#1) [172], DDX46 (#3)

[173], EF2 (#15 & #34) [174], hnRNP K (#16) [175], and eRF1 (# 26) [176] are all involved in mRNA splicing or processing and RNA translation initiation or termination, indicating alteration of mRNA secondary structure and protein synthesis may be targeted by both TNT and RDX. More work should be devoted to exploring biological functions and interactions of the 58 genes that may lead or be linked to toxicological effects or biochemical endpoints.

This study addresses a sophisticated issue of discovering and optimizing classifier gene sets in environmentally relevant animal models. Although a perfect or the best solution to it is yet to be found, we have demonstrated that the ISML pipeline can reduce the dimensionality of microarray datasets, identify and rank classifier genes, generate a small set of classifier genes, produce an SVM classification model with high accuracy, and select a small group of biomarker candidate genes for biological validation. This approach can also be applied to discover diagnostic biomarker genes exhibiting toxicity- or disease-dependent response in environmental species from fish and springtail to water flea and earthworm.

We report here some preliminary results of a much larger effort. Our future work include: (1) compare the performance of the ISML approach with that of other popular and existing feature selection techniques such as SVM-RFE (SVM Recursive Feature Elimination), CFS (Correlation based Feature Selection) and χ^2 using the earthworm dataset and other microarray datasets; (2) validate the final 58- gene set using other experimental methods such as real-time quantitative PCR; (3) further test the classifiers in field samples; (4) identify TNT/RDX concentration-related classifier genes; and (5) validate the biochemical outcome regulated by the biomarker candidate genes. We

believe that these consorted efforts will lead us to discovery of novel classifier genes useful for environmental risk assessment.

Time-Series Earthworm Microarray Dataset

Experimental Design and Dataset Generation

The following experiment id designed and conducted by Dr. Ping Gong at the Environmental Laboratory of U.S. Army Engineer Research and Development Center. A new earthworm array containing 43,803 non-redundant 60-mer probes was used to generate the dataset. The probes were selected from 63,641 previously validated oligonucleotide probes, each targeting a unique *Eisenia fetida* transcript, and 37,439 (59%) of probed targets had meaningful biological annotation [157]. A synchronized earthworm culture (starting from cocoons) was created and mature worms bearing clitellum and weighing 0.4~0.6 g were chosen for this experiment. Each worm was transferred from artificial soil-based bedding (culture) and housed in an individual glass vial (115 mL in volume) [177]. These worms were exposed to carbaryl (20 ng/cm^2) or RDX (2 $\mu g/cm^2$) or acetone (solvent control) on moistened filter paper lined up inside the vial. These chemical concentrations were selected because they did not cause lethality (based on results from preliminary tests). The entire experiment was divided into three phases (Figure 6.8): acclimation (4 days), exposure (6 days) and recovery (7 days). The acclimation phase was necessary for the worms to adapt from soil culture to filter paper, and four samplings were taken to establish the "background" baseline under the control condition. Worms were sampled at 13 and 14 time points for all three treatments (control, RDX and carbaryl) during the exposure and the recovery phase, respectively. Sampled worms were measured for conduction velocity of the medial giant nerve fiber (MGF) before being sacrificed by snap-freezing in liquid nitrogen. All yet-to-be-sampled worms

were transferred to new vials at the beginning of the next phase. For instance, at the end of exposure phase, all remaining worms were transferred from exposure vials (containing spiked filter paper) to recovery vials (containing non-spiked clean filter paper). No mortality occurred throughout the whole experiment. Sampled worms were fixed in RNAlater-ICE to preserve RNA integrity at -80°C.

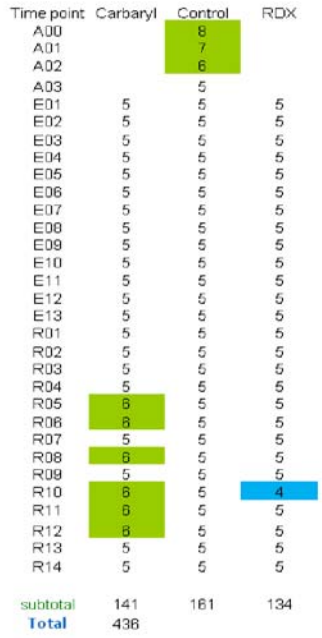

Time point	Carbaryl	Control	RDX
A00		8	
A01		7	
A02		6	
A03		5	
E01	5	5	5
E02	5	5	5
E03	5	5	5
E04	5	5	5
E05	5	5	5
E06	5	5	5
E07	5	5	5
E08	5	5	5
E09	5	5	5
E10	5	5	5
E11	5	5	5
E12	5	5	5
E13	5	5	5
R01	5	5	5
R02	5	5	5
R03	5	5	5
R04	5	5	5
R05	6	5	5
R06	8	5	5
R07	5	5	5
R08	6	5	5
R09	5	5	5
R10	6	5	4
R11	8	5	5
R12	8	5	5
R13	5	5	5
R14	5	5	5
subtotal	141	161	134
Total	436		

Figure 6.7. Array distributions of three treatments and 31 time points.

Total RNA were extracted from at least 5 worms per time point per treatment, except for the 10th time point of RDX treatment in recovery stage (R10-RDX) where only 4 replicates remained after removing an array due to the poor RNA quality in the second replicate. RNA samples were hybridized to the custom-designed 44K-oligo array using Agilent's one-color Low RNA Input Linear Amplification Kit. After hybridization and scanning, gene expression data were acquired using Agilent's Feature Extraction Software (v.9.1.3). In the current study, a total of 436 good quality arrays were generated, corresponding to 436 worm RNA samples (= 4~8 replicate worms × (1 control treatment

× 31 time points + 2 chemical treatments × 27 time points) (see Figure 6.7). There were 161 untreated controls, 141 carbaryl-treated, and 134 RDX-treated. Three manufacturing batches of arrays were used, so the replicates within the same treatment condition and sampling time point were distributed into three batches in order to minimize batch effects. For example, five replicate worms exposed to RDX were sampled at E01, and 2, 2 and 1 replicate worm was hybridized to arrays of batch 1, 2 and 3, respectively. A multidimensional scaling was used to examine batch effects, and results show that samples are not grouped by batch, suggest batch had no significant effect in this dataset. Figure 6.8 shows the sampling scheme and time points of sample collections.

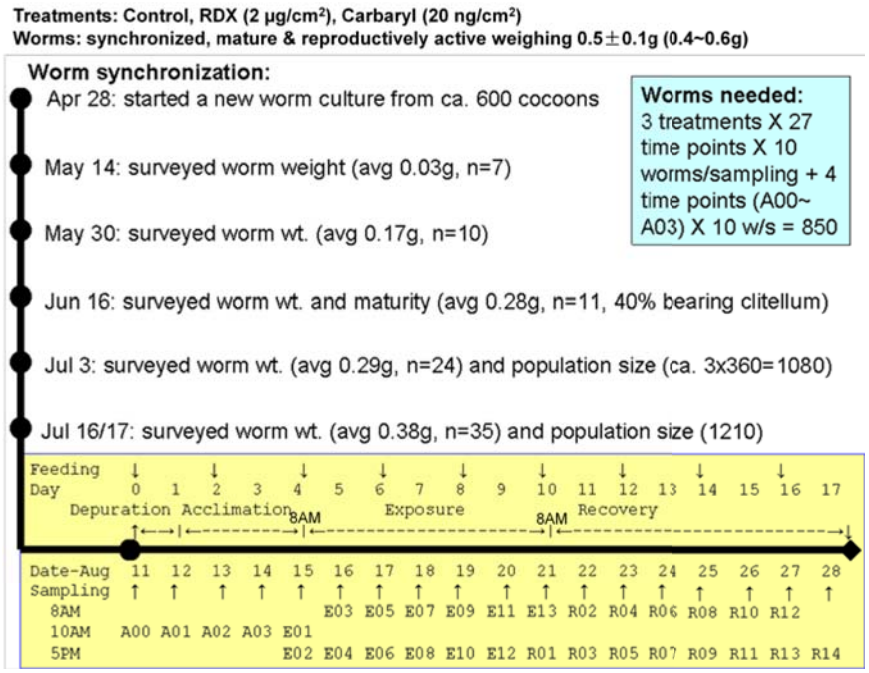

Figure 6.8. Sampling scheme of 44K time-series earthworm microarray dataset.

Integrated Statistical and Machine Learning (ISML) Approach

The ISML pipeline was applied to the 44K earthworm dataset. Figure 6.10 shows the overall process, which identified 70 classifier genes from 44K genes. The pipeline illustrates the analytical procedure that integrates statistical analysis with supervised

machine learning and unsupervised clustering. Numbers in brackets indicate the amount of genes remaining.

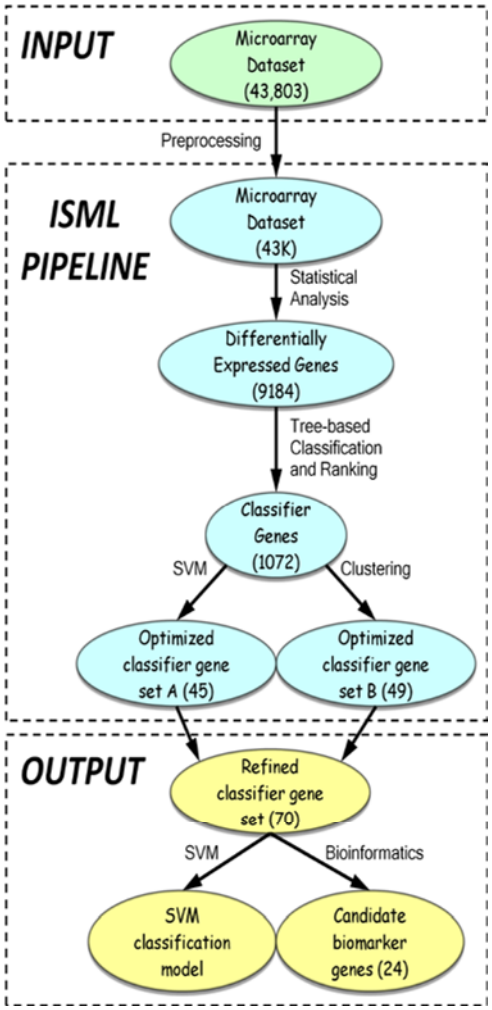

Figure 6.9. Application of ISML pipeline in time-series earthworm dataset.

Data Preprocessing

The following data pre-treatment steps were applied prior to further statistical and computational analyses: (1) feature filtering: flag out spots with signal intensity outside the linear range as well as non-uniform spots; (2) conversion: convert signal intensity into relative RNA concentration based on the linear standard curve of spike-in RNAs; (3) normalization: normalize the relative RNA concentration to the median value on each array; and (4) gene filtering: filter out genes appearing in less than 50% of arrays (i.e.,

present on at least 219 arrays). There were more than 43,000 genes remaining after this procedure.

Feature Filtering by Univariate Statistical Analysis

The Class Comparison Between Groups of Arrays Tool in BRB-ArrayTools v.3.8 software package ([103]) was used to identify significantly changed genes. The collated earthworm array dataset was imported without any further normalization or transformation. The tool runs a random variance version of the t-test or F-test separately for each gene. It performs random permutations of the class labels and computes the proportion of the random permutations that give as many genes significant at the level set by the user as are found in comparing the true class labels. The following class-comparison analyses were conducted to infer genes differentially expressed in response to Carbaryl or RDX: two 2-class comparisons: pooled controls vs. pooled Carbaryl or RDX treatments. The following settings were employed: a univariate test random variance model, multivariate permutation tests with 10,000 random permutations, a confidence level of false discovery rate assessment = 99%, and a maximum allowed number of false-positive genes = 10. A total of 9184 unique genes were obtained after combining all significantly changed gene lists from Carbaryl- and RDX-exposures. The frequency of changes of gene expression values for each gene across 31 time points are counted, and among the 9184 differentially expressed genes (DEGs), 2574 unique genes were identified as DEGs for at least two time points.

Identification and Optimization of Classifier Genes

Classifier Gene Selection and Ranking

We used seven different tree-based machine learning algorithms to select classifier genes from the 2574 statistically significant genes. Each algorithm in combination with

bagging or boosting generated decision trees, separating earthworm samples into three pre-defined classes based on the expression of classifier genes. A different set of classifier genes was selected by each algorithm (Table 6.6). The classification accuracy varied from 75.0% for SimpleCart with boosting to 84.7% for LMT with bagging. There is a significant correlation between ROC area and accuracy (correlation coefficient = 0.94).

A total of 1072 unique classifier genes were obtained after pooling classifier genes from all decision trees. Each classifier gene was then ranked by an overall weight of significance. The distribution and histogram of overall weights of these genes are shown in Figure 6.10. The overall weight of 550 (or 36%) of classifier genes are below 0.1 (Figure 6.10a). Only the top 68 genes had an overall weight between 0.5 and 1.0 (Figure 6.10b), respectively. Over 90% of these genes have one or more strings of annotation information obtained using such bioinformatics programs as BLASTX, BLASTN, InterProScan and PIPA [159].

Table 6.6

Summary of Classification Results Using Tree-Based Classification Algorithms

Ensemble Method	Tree-Based Algorithm	Accuracy (%)	ROC Area
Boosting	LADTree	77.3	0.918
Boosting	SimpleCart	78.0	0.913
Boosting	REPTree	74.8	0.889
Boosting	LMT	83.9	0.961
Bagging	J48	78.4	0.919
Bagging	LADTree	77.8	0.918
Bagging	REPTree	79.4	0.914
Bagging	SimpleCart	78	0.904
Bagging	LMT	84.9	0.965

(a) (b)

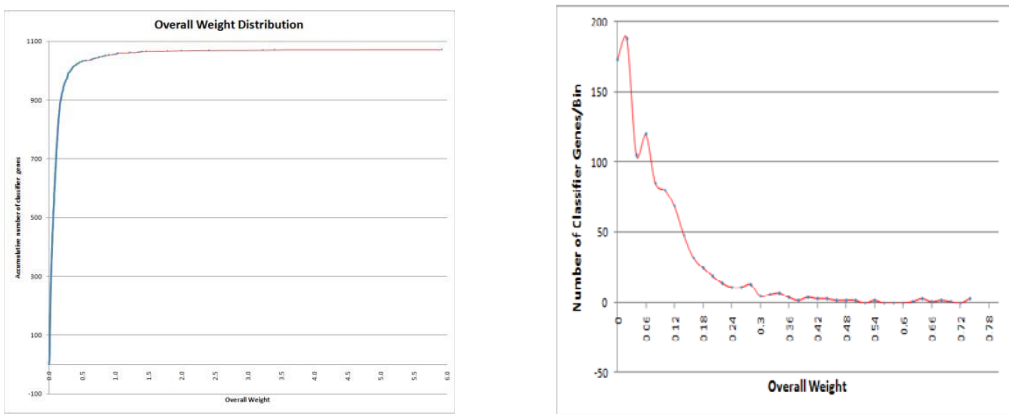

Figure 6.10. The accumulative distribution (a) and histogram (b) of weights of 1074 classifier genes. In the histogram, the bin size is set at 0.02.

Refinement of Classifier Gene Set Using MC-SVM or Clustering

Two different algorithms, SMO and K-mean clustering, were employed to optimize the number and set of genes from the 1074 ranked classifier genes. Composition of the classifier gene set had a significant influence on classification accuracy (Figure 6.11). Using SMO, as few as 22 top ranked genes classified 82% of the 436 samples into correct classes (Figure 6.11a). Starting at the 268th gene, the inclusion of additional classifier genes not only did not improve the classification accuracy for the TNT and the RDX classes as well as the weighted average accuracy, but deteriorated the accuracy for the control class (Figure 6.11a). Similarly, with the clustering approach, the top ranked 23 genes correctly clustered 72% of the samples, while addition of other genes did little, if any, to improve the accuracy of either individual classes or the weighted average (Figure 6.11b). Clearly, individual classifier genes vary remarkably in its contribution to the change of classification accuracy, which also depends on the choice of machine learning algorithms. In Figure 6.11, the weighted average accuracy and the accuracy for each of the three classes (control, RDX and Carbaryl) are shown for each set of genes (1~1074

genes). Genes were added to the increasing gene set one at a time in the order of decreasing overall weight (see also Figure 6.10a). The iterative optimization process effectively removed many genes that made no or negative contribution to the classification performance. As a result, this process produced a SVM- and a clustering-optimized subset consisting of 45 and 49 genes, respectively (Figure 6.12).

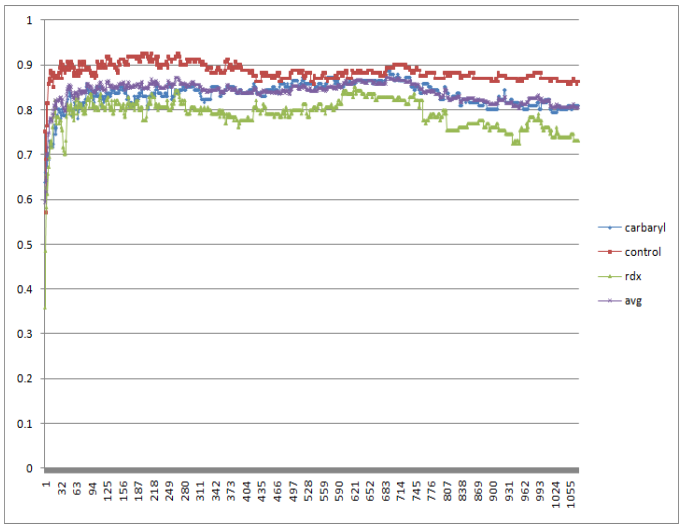

(a)

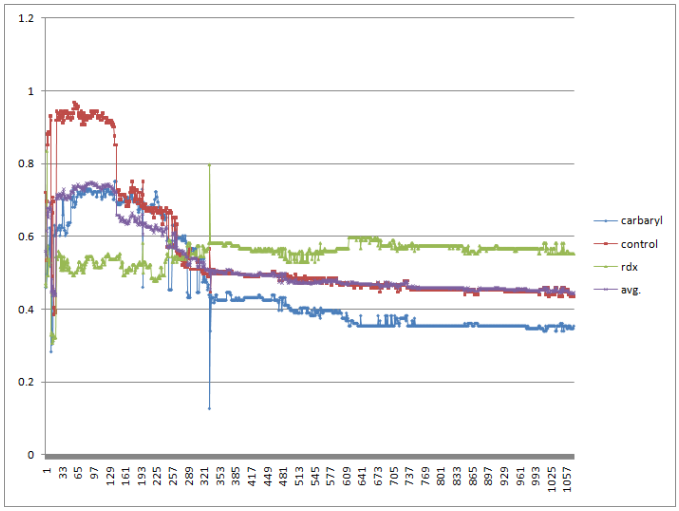

(b)

Figure 6.11. Classification accuracy using 1074 classifier genes by SVM or Clustering. Classification accuracy of 436 earthworm samples using SVM (a) or clustering (b) with an increasing number of top ranked classifier genes.

The first 28 genes of the SVM-optimized subset clearly played more important roles than the remaining 17 genes that only slightly improved the accuracy for the control class and changed very little the accuracy for the Carbaryl and the RDX classes (Figure 6.11a). The subset of 45 genes performed well in terms of accuracy, ROC area, and precision, with 85~89% in accuracy and precision except for the 85% precision of the carbaryl class (Table 6.7). The case for the clustering-optimized subset is a bit perplexing as the accuracy of the control and the RDX classes changed in opposite directions after adding the 2^{nd}, 5^{th}, 7^{th}, 9^{th} genes (Figure 6.11b). Nevertheless, the whole subset of 49 genes evened up the accuracy for all classes (Figure 6.12b and Table 6.8) and gave an average of 80.7% precision for the three classes (Table 6.8).

Table 6.7

Confusion Matrix Showing Classification Results Using 45 Classifier Genes by SVM

True Class (No. Samples)	No. Samples Classified as			Accuracy (%)	ROC Area
	Control	RDX	Carbaryl		
Control (161)	140	14	7	87.0	0.938
RDX (134)	8	120	6	89.6	0.887
Carbaryl (141)	5	15	121	85.8	0.913
Precision (%)	91.5	80.5	90.3		
Weighted average (436)	89.4 (precision)			88.6	0.904

Note. Confusion matrix showing classification results for testing datasets obtained by MC-SVM using the optimized set of 45 classifier genes.

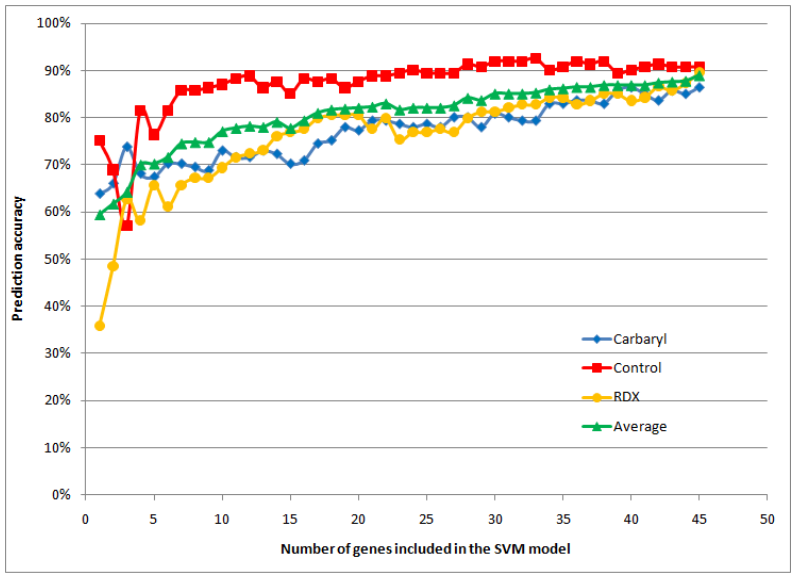

(a)

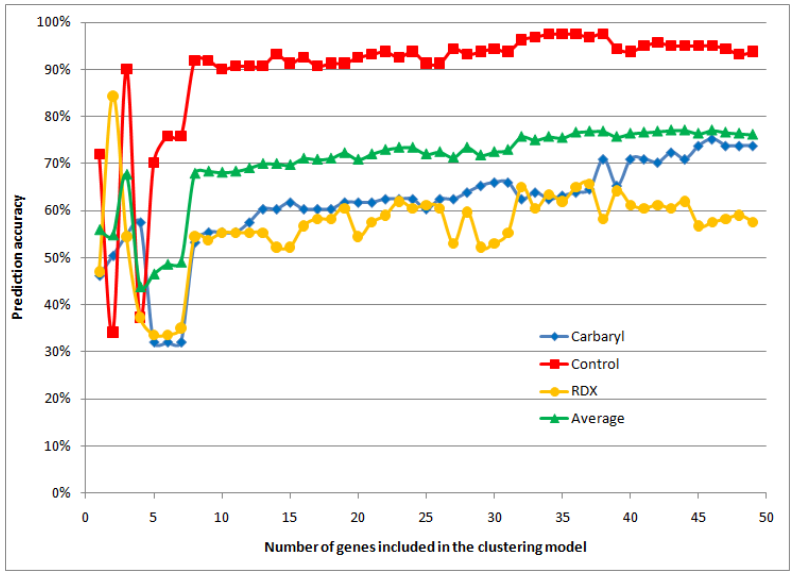

(b)

Figure 6.12. Classification accuracy using 45 or 49 classifier genes by SVM or clustering, respectively. Classification accuracy of the 436 earthworm samples using an increasing number of classifier genes optimized by SVM (a) or clustering (b). The weighted average accuracy and the accuracy for each of the three classes (control, RDX and Carbaryl) are shown for each set of genes (1~45 genes in 6.12(a) or 1~49 genes in 6.12(b)). One gene (the next highest ranked gene) at a time was added to the previous gene set to generate a new gene set (see also Figure 6.10(a)).

Table 6.8

Confusion Matrix Showing Classification Results Using 49 Classifier Genes by Clustering

True Class (No. Samples)	No. Samples Classified as			Accuracy (%)
	Control	RDX	Carbaryl	
Control (161)	140	3	18	87
RDX (134)	24	100	10	74.6
Carbaryl (141)	30	9	102	72.3
Precision (%)	72.2	89.3	78.5	
Weighted average (436)	80.7 (precision)			77.2

Note. Confusion matrix showing classification results obtained by clustering. [a] The optimized set of 49 classifier genes were used. ROC area was not computable for clustering.

Optimized Gene Subset for Classification

The two subsets of classifier genes optimized by SVM and clustering share 24 common genes, and the combination of these two resulted in a set of 70 unique genes that represents a refined gene set for the three-class classification. Using this gene set, we were able to build a SVM model with high performance parameters including accuracy, sensitivity and ROC area (Table 6.9). The classification results for both supervised SVM and unsupervised clustering are slightly less superior with the 70-gene set (Table 6.9) than with the 45- or the 49-gene set (Tables 6.7 and 6.8).

Reconstruction of GRNs for Chemical-Induced Neurotoxicity

Identification of Significant Pathways/GRNs

A total of 240 KEGG pathways, including 121 metabolism pathways and 119 non-metabolism pathways contain KO ortholog genes that can be mapped with earthworm target genes. Among those 2574 significant differential expressed genes, 604 of them

were found in the 240 KEGG pathways with 218 genes mapped to metabolic pathways, 460 to non-metabolic pathways and 74 genes to both. Figure 6.13 gives an example of a customized pathway built by RefNet toolbox. The red-highlighted KEGG genes have homologous *E. fetida* transcripts.

Table 6.9

Confusion Matrix Showing Classification Results Using 70 Classifier Genes by SVM or Clustering

True Class (No. Samples)	No. Samples Classified as			Accuracy (%)	ROC Area
	Control	RDX	Cararyl		
SVM					
Control (161)	135	20	6	83.9	0.936
RDX (134)	14	100	20	74.6	0.856
Carbaryl (141)	6	20	115	81.6	0.913
Precision (%)	87.1	71.4	81.6		
Weighted average (436)	81.8 (precision)			79.5	0.904
Clustering [a]					
Control (161)	121	4	36	75.2	NA
RDX (134)	30	90	14	67.2	NA
Carbaryl (141)	26	12	103	73	NA
Precision (%)	68.4	84.9	63.2		
Weighted average (436)	70.9 (precision)			72.3	NA

Note. Confusion matrix of classification results obtained using the refined set of 70 classifier genes combined from the SVM- and the clustering-optimized gene sets. [a] ROC area was not computable with clustering.

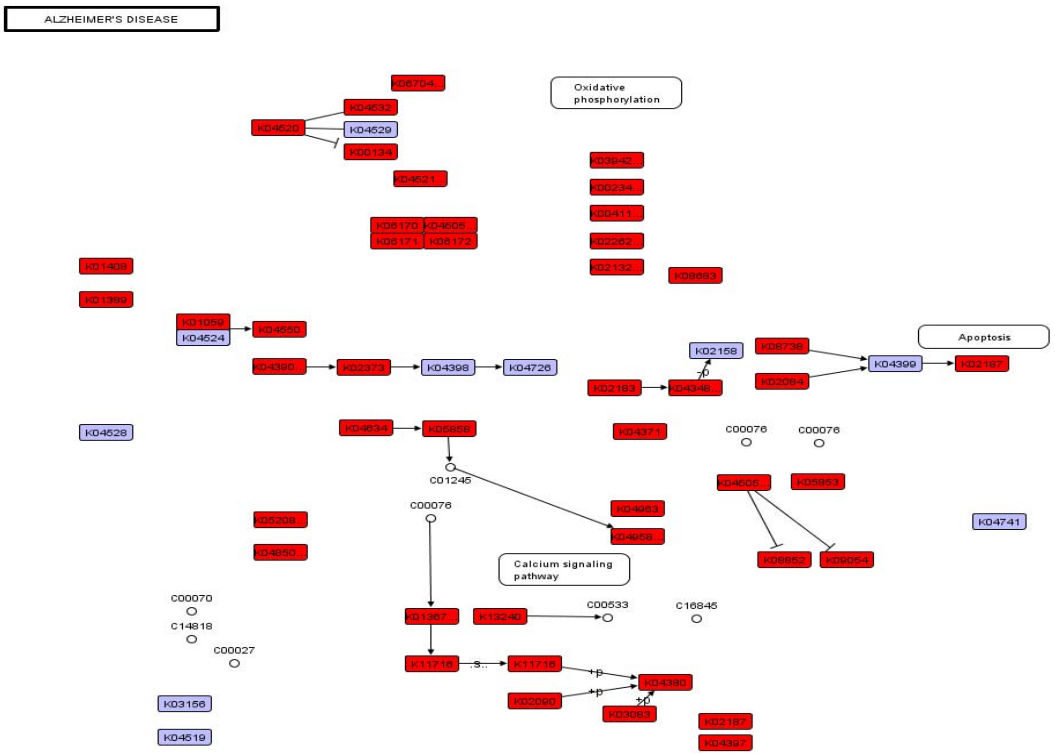

Figure 6.13. Reference pathway for Alzheimer's disease built by RefNet.

By comparing all the mapped earthworm genes in KEGG pathways with 2574 significantly differentially expressed genes, nine pathways were identified that are significantly affected by chemical treatments. The nine pathways are related to signaling and neurological functions. Table 6.10 summarized the selected 9 pathways and they are ordered by the number of differentially expressed genes found in mapped KEGG pathways. Then, the top two pathways, namely MAPK Signaling Pathway (Ko04010) and Huntington's disease pathway (Ko05016) were chosen to perform detailed analysis and sets of relevant genes were selected to reconstruct gene regulatory network using time-lagged DBN model. From Table 6.10, a total of 327 mapped earthworm genes were included in the MAPK Signaling Pathway and 181 unique KO orthologs in the KEGG database. That is, roughly one KO gene is matched by two earthworm genes. Due to the high computational costs and huge searching space of time-lagged DBN model, the set of

372 genes was difficult to accomplish and demanded high performance computing facility to model GRN. Therefore, a part of the MAPK pathway was selected to infer GRN, given current computing power. Figure 6.14 shows the reference networks for MAPK Signaling Pathway (6.14a) and Huntington's Disease Pathway (6.14b) built by RefNet.

Table 6.10

Summary of Nine Identified Significant Pathways

Pathway	Description	#KO in KEGG	#Probe Mapped in KEGG (#Probe Mapped if Evalue<10E-6)	#DEG in KEGG (in 2574g / in 9184g /in 1072g)	#DEG in KEGG (in 2574g / in 9184g) Evalue<10E-6
Ko04010	MAPK Signaling Pathway	181	327 (46)	26/71/15	5/9
Ko05016	Huntington's Disease	147	372 (141)	43/94/15	32/51
Ko04360	Axon Guidance	80	189 (15)	20/48/13	0/3
Ko05010	Alzheimer's Disease	140	349 (129)	44/95/13	29/46
Ko04141	Protein Processing in ER	137	409 (121)	25/81/12	6/20
Ko04110	Cell Cycle	103	233 (29)	17/60/11	4/10
Ko04740	Olfactory transduction	16	593 (12)	20/117/11	0/1
Ko04810	Regulation of actin Cytoskeleton	144	296 (47)	25/73/11	3/13
Ko05200	Pathways in Cancer	239	448 (32)	29/115/11	0/8

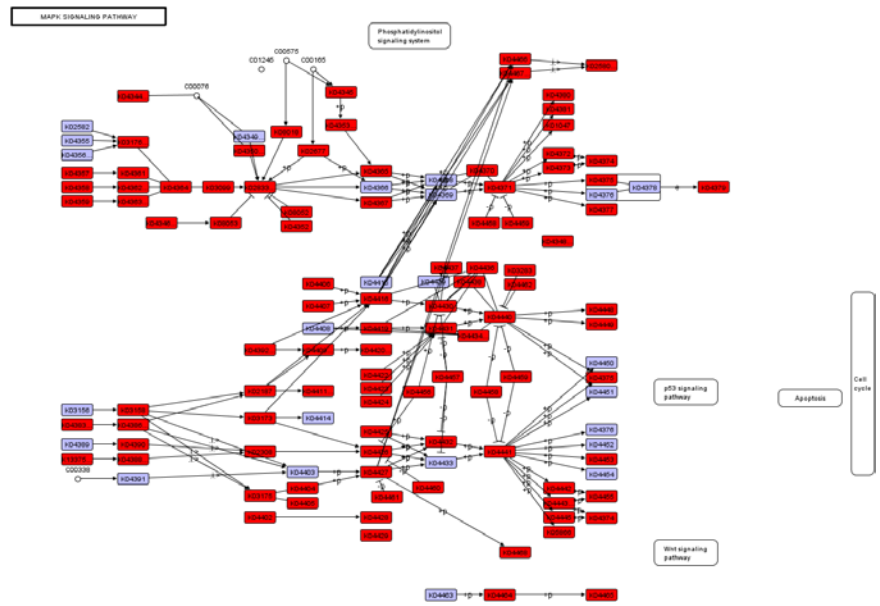

(a)

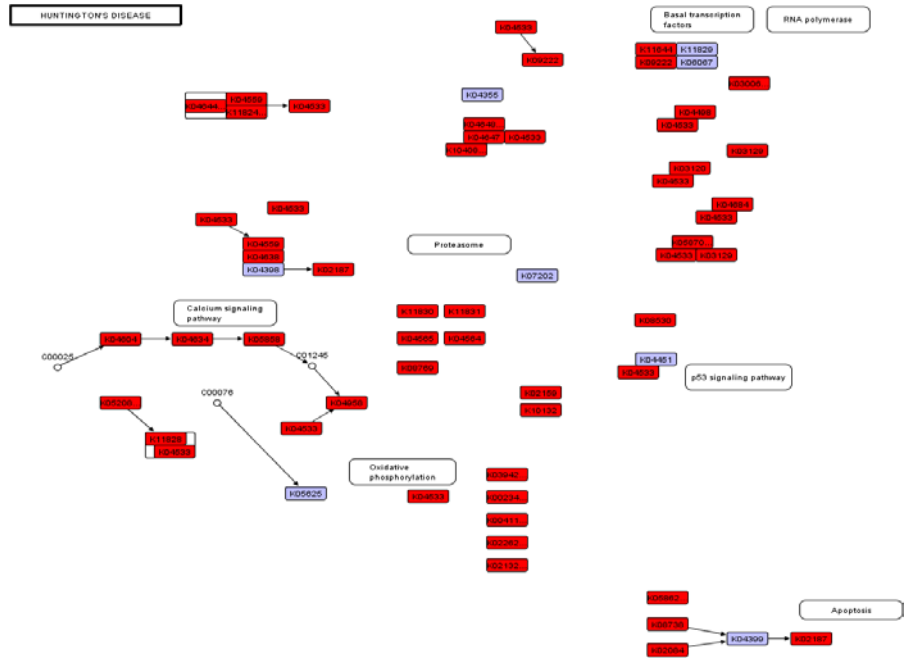

(b)

Figure 6.14. Reference pathways of (a) MAPK and (b) Huntington's disease built by RefNet.

Mitogen-activated protein (MAP) kinases are serine/threonine-specific protein kinases that respond to extracellular stimuli (mitogens, osmotic stress, heat shock and

proinflammatory cytokines) and regulate various cellular activities, such as gene expression, mitosis, differentiation, proliferation, and cell survival/apoptosis. ERK1 and ERK2 were the first of the ERK/MAP kinase subfamily to be cloned. Other related mammalian enzymes have been detected including: two ERK3 isoforms, ERK4, Jun N-terminal kinases/stress-activated protein kinases (JNK/SAPKs), p38/HOG, and p57 MAP kinases (38).

1. Extracellular signal-regulated kinases (ERK1, ERK2). The ERK1/2 (also known as classical MAP kinases) signaling pathway is preferentially activated in response to growth factors and phorbol ester (a tumor promoter), and regulates cell proliferation and cell differentiation.
2. C-Jun N-terminal kinases (JNKs), (MAPK8, MAPK9, MAPK10) also known as stress-activated protein kinases (SAPKs).
3. P38 isoforms. (p38-α (MAPK14), -β (MAPK11), -γ (MAPK12 or ERK6) and -δ (MAPK13 or SAPK4)) Both JNK and p38 signaling pathways are responsive to stress stimuli, such as cytokines, ultraviolet irradiation, heat shock, and osmotic shock, and are involved in cell differentiation and apoptosis.
4. ERK5. ERK5 (MAPK7), which has been found recently, is activated both by growth factors and by stress stimuli, and it participates in cell proliferation.
5. ERK3/4. ERK3 (MAPK6) and ERK4 (MAPK4) are structurally-related atypical MAPKs possessing SEG motifs in the activation loop and displaying major differences only in the C-terminal extension. ERK3 and ERK4 are primarily cytoplasmic proteins that bind, translocate, and activate MK5 (PRAK, MAPKAP5). ERK3 is unstable, unlike ERK4, which is relatively stable [178].

6. ERK7/8. (MAPK15) is the newest member of MAPKs and behaves like atypical MAPKs. It possesses a long C terminus similar to ERK3/4.

The JNK/SAPK pathway and p38 isoforms pathway are the mammalian ortholog of the yeast HOG kinase, which participate in a signaling cascade controlling cellular responses. Therefore, we choose these two parallel pathways to infer GRNs using 44K time-series earthworm microarray dataset. Based on the annotation information from NCBI, InterProScan and PIPA databases, a total of 38 genes related to the JNK/SAPK and p38 isoforms pathways were selected. Figure 6.16 contains the annotation information for the 38 genes from MAPK Signaling Pathway. Based on the MAPK pathway map from the KEGG database, a manually curated reference pathway using the 38 genes was constructed (Figure 6.15) and biologically significant genes were highlighted as red nodes.

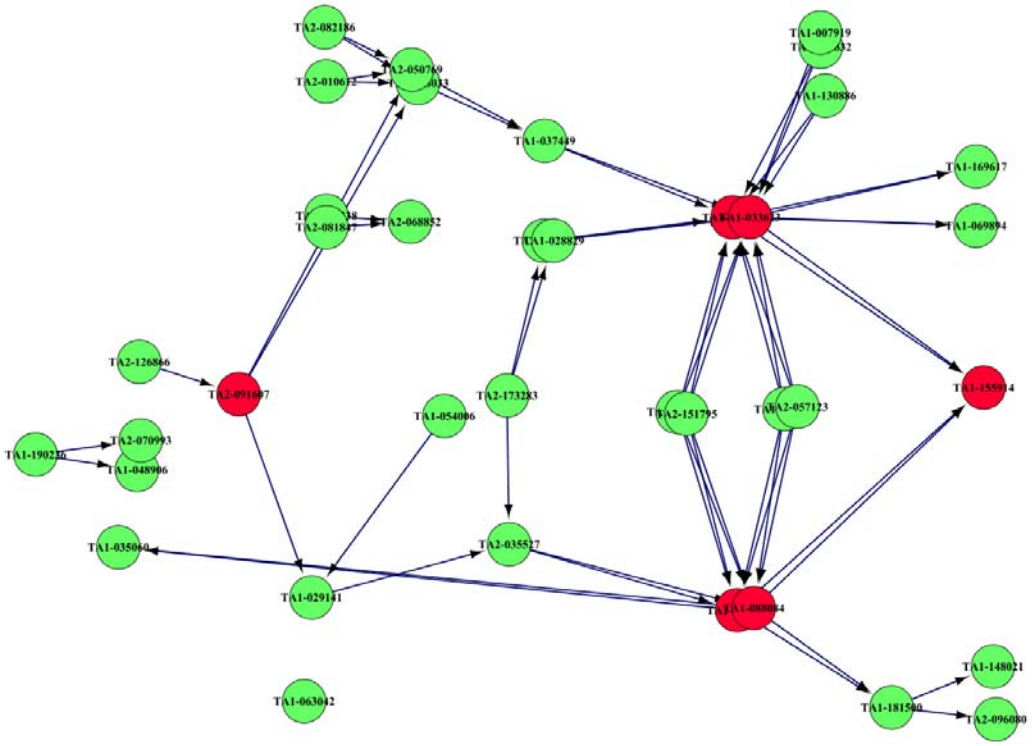

Figure 6.15. A curated reference network of 38 genes from MAPK Pathway.

probeid	koid	targetid	blastn_go	blastx_go	ips_go	pipa_go	evalue	sigevent
TA2-126866	K03158	SMcontig_53030					5.3	1
TA2-091607	K03173	SMcontig_40747	" Mus musculus Tnf rec	PREDICTED: similar to			1E-19	
TA1-007919	K03283	DQ286711.1					0	
TA1-107832	K03283	contig00900				Cytoplasmic	4.1	1
TA2-096080	K04374	contig26722		activating transcription fa			2E-12	
TA1-155914	K04375	contig07787				Cytoplasmic	2.3	
TA1-190236	K04383	EW1_F1P03_F07				Cytoplasmic	1.1	
TA2-070993	K04386	contig02072				Transmembrane Locati	1.1	2
TA1-048906	K04387	EB3O8BM02H1SF8				Cytoplasmic	6.8	
TA2-082186	K04406	EW1_F1P02_A02		fucolectin			1.4	
TA2-010612	K04407	contig14403			"""Molecular unctiofi:		0.37	2
TA1-177238	K04409	EB3ZX6E02JKG87				Transmembrane Locati	5.2	2
TA2-081847	K04410	EB3ZX6E02H35FR		unnamed protein produc		IPR017442;name kina	8E-07	
TA1-158033	K04416	contig26439				Signal_peptide Locatio	2	
TA2-050769	K04416	SMcontig_340					2.6	
TA2-068852	K04421	SMcontig_39284					6.9	1
TA1-029141	K04426	contig15518	" Eisenia fetida evcp-1 g				5.2	2
TA1-063042	K04428	contig24900				Transmembrane Locati	1.9	
TA1-037449	K04430	SMcontig_16164					9.2	4
TA1-028829	K04431	EB3O8BM01BYSQT				Signal_peptide Locatio	1.8	1
TA2-059291	K04431	contig25936					3.1	1
TA2-035527	K04432	EB3O8BM02I9JL3				Cytoplasmic	4	
TA1-033623	K04440	contig24419				Cytoplasmic	1.3	
TA1-190111	K04440	SMcontig_1640					7	
TA1-088084	K04441	EB3O8BM02G38M8				Cytoplasmic	0.057	
TA1-015495	K04441	contig08069			Molecular Function: hyd		1.8	
TA1-181500	K04443	EB3ZX6E02JKLS7	" PREDICTED: Apis m	"PREDICTED: similar t		IPR015731;name MAP	2E-08	1
TA1-169617	K04448	contig02521				Cytoplasmic	1.1	
TA1-069894	K04449	SMcontig_24452		JunDLb			1E-08	
TA1-035060	K04453	contig00402		AGAP003177-PA		Transmembrane Locati	1E-19	
TA1-148021	K04455	EB3O8BM02I5ZVH				NULL;name SMALL F	0.002	2
TA1-054006	K04456	EB3ZX6E02HBMTJ	Corynebacterium ureal			Cytoplasmic	2.4	
TA2-173283	K04457	EB3ZX6E01EEPBN		PREDICTED: similar to		IPR015655;name PRO	6E-06	2
TA1-015759	K04458	EB3O8BM02JRER0				Cytoplasmic	3	
TA2-151795	K04458	SMcontig_61478					3.1	
TA1-203999	K04459	EW1_F1P02_E08		MGC84083 protein		Cytoplasmic	3E-34	
TA2-057123	K04459	EB3ZX6E01BHTE0		MGC79099 protein		NULL;name DUAL SP	6E-06	2
TA1-130886	K04462	contig29646				Transmembrane Locati	4.1	1

Figure 6.16. List of 38 genes from MAPK pathway for reconstruction of GRN.

Then, the time-lagged DBN model was used to infer 6 GRNs using the 38 genes for different chemical treatments and different stages. Figure 6.17 (a)-(f) are inferred GRNs of the 38 genes: (a) Control Exposure; (b) Carbaryl Exposure; (c) RDX Exposure; (d) Control Recovery; (e) Carbaryl Recovery; and (f) RDX Recovery. The nodes highlighted in red are biologically significant genes based on annotations from the KEGG database, while the green nodes are selected genes to model GRNs.

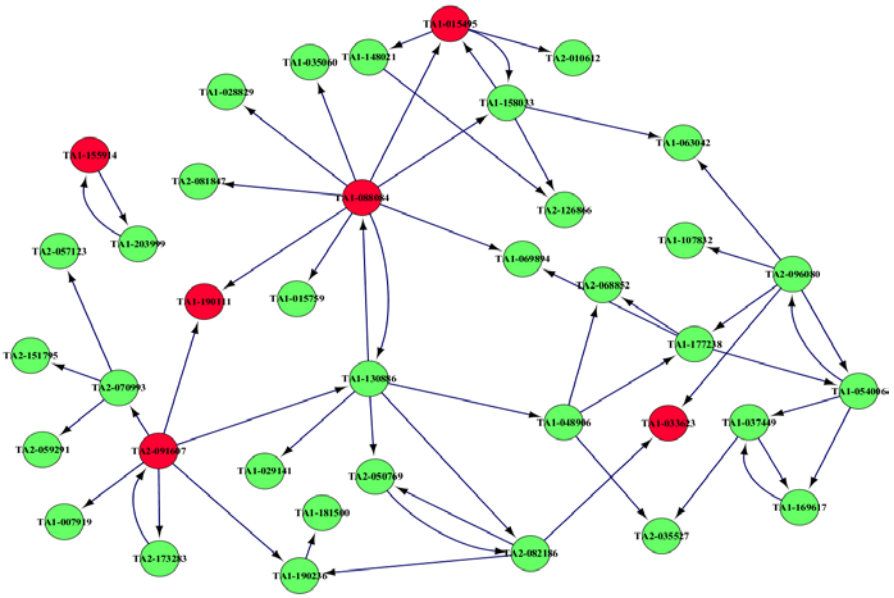

(a)

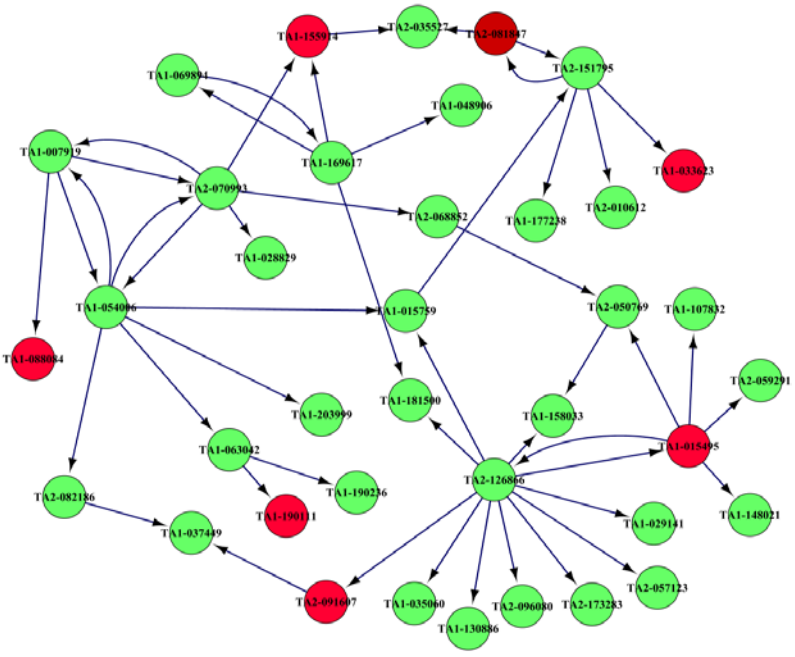

(b)

Figure 6.17. Inferred GRNs of 38 genes from MAPK pathway. (a)-(f) are inferred GRNs of the 38 genes: (a) Control Exposure; (b) Carbaryl Exposure; (c) RDX Exposure; (d) Control Recovery; (e) Carbaryl Recovery; and (f) RDX Recovery.

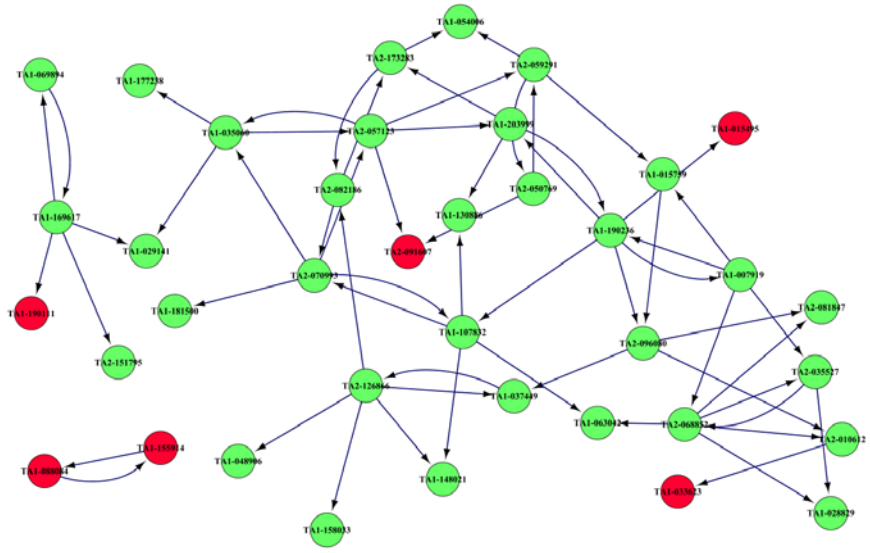

(c)

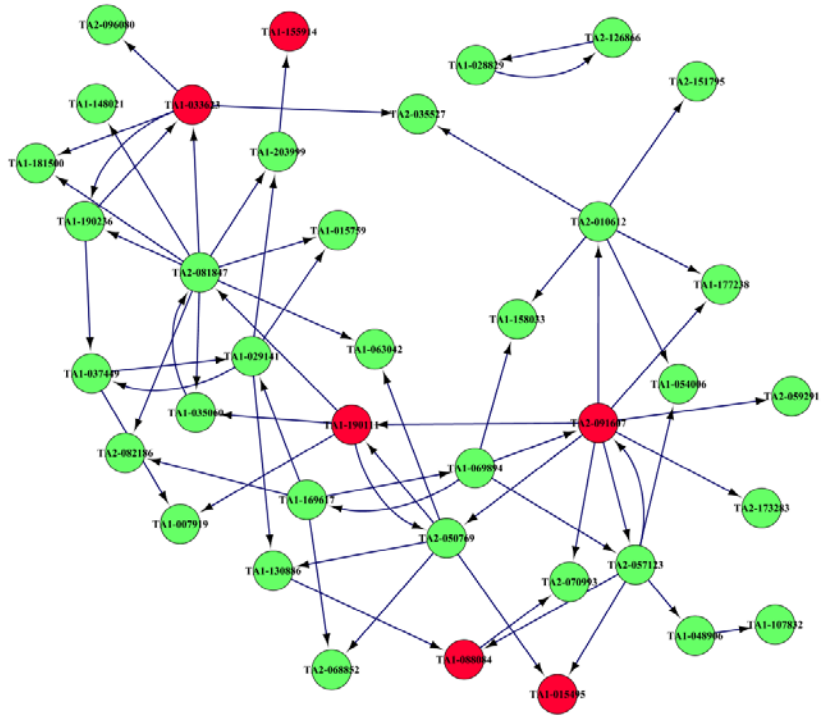

(d)

Figure 6.17. (continued).

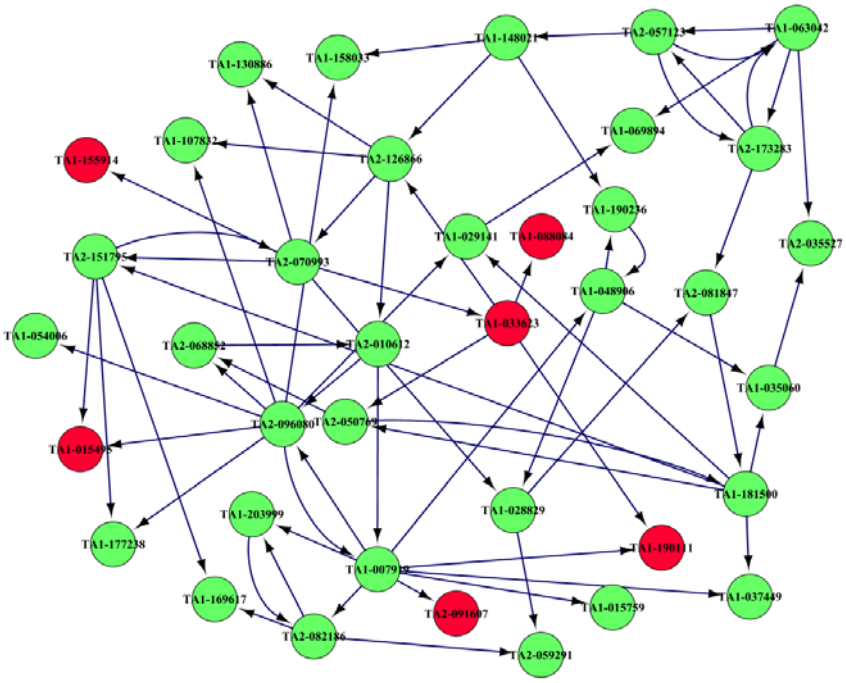

(e)

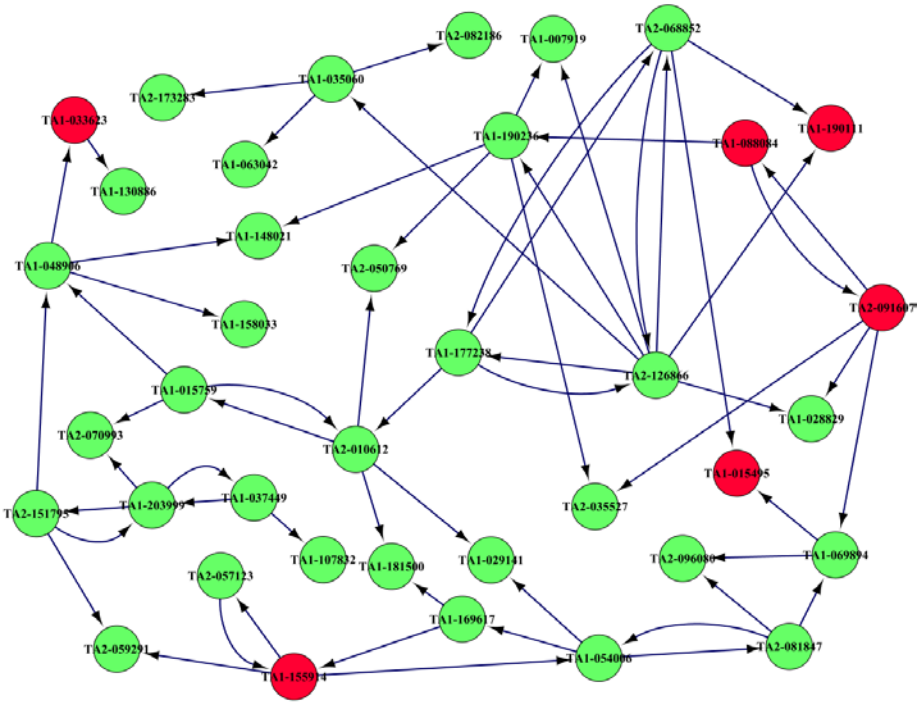

(f)

Figure 6.17. (continued).

Table 6.11 lists the number of inferred edges for each chemical treatment condition in either stage. By comparing these six constructed networks with the curated reference network, Figure 6.18 summarizes the common connections (edges) for the 6 GRNs, respectively.

Table 6.11

Summary of Inferred GRNs for MAPK Pathway by DBN Model

Sample	# Edges Inferred
Refnet	62
Control, Exposure	55
Carbaryl, Exposure	49
RDX, Exposure	61
Control, Recovery	63
Carbaryl, Recovery	69
RDX, Recovery	60

RefNet and Conexp			**RefNet and Conrec**	
TA1-015759	TA1-088084		TA2-010612	TA1-158033
TA1-088084	TA1-035060		TA2-057123	TA1-015495
TA2-082186	TA2-050769		TA2-057123	TA1-088084
			TA2-091607	TA2-050769
RefNet and Carexp			**RefNet and Carrec**	
TA2-126866	TA2-091607		TA1-190236	TA1-048906
TA2-151795	TA1-033623		TA2-151795	TA1-015495
RefNet and RDXexp			**RefNet and RDXrec**	
TA1-088084	TA1-155914		TA1-054006	TA1-029141
TA1-190111	TA1-169617		TA1-130886	TA1-033623
TA2-081847	TA2-068852		TA2-010612	TA2-050769
TA2-091607	TA2-050769			

Figure 6.18. Summary of common edges between six inferred GRNs with curated reference network, respectively.

From Figure 6.18 we can see that inferred GRN of control treatment in recovery stage have the maximum number of conserved connections with curated reference network. Table 6.12 summaries pairwise comparisons between six inferred GRNs by DBN in various treatment conditions and stages.

Table 6.12

Summary of Comparing Inferred GRNs in Three Treatment Conditions

Pair of GRNs	Common Connections	
Conexp and Conrec	TA1-088084	TA1-130886
	TA1-130886	TA1-029141
	TA1-130886	TA1-088084
	TA1-130886	TA2-050769
	TA1-155914	TA1-203999
	TA1-203999	TA1-155914
	TA2-091607	TA1-190111
	TA2-091607	TA2-070993
	TA2-091607	TA2-173283
	TA2-096080	TA1-033623
	TA2-173283	TA2-091607
Conexp and Carexp	TA1-015495	TA1-148021
	TA1-158033	TA2-126866
Conexp and RDXexp	TA1-148021	TA2-126866
	TA1-158033	TA2-126866
	TA2-070993	TA2-057123
Carexp and RDXexp	TA1-069894	TA1-169617
	TA1-169617	TA1-069894
	TA2-126866	TA1-158033
Conrec and Carrec	TA1-007919	TA1-037449
	TA2-082186	TA1-169617
	TA1-007919	TA1-190111
	TA2-050769	TA2-068852
	TA2-081847	TA1-181500
Conrec and RDXrec	TA2-010612	TA1-177238
	TA1-069894	TA2-091607
	TA1-028829	TA2-126866
Carrec and RDXrec	TA1-148021	TA1-190236

Huntington's Disease

Huntington's disease, chorea, or disorder (HD), is a neurodegenerative genetic disorder that affects muscle coordination and leads to cognitive decline and dementia. It typically becomes noticeable in middle age. HD is the most common genetic cause of abnormal involuntary writhing movements called chorea. The disease is caused by an autosomal dominant mutation on either of an individual's two copies of a gene called Huntingtin (Htt gene in KEGG pathway), which means that any child of an affected parent has a 50% risk of inheriting the disease. The Huntingtin gene normally provides the genetic information for a protein that is also called "Huntingtin." The mutation of the Huntingtin gene codes for a different form of the protein, whose presence results in gradual damage to specific areas of the brain.

All humans have the Huntingtin gene, which codes for the protein Huntingtin (Htt). Part of this gene is a repeated section called a trinucleotide repeat, which varies in length between individuals and may change length between generations. When the length of this repeated section reaches a certain threshold, it produces an altered form of the protein, called mutant Huntingtin protein (mHtt). The differing functions of these proteins are the cause of pathological changes which in turn cause the disease symptoms. The Huntington's disease mutation is genetically dominant and almost fully penetrant: mutation of either of a person's HTT genes causes the disease. It is not inherited according to sex, but the length of the repeated section of the gene, and hence its severity, can be influenced by the sex of the affected parent [179, 180].

By mapping the 44K earthworm genes to KEGG ortholog genes, a total of 372 transcripts were mapped in the KEGG Huntington's disease pathway and 43 of them are DEGs from the set of 2574 DEGs. Again, a part of the Huntington's disease pathway has

been selected and a set of 40 biological significant genes was used to infer GRNs under various circumstances. Figure 6.19 are the list of the 40 genes with their annotation information from NCBI, InterProScan and PIPA databases.

probeid	koid	targetid	blastn_go	blastx_go	ips_go	pipa_go	evalue	sigevent
TA1-110674	K00234	EB3ZX6E02F5UO2		hypothetical p			4E-12	2
TA1-124713	K00235	contig26540	" Dinoroseobacter shiba	unnamed prot		Transmembrane Locati	0	
TA1-167099	K00412	contig24442	" Lumbricus terrestris m	CYTB_1059		IPR005797;name yto	1E-27	2
TA1-080260	K00412	contig29848	" Tetraogallus tibetanus	CYTB_1059			6E-20	4
TA1-151920	K02084	SMcontig_61192		PREDICTED			0.025	
TA1-052474	K02127	SMcontig_36607		putative ATP			1E-24	
TA1-030538	K02128	EW2_R1P10_E09	" Ixodes pacificus clone	mitochondrial			3E-19	
TA1-185327	K02132	contig23278	Platynereis dumerilii ES	mitochondrial		"""IPR004100;name -	6E-12	3
TA1-056208	K02133	contig28741	Aedes aegypti ATP syr	hypothetical p		Signal_peptide Location	2E-29	1
TA2-021709	K02137	contig02700		ATP synthase	"""Molecular Function: e		2E-18	
TA2-141273	K02159	contig24085		bcl2-associat		IPR000712;name Bcl-2	0.00002	
TA1-204993	K02187	SMcontig_25193		GD24332			3.1	1
TA2-122460	K02266	contig24873		AGAP00085		Cytoplasmic	7E-31	
TA1-088917	K03129	SMcontig_12304					1.1	1
TA2-082037	K03940	contig25313	" Drosophila willistoni G	GH21035		Signal_peptide Location	0	1
TA2-144557	K03954	contig26178		GK14239		Cytoplasmic	9E-21	
TA1-062050	K04533	contig07159			"""Biological Process: pr	Cytoplasmic	0.37	
TA2-158820	K04533	SMcontig_41013					6.8	1
TA1-153843	K04564	contig28172	" Callinectes sapidus mit	AF264029_1		Cytoplasmic	0	
TA1-115451	K04565	EW2_R1P04_A07		SJCHGC056		Cytoplasmic	1E-08	1
TA2-084557	K04604	contig21397					5.2	
TA1-231349	K04634	contig26701				Cytoplasmic	5.2	3
TA1-023347	K04958	SMcontig_40677					1.4	
TA1-030855	K05208	contig24936				Transmembrane Locati	1.6	
TA2-161461	K05210	EW2_R1P09_G11					0.096	
TA1-043128	K05858	EB3ZX6E01DWRZB				NULL;name METHYL	0.28	
TA1-006086	K05862	contig02841	" Mus musculus voltage-	voltage-depe		NULL;name VOLTAG	6E-23	2
TA2-047090	K05863	contig10190	" Platynereis dumerilii pa	hypothetical p	"""Molecular unction:	Cytoplasmic	9E-27	2
TA2-000741	K05863	SMcontig_12917		SJCHGC027			5E-08	2
TA2-090805	K05864	contig13426				NULL;name TPR-like	0.043	
TA2-106990	K05870	EB3O8BM01D3TAQ				"""IPR003102;name	0.004	
TA2-079359	K08530	SMcontig_14039					6.9	
TA2-093641	K08738	SMcontig_79	" PREDICTED: Equus c	GJ16722			3E-28	
TA2-157407	K08769	SMcontig_21734		PREDICTED			0.015	2
TA1-093839	K09047	EW1_F2P20_G01	" Eisenia foetida mRNA			IPR001396;name Meta	1.1	
TA1-111713	K09048	SMcontig_8876					1.1	2
TA1-070849	K10132	EB3O8BM01A2T70				Cytoplasmic	0.62	1
TA1-138641	K11828	SMcontig_7092					0.82	
TA1-178978	K11830	SMcontig_45447	" Rattus norvegicus coil	PREDICTED			1.1	1
TA2-045009	K11831	contig23638				Signal_peptide Locatio	1.3	

Figure 6.19. List of 40 genes from huntington's disease pathway for reconstruction of GRN.

K04533 is the Htt gene, which could produce mHtt protein if it is mutant under certain condition. Figure 6.20 (a)-(f) are inferred GRNs using the selected 40 genes from the Huntington's disease pathway by time-lagged DBN model: (a) Control Exposure; (b) Carbaryl Exposure; (c) RDX Exposure; (d) Control Recovery; (e) Carbaryl Recovery; and (f) RDX Recovery.

Table 6.13 lists the number of inferred edges for each chemical treatment condition in either stage. Table 6.14 summaries pairwise comparison between six inferred GRNs by DBN in various treatment conditions and stages in the Huntington's disease Pathway.

Table 6.13

Summary of Inferred GRNs for Huntington's Disease Pathway by DBN Model

Sample	# Edges Inferred
Refnet	51
Control, Exposure	55
Carbaryl, Exposure	62
RDX, Exposure	64
Control, Recovery	64
Carbaryl, Recovery	68
RDX, Recovery	64

In summary, after exposure to sublethal concentrations of RDX or carbaryl, physiological recovery reflected in MGF conduction velocity correlates with both the number and the restored expression level of altered genes (results not shown). RDX and carbaryl affected different biological pathways and gene interactions in a network context, suggesting that they have different targets. Network landscape change caused by neurotoxicant RDX or carbaryl did not recover even after full physiological recovery.

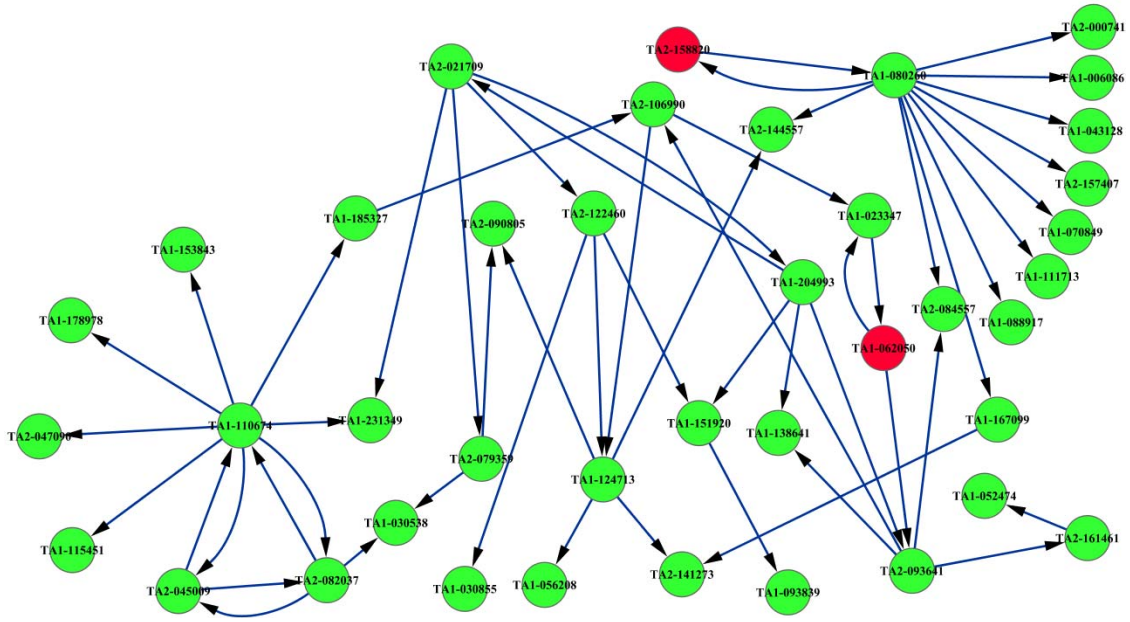

(a)

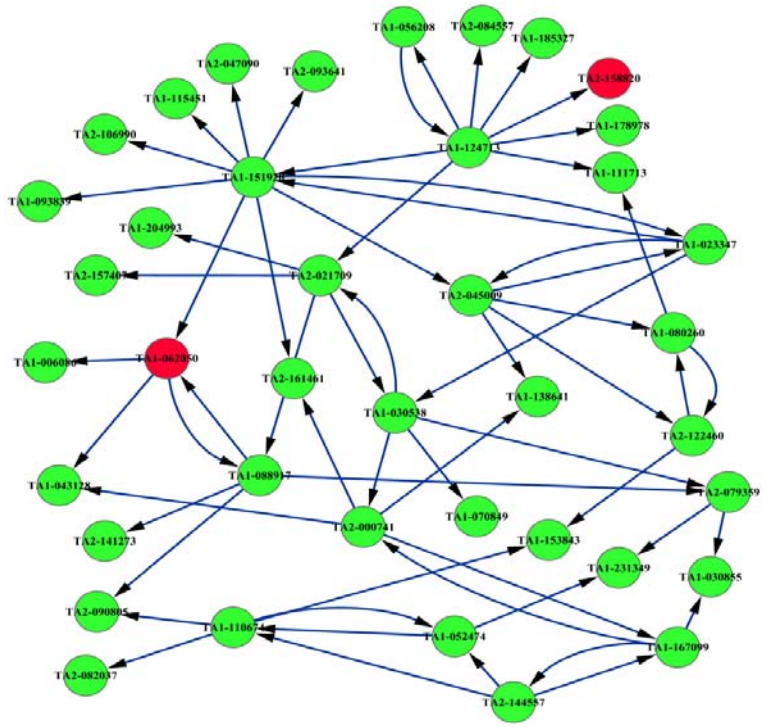

(b)

Figure 6.20. Inferred GRNs of 40 genes from Huntington's disease pathway. (a)-(f) are inferred GRNs using the selected 40 genes from Huntington's disease pathway by time-lagged DBN model: (a) Control Exposure; (b) Carbaryl Exposure; (c) RDX Exposure; (d) Control Recovery; (e) Carbaryl Recovery; and (f) RDX Recovery.

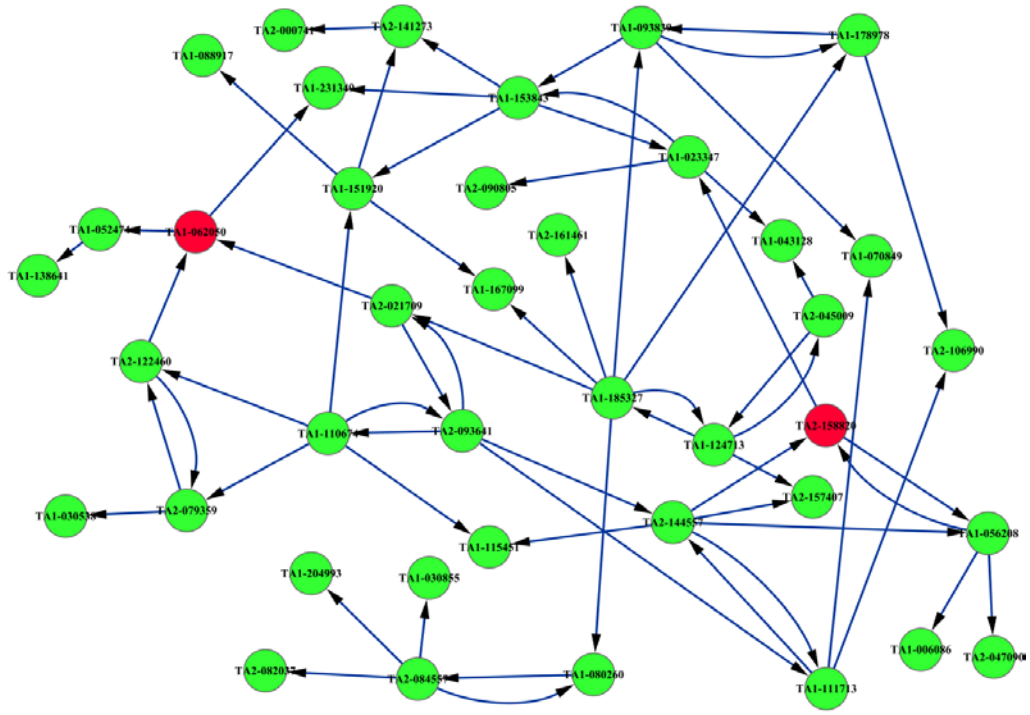

(c)

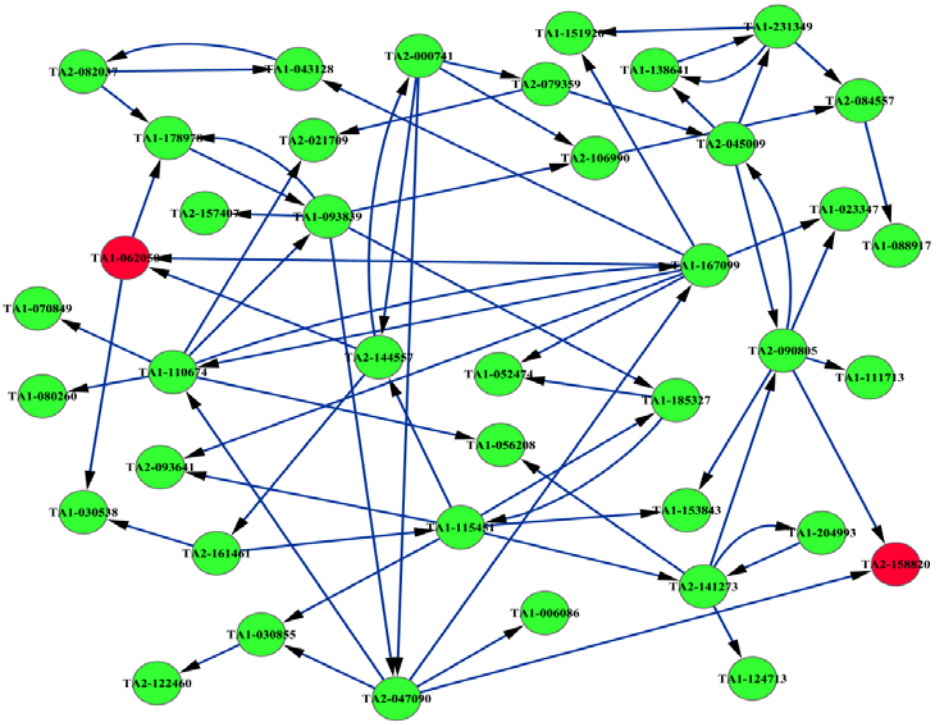

(d)

Figure 6.20. (continued).

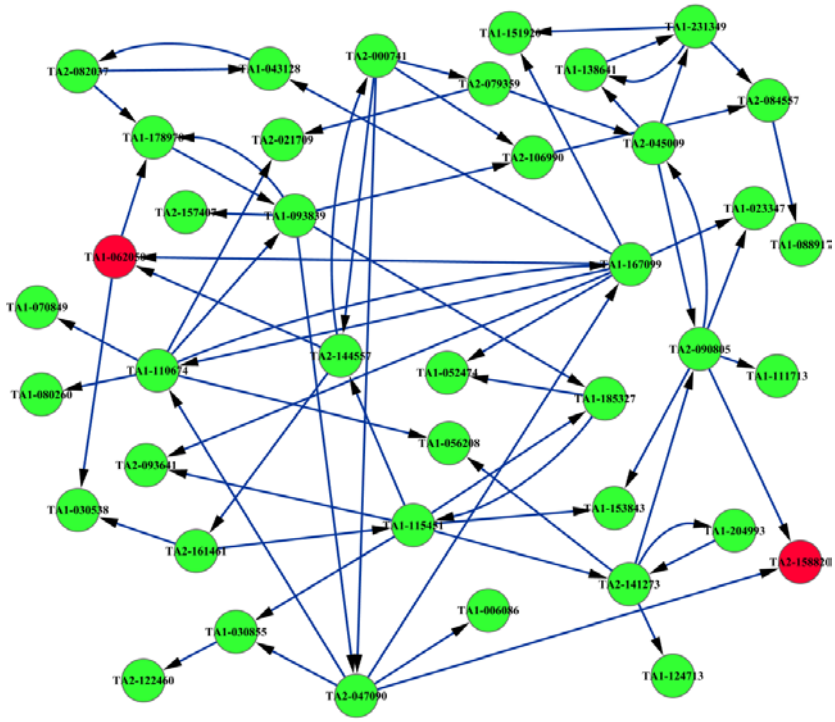

(e)

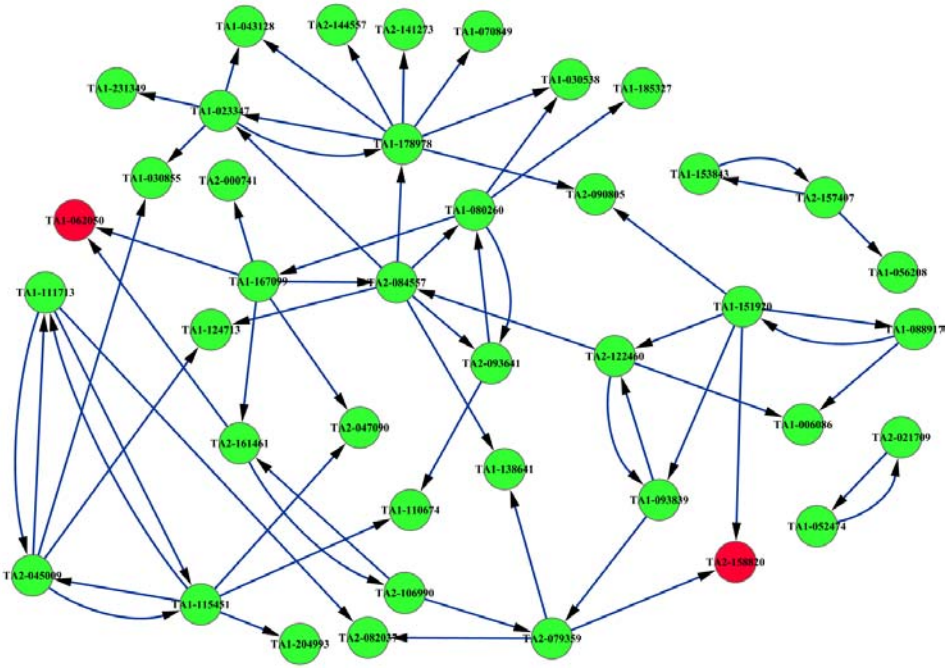

(f)

Figure 6.20. (continued).

Table 6.14

Summary of Comparing Inferred GRNs in Three Treatment Conditions

Pair of GRNs	Common Connections	
Conexp and Conrec	TA1-080260	TA1-111713
	TA1-080260	TA2-084557
	TA1-080260	TA2-158820
	TA1-110674	TA1-178978
	TA1-110674	TA1-185327
	TA1-110674	TA2-047090
	TA2-021709	TA1-231349
	TA2-093641	TA2-161461
	TA2-158820	TA1-080260
Conexp and Carexp	TA1-080260	TA1-111713
	TA1-110674	TA1-153843
	TA1-110674	TA2-082037
	TA1-124713	TA1-056208
	TA1-151920	TA1-093839
	TA1-204993	TA2-021709
	TA2-021709	TA1-204993
	TA2-079359	TA1-030538
	TA2-082037	TA1-110674
Conexp and RDXexp	TA1-080260	TA2-084557
	TA1-110674	TA1-115451
	TA2-079359	TA1-030538
Carexp and RDXexp	TA1-030538	TA2-079359
	TA1-124713	TA1-185327
Conrec and Carrec	TA1-110674	TA1-056208
	TA2-047090	TA1-110674
	TA1-231349	TA1-151920
	TA2-141273	TA2-090805
Conrec and RDXrec	TA1-023347	TA1-043128
	TA1-111713	TA1-115451
	TA1-115451	TA1-111713
	TA1-115451	TA2-045009
	TA2-045009	TA1-115451
	TA2-084557	TA1-080260
Carrec and RDXrec	TA1-167099	TA1-062050
	TA1-167099	TA2-047090

CHAPTER VII

CONCLUSIONS

Summary and Conclusions

Gene Regulatory Networks (GRNs) provide integrated views of gene interactions that control biological processes. Reconstruction of GRNs from time-series microarray gene expression data is a very challenging problem for bioinformatics researchers. Although a number of computational models and algorithms have been developed to infer GRNs, there is no single outstanding approach that can model GRNs with the best performances for any given data set. Here, we have developed ISML and RefNet toolboxs that have shown promising potential in overcoming some of the difficulties in inference of GRNs and have had some novel biological discovery.

By applying ISML to two microarray datasets, we have identified and optimized small subsets of classifier/biomarker genes from high dimensional datasets and generated classification models of acceptable precision for multiple classes.

In the RefNet toolbox, we have developed a cyber-based integrated environment to (1) build reference GRN/Pathway for non-model organisms; (2) provide biological prior knowledge of GRN to improve computational models, (3) interpret and compare the GRNs built from computational models with wet-lab experiments; and (4) serve as a gene selection tool for GRN reconstruction. This tool was applied to the earthworm *Eisenia fetida*, an environmentally important species without a complete genome sequence and helped identify pathway-related genes from transcriptomic-wide transcripts.

By applying ISML, RefNet and time-lagged DBN to a time-course microarray dataset, GRNs were inferred for the exposure and the recovery phases of unexposed earthworms and earthworms exposed to RDX and carbaryl. Differences between these networks are

attributed to perturbations caused by chemical exposure. These differences warrant further biological experiments for validation and validated changes have the great potential of providing new clues to toxicity targets and modes of action (mechanisms).

Future Directions

There are several areas that we can extend the current work to in the future:

- Identification of exposure dose- and duration-specific classifier genes from the 15K earthworm multi-class microarray dataset. Instead of separating the biological samples into three classes of treatment types, they can be further classified into six classes: (1) Control day_0 & day_14; (2) Control day_4; (3) TNT day_0 & day_14; (4) TNT day_4; (5) RDX day_0 & day_14; (6) RDX day_4. Currently, we are investigating which factor (dose or exposure time) has more pronounced effects on the gene expression of biological samples.
- Many other biological interaction resources and databases may be incorporated in the RefNet toolbox. To integrate the organism specific reference pathways, genes and interaction relations in all organism-specific reference pathways will be merged to form a unified pathways graph. This graph contains the maximum (but, may be redundant or inaccurate) information extracted from the experimental validated pathways. The graph will be pruned based on the importance score of the nodes, which will be computed using a graph ranking algorithm, e.g. page rank algorithm. Different similarity metrics for comparing pathways can be tested to generate gene interaction relationships in pathway-pathway relationships for whole genome of query organism. Furthermore, to validate the pruned pathways, leave-one-out cross validation can be applied. For the eight model organisms, one can be used as query, and a pathway based on homologues search against the

other seven model organisms can be built. The number of genes and the number of interaction relations can be used to evaluate the accuracy and the precision of the proposed method. In addition, we can interpret and display the pathway in web-based Cytoscape and integrate confirmed prior interaction information to computational model. Meanwhile, the generated GRN can be used to develop a gene selection tool to generate a gene set for GRN reconstruction.

- Currently, I only used the time-lagged DBN model to reconstruct gene regulatory networks and only small parts of the constructed reference network by RefNet are reconstructed. I intend to try other computational approaches such as information theory based method (e.g., ARACNE), Probabilistic Boolean network model, or differential equations method to infer gene regulatory network using the same sets of genes from a specific pathway of interest. Based on the inferred networks from various methods, their performances such as precision, recall, and run time will be compared with current inferred results. Furthermore, I also plan to integrate results of different computational approaches by combining each inferred network with their performance/scores to generate a more reliable gene regulatory network. For example, certain connections may exist in the multiple GRNs inferred using different computational methods, and such connections are considered more reliable than others inferred by a single method.

REFERENCES

[1] Crick, F. (1970): Central Dogma of Molecular Biology. *Nature* **227**, 561-563.

[2] Bodenreider, O. (2004). The unified medical language system (umls): Integrating biomedical terminology. *Nucleic Acids Res*, **32** (Database issue):D267–D270.

[3] David P. Clark (2005). Molecular Biology (Understanding the Genetic Revolution), **Chapter 6**. *Elsevier academic press.*

[4] Adomas A, Heller G, Olson A, Osborne J, Karlsson M, Nahalkova J, Van Zyl L, Sederoff R, Stenlid J, Finlay R, Asiegbu FO (2008). Comparative analysis of transcript abundance in Pinus sylvestris after challenge with a saprotrophic, pathogenic or mutualistic fungus. *Tree Physiol.* **28** (6): 885–897.

[5] Pollack JR, Perou CM, Alizadeh AA, Eisen MB, Pergamenschikov A, Williams CF, Jeffrey SS, Botstein D, Brown PO (1999). Genome-wide analysis of DNA copy-number changes using cDNA microarrays. *Nat Genet* **23** (1): 41–46.

[6] Moran G, Stokes C, Thewes S, Hube B, Coleman DC, Sullivan D (2004). Comparative genomics using Candida albicans DNA microarrays reveals absence and divergence of virulence-associated genes in Candida dubliniensis. *Microbiology* **150** (Pt 10): 3363–3382.

[7] Kulesh DA, Clive DR, Zarlenga DS, Greene JJ (1987). Identification of interferon-modulated proliferation-related cDNA sequences. *Proc Natl Acad Sci USA* **84** (23): 8453–8457.

[8] Hacia JG, Fan JB, Ryder O, Jin L, Edgemon K, Ghandour G, Mayer RA, Sun B, Hsie L, Robbins CM, Brody LC, Wang D, Lander ES, Lipshutz R, Fodor SP, Collins FS (1999). Determination of ancestral alleles for human single-nucleotide polymorphisms using high-density oligonucleotide arrays. *Nat Genet* **22**: 164–167.

[9] Churchill, GA (2002). Fundamentals of experimental design for cDNA microarrays. *Nature genetics supplement* **32**: 490.

[10] Patterson, T.A., Lobenhofer, E.K., Fulmer-Smentek, S.B., Collins, P.J., Chu, T.M., Bao, W., Fang, H., Kawasaki, E.S., Hager, J., Tikhonova, I.R. *et al.* Performance comparison of one-color and two-color platforms within the MicroArray Quality Control (MAQC) project. *Nat Biotechnol*, **24**(9):1140-1150, 2006.

[11] Shi, L., Reid, L.H., Jones, W.D., Shippy, R., Warrington, J.A., Baker, S.C., Collins, P.J., de Longueville, F., Kawasaki, E.S., Lee, K.Y. *et al*. The MicroArray Quality Control (MAQC) project shows inter- and intraplatform reproducibility of gene expression measurements. *Nat Biotechnol*, **24**(9):1151-1161, 2006.

[12] Ben-Gal I., Shani A., Gohr A., Grau J., Arviv S., Shmilovici A., Posch S. and Grosse I. (2005), Identification of Transcription Factor Binding Sites with Variable-order Bayesian Networks, *Bioinformatics*, **21**(11): 2657-2666.

[13] Yuk Fai Leung and Duccio Cavalieri, Fundamentals of cDNA microarray data analysis. *TRENDS in Genetics* **19**(11), November 2003

[14] Priness I., Maimon O., Ben-Gal I. (2007), Evaluation of Gene-Expression Clustering by Mutual Information Distance Measures, *BMC Bioinformatics*, *8(1)*:111.

[15] Wei C, Li J, Bumgarner RE. (2004). Sample size for detecting differentially expressed genes in microarray experiments. *BMC Genomics* **5** (1): 87.

[16] Emmert-Streib, F. and Dehmer, M. (2008). Analysis of Microarray Data A Network-Based Approach. *Wiley-VCH*.

[17] Wouters L, Gõhlmann HW, Bijnens L, Kass SU, Molenberghs G, Lewi PJ (2003). Graphical exploration of gene expression data: a comparative study of three multivariate methods. *Biometrics* **59** (4): 1131–1139.

[18] Yang Y, Adelstein SJ, Kassis AI (2009) Target discovery from data mining approaches. *Drug Discov Today* **14**: 147–154.

[19] Huang LT (2009) An integrated method for cancer classification and rule extraction from microarray data. *J Biomed Sci* **16**: 25.

[20] Powell WB (2007) Approximate Dynamic Programming: Solving the Curse of Dimensionality. Hoboken, *NJ: Wiley*.

[21] Trevino V, Falciani F (2006) GALGO: an R package for multivariate variable selection using genetic algorithms. *Bioinformatics* **22**: 1154–1156.

[22] Shmulevich I., E.R. Dougherty, K. Seungchan, W. Zhang (2002). Probabilistic Boolean networks: a rule-based uncertainty model for gene regulatory networks. *Bioinformatics*, **18**(2): 261–274.

[23] Shmulevich I., Dougherty E. R. and Zhang W (2002). Gene perturbation and intervention in probabilistic Boolean networks. *Bioinformatics*, **18** (10):1319-1331.

[24] X. Zhou, X. Wang, and E. R. Dougherty (2003): Construction of genomic networks using mutual information clustering and reversible-jump Markov-Chain-Monte-Carlo predictor design. *Signal Processing*, **83**(4), pp. 745--761.

[25] Dougherty, E. R., Kim, S. and Chen, Y (2000). Coefficient of determination in nonlinear signal processing. *Signal Processing*, **80**:10, pp. 2219-2235. 16.

[26] N. Friedman, K. Murphy, S (1998). Russell: Learning the structure of dynamic probabilistic networks. *Proceedings of the Fourteenth Conference on Uncertainty in Artificial Intelligence (UAI)*, 139–147.

[27] J. Yu, V. Smith, P. Wang, A. Hartemink and E Jarvis (2004). Advances to Bayesian network inference for generating causal networks from observational biological data. *Bioinformatics* **20**: 3594-603.

[28] M. Zou and S. D. Conzen (2005). A new dynamic Bayesian network (DBN) approach for identifying gene regulatory networks from time course microarray data. *Bioinformatics* **21**(1): 71-79.

[29] Perrin BE, Ralaivola L et al (2003). Gene networks inference using dynamic Bayesian networks. *Bioinformatics,* **19** Suppl 2:II138-II148.

[30] Zhengzheng Xing, Dan Wu (2006): Modeling Multiple Time Units Delayed Gene Regulatory Network Using Dynamic Bayesian Network. *ICDM Workshops,* 190-195.

[31] Zhang, L., Samaras, D., Alia-Klein, N., Volkow, N., and Goldstein, R (2006). Modeling neuronal interactivity using dynamic Bayesian networks. *Advances in Neural Information Processing Systems **18.*** Eds. Y. Weiss and B. Scholkopf, and J. Platt. Cambridge, *MA: MIT Press*.

[32] Li P, Zhang C, Perkins E, Gong P, Deng Y. Comparison of probabilistic boolean network and dynamic bayesian network approaches for inferring gene regulatory networks. *BMC Bioinformatics.* 2007;**8**(Suppl 7):S13.

[33] Affymetrix: http://www.affymetrix.com/index.affx

[34] Lausted C et al. (2004). POSaM: a fast, flexible, open-source, inkjet oligonucleotide synthesizer and microarrayer. *Genome Biology* **5** (8): R58.

[35] Nagaraj SH, Gasser RB, Ranganathan S (Jan 2007). A hitchhiker's guide to expressed sequence tag (EST) analysis. *Brief. Bioinformatics* **8** (1): 6–21.

[36] Bammler T, Beyer RP; Consortium, Members of the Toxicogenomics Research; Kerr, X; Jing, LX; Lapidus, S; Lasarev, DA; Paules, RS; Li, JL et al. (2005). Standardizing global gene expression analysis between laboratories and across platforms. *Nat Methods* **2** (5): 351–356.

[37] Pease AC, Solas D, Sullivan EJ, Cronin MT, Holmes CP, Fodor SP. (1994). Light-generated oligonucleotide arrays for rapid DNA sequence analysis. *PNAS* **91** (11): 5022–5026.

[38] Nuwaysir EF, Huang W, Albert TJ, Singh J, Nuwaysir K, Pitas A, Richmond T, Gorski T, Berg JP, Ballin J, McCormick M, Norton J, Pollock T, Sumwalt T, Butcher L, Porter D, Molla M, Hall C, Blattner F, Sussman MR, Wallace RL, Cerrina F, Green RD. (2002). Gene expression analysis using oligonucleotide arrays produced by maskless photolithography. *Genome Res* **12** (11): 1749–1755.

[39] D. J. Duggan, M. Bittner, Y. Chen, P. Meltzer and J. M. Trent (1999). Expression profiling using cDNA microarrays. *Nature Genetics*, **21**(1 Suppl.):10–14.

[40] Y. H. Yang, S. Dudoit, P. Luu and T. P. Speed. Normalization for cDNA Microarray Data. *SPIE BiOS* 2001, San Jose, California, January 2001.

[41] Yang, Y.H. et al (2002). Normalization for cDNA microarray data: a robust composite method addressing single and multiple slide systematic variation. *Nucleic Acids Res.* **30**, e15.

[42] Yang, I.V. et al (2002). Within the fold: assessing differential expression measures and reproducibility in microarray assays. *Genome Biol* **3**, research0062.1–0062.12.

[43] Cleveland, W.S (1979). Robust locally weighted regression and smoothing scatterplots. *J. Amer. Stat. Assoc*. **74**, 829–836.

[44] Olga Troyanskaya, Michael Cantor, Gavin Sherlock, Pat Brown, Trevor Hastie, Robert Tibshirani, David Botstein, and Russ B. Altman, Missing value estimation methods for DNA microarrays. *Bioinformatics* (2001) **17**(6): 520-525.

[45] Alter,O., Brown,P.O. and Botstein,D. (2000) Singular value decomposition for genome-wide expression data processing and modeling. *Proc. Natl Acad. Sci. USA*, **97**, 10101–10106.

[46] Anderson,T.W. (1984) An Introduction to Multivariate Statistical Analysis. *Wiley, New York.*

[47] Golub,G.H. and Van Loan,C.F. (1996) Matrix Computations. *Johns Hopkins University Press, Baltimore, MD.*

[48] Eisen, M.B., Spellman, P.T., Brown, P.O (1998). Cluster analysis and display of genome-wide expression patterns. *Proc. Natl Acad. Sci. USA* **95,** 14863-14868.

[49] Wen, X., Fuhrman, S., Michaels, G.S., Carr, D.B., Smith, S., Barker, J.L. & Somogy, R (1998). Large-scale temporal gene expression mapping of central nervous system development. *Proc. Natl Acad. Sci. USA* **95**, 334–339.

[50] Tamayo, P. *et al* (1999). Interpreting patterns of gene expression with self-organizing maps: methods and application to hematopoietic differentiation. *Proc. Natl Acad. Sci. USA* **96**, 2907–2912.

[51] Quackenbush, J (2002). Microarray data normalization and transformation. *Nature Genetics* **32**, 496-501.

[52] Somorjai R, et al. Class prediction and discovery using gene microarray and proteomics mass spectroscopy data: curses, caveats, cautions. *Bioinformatics* 2003;**19**:1484-1491.

[53] Alon U, et al. Broad patterns of gene expression revealed by clustering analysis of tumor and normal colon tissues probed by oligonucleotide arrays. *Proc. Nat. Acad. Sci. USA* 1999;**96**:6745-6750

[54] Ben-Dor A, et al. Tissue classification with gene expression profiles. *J. Comput. Biol.* 2000;**7**:559-584

[55] Golub T, et al. Molecular classification of cancer: class discovery and class prediction by gene expression monitoring. *Science* 1999;**286**:531-537

[56] Ross D, et al. Systematic variation in gene expression patterns in human cancer cell lines. *Nat. Genet.* 2000;**24**:227-234

[57] Jafari P, Azuaje F. An assessment of recently published gene expression data analyses: reporting experimental design and statistical factors. *BMC Med. Inform. Decis. Mak.* 2006;**6**:27.

[58] Yvan Saeys, Iñaki Inza, and Pedro Larrañaga, A review of feature selection techniques in bioinformatics. *Bioinformatics* (2007) **23**(19): 2507-2517.

[59] Dudoit S, et al. Comparison of discriminant methods for the classification of tumors using gene expression data. *J. Am. Stat. Assoc* 2002;**97**:77-87.

[60] Lee J, et al. An extensive comparison of recent classification tools applied to microarray data. *Comput. Stat. and Data Anal.* 2005;**48**:869-885.

[61] Li L, et al. Applications of the GA/KNN method to SELDI proteomics data. *Bioinformatics* 2004;**20**:1638-1640.

[62] Statnikov A, et al. A comprhensive evaluation of multicategory classification methods for microarray gene expression cancer diagnosis. *Bioinformatics* 2005;**21**:631-643.

[63] Ben-Dor A, et al. Tissue classification with gene expression profiles. *J. Comput. Biol.* 2000;**7**:559-584.

[64] Thomas J, et al. An efficient and robust statistical modeling approach to discover differentially expressed genes using genomic expression profiles. Genome Res. 2001;11:1227-1236.

[65] Newton M, et al. On differential variability of expression ratios: improving statistical inference about gene expression changes from microarray data. *J. Comput. Biol.* 2001;**8**:37-52.

[66] Bø T, Jonassen I. New feature subset selection procedures for classification of expression profiles. *Genome Biol.* 2002;**3**.

[67] Wang Y, et al. Gene selection from microarray data for cancer classification–a machine learning approach. *Comput. Biol. Chem.* 2005;**29**:37-46.

[68] Yeoh E, et al. Classification, subtype discovery, and prediction of outcome in pediatric lymphoblastic leukemia by gene expression profiling. *Cancer Cell* 2002;**1**:133-143.

[69] Gevaert O, et al. Predicting the prognosis of breast cancer by integrating clinical and microarray data with Bayesian networks. *Bioinformatics* 2006;**22**:e184-e190.

[70] Mamitsuka H. Selecting features in microarray classification using ROC curves. *Pattern Recognit.* 2006;**39**:2393-2404.

[71] Xing EP, et al. Feature selection for high-dimensional genomic microarray data. *Proceedings of the Eighteenth International Conference on Machine Learning.* 2001. pp. 601-608.

[72] Blanco R, et al. Gene selection for cancer classification using wrapper approaches. *Int. J. Pattern Recognit. Artif. Intell.* 2004;**18**:1373-1390.

[73] Jirapech-Umpai T, Aitken S. Feature selection and classification for microarray data analysis: evolutionary methods for identifying predictive genes. *BMC Bioinformatics* 2005;**6**:148.

[74] Li L, et al. Gene selection for sample classification based on gene expression data: study of sensitivity to choice of parameters of the GA/KNN method. *Bioinformatics* 2001;**17**:1131-1142.

[75] Ooi C, Tan P. Genetic algorithms applied to multi-class prediction for the analysis of gene expression data. *Bioinformatics* 2003;**19**:37-44.

[76] Inza I, et al. Filter versus wrapper gene selection approaches in DNA microarray domains. *Artif. Intell. Med*. 2004;**31**:91-103.

[77] Xiong M, et al. Biomarker identification by feature wrappers. *Genome Res.* 2001;**11**:1878-1887.

[78] Segal, E., Shapira, M., Regev, A., Pe'er, D., Botstein, D., Koller, D., and Friedman, N (2003). Module networks: identifying regulatory modules and their condition-specific regulators from gene expression data. *Nat. Genet*. **34**, 166-176.

[79] Gardner, T. S., di Bernardo, D., Lorenz, D., and Collins, J. J. (2003). Inferring genetic networks and identifying compound mode of action via expression profiling. *Science* **301**, 102-105.

[80] Steuer, R., Kurths, J., Daub, C.O., Weise, J., Selbig, J (2002). The mutual information: detecting and evaluating dependencies between variables. *Bioinformatics* **18** (Suppl 2), S231–S240.

[81] Butte, A., Kohane, I (2000). Mutual information relevance networks: Functional genomics clustering using pairwise entropy measurements. *Proceeding of the Pacific Symposium on Biocomputing*, pp. 418–429.

[82] Basso, K., Margolin, A.A., Stolovitzky, G., Klein, U., Dalla-Favera (2005). Reverse engineering of regulatory networks in human B cells. *Nat. Genet* **37**, 382–390.

[83] Opgen-Rhein, R., Strimmer, K (2007). From correlation to causation networks: a simple approximate learning algorithm and its application to high-dimensional plant gene expression data. *BMC Syst. Biol*. **1**, 37.

[84] W. Zhao, E. Serpedin, and E. R. Dougherty (2008). Inferring connectivity of genetic regulatory networks using information-theoretic criteria," *IEEE/ACM Transactions on Computational Biology and Bioinformatics*, vol. **5**, no. 2, pp.262-274.

[85] Huang S (1999). Gene expression profiling, genetic networks and cellular states: An integrating concept for tumorigenesis and drug discovery. *Journal of Molecular Medicine*, **77**:469-480.

[86] Shmulevich I, Gluhovsky I, Hashimoto RF, Dougherty ER, Zhang W (2003). Steady-state analysis of genetic regulatory networks modeled by probabilistic Boolean networks. *Comparative and Functional Genomics*, **4**:601-608.

[87] Shmulevich I., Dougherty R., Zhang W (2002). From Boolean to Probabilistic Boolean Networks as Models of Genetic Regulatory Networks. *Proceeding of the IEEE*, **90**(11), 1778-1792.

[88] H. Lähdesmäki, I. Shmulevich, and O. Yli-Harja (2003). On Learning Gene **52**, pp. 147 167.

[89] Voit, E.O (2000). Computational analysis of biochemical systems: a practical guide for biochemists and molecular biologists. Cambridge University Press, Cambridge, New York.

[90] De Jong, H (2002). Modeling and simulation of genetic regulatory systems: a literature review. *J. Comput. Biol.* **9**, 67–103.

[91] P. Smolen, D.A. Baxter, and J.H. Byrne (2000). Modeling transcriptional control in gene networks: Methods, recent results, and future directions. *Bulletin of Mathematical Biology*, **62**:247_292.

[92] H.D. Landahl (1969). Some conditions for sustained oscillations in biochemical chaines. *Bulletin of Mathematical Biophysics*, **31**:775_787.

[93] Spieth, C., Hassis, N., Streichert, F (2006). Comparing mathematical models on the problem of network inference. In: *Proceeding of the 8th Annual Conference on Genetic and evolutionary computation (GECCO 2006)*,Washington, USA, pp. 279–285.

[94] N. Friedman, et al (2000) Using Bayesian Networks to Analyze Expression Data. *Journal of Computational Biology* **7**(3-4): 601-620.

[95] N. Dojer, et al (2006). Applying dynamic Bayesian networks to perturbed gene expression data. BMC *Bioinformatics* **7**(1): 249.

[96] H. Lahdesmki, S. Hautaniemi, I. Shmulevich, O.Yli-Hrja (2006): Relationships between probabilistic Boolean networks and dynamic Bayesian networks as models of gene regulatory networks. *Signal Processing,* volume **86**, issue 4, 814 - 834.

[97] Lockhart, D. J. and Winzeler, E. A. (2000). Genomics, gene expression and DNA arrays. *Nature*, **405**(6788):827–836.

[98] Ankley GT, Daston GP, Degitz SJ, Denslow ND, Hoke RA, et al. (2006) Toxicogenomics in regulatory ecotoxicology. *Environ Sci Technol* **40**: 4055–4065.

[99] Falciani F, Diab AM, Sabine V, Williams TD, Ortega F, et al. (2008) Hepatic transcriptomic profiles of European flounder (*Platichthys flesus*) from field sites and computational approaches to predict site from stress gene responses following exposure to model toxicants. *Aquat Toxicol* **90**: 92–101.

[100] Nota B, Verweij RA, Molenaar D, Ylstra B, van Straalen NM, et al. (2010) Gene expression analysis reveals a gene set discriminatory to different metals in soil. *Toxicol Sci* **115**: 34–40.

[101] Powell WB (2007) Approximate Dynamic Programming: Solving the Curse of Dimensionality. *Hoboken, NJ: Wiley.*

[102] Trevino V, Falciani F (2006) GALGO: an R package for multivariate variable selection using genetic algorithms. *Bioinformatics* **22**: 1154–1156.

[103] Simon R, Lam A, Li MC, Ngan M, Menenzes S, et al. (2007) Analysis of Gene Expression Data Using BRB-Array Tools. *Cancer Inform* **3**: 11–17.

[104] Horng J, Wu L, Liu B, Kuo J, Kuo W, et al. (2009) An expert system to classify microarray gene expression data using gene selection by decision tree. *Expert Systems with Applications* **36**: 9072–9081.

[105] Tan PJ, Dowe DL, Dix TI (2007) Building classification models from microarray data with tree-based classification algorithms. In: Orgun MA, Thornton J, editors. Advances in Artificial Intelligence. *Berlin, Heidelberg: Springer-Verlag*. pp. 589–598.

[106] Abeel T, Helleputte T, Van de PY, Dupont P, Saeys Y (2010) Robust biomarker identification for cancer diagnosis with ensemble feature selection methods. *Bioinformatics* **26**: 392–398.

[107] Frank E, Hall M, Trigg L, Holmes G, Witten IH (2004) Data mining in bioinformatics using Weka. *Bioinformatics* **20**: 2479–2481.

[108] Signal detection theory and ROC analysis in psychology and diagnostics: collected papers; *Swets*, 1996.

[109] Platt JC (1998) Fast training of support vector machines using sequential minimal optimization. In: Schoelkopf B, Burges CJC, Smola AJ, editors. Advances in Kernel Methods: Support Vector Learning. Cambridge, *MA: MIT Press*. pp. 185–208.

[110] Zhang C, Li P, Rajendran A, Deng Y, Chen D (2006) Parallelization of multicategory support vector machines (PMC-SVM) for classifying microarray data. *BMC Bioinformatics* **7**: Suppl 4S15.

[111] Statnikov A, Aliferis CF, Tsamardinos I, Hardin D, Levy S (2005) A comprehensive evaluation of multicategory classification methods for microarray gene expression cancer diagnosis. *Bioinformatics* 21: 631–643.

[112] McLachlan GJ, Chevelu J, Zhu J (2008) Correcting for selection bias via cross-validation in the classification of microarray data. In: Balakrishnan N, Pena E, Silvapulle MJ, editors. Beyond Parametrics in Interdisciplinary Research: Festschrift in Honor of Professor Pranab K. Sen. Institute of Mathematical Statistics. pp. 364–376.

[113] Salwinski L, Miller CS, Smith AJ, Pettit FK, Bowie JU, Eisenberg D. (2004) The Database of Interacting Proteins: 2004 update. *NAR* **32**:D449-51.

[114] Bader GD, Donaldson I, Wolting C, Ouellette BF, Pawson T, Hogue CW. BIND--The Biomolecular Interaction Network Database. *Nucleic Acids Res.* 2001;**29**(1):242–245.

[115] Stark C, Breitkreutz BJ, Reguly T, Boucher L, Breitkreutz A, Tyers M. BioGRID: a general repository for interaction datasets. *Nucleic Acids Res.* 2006;**34**(Database issue):D535–539.

[116] Ceol A, Chatr Aryamontri A, Licata L, Peluso D, Briganti L, Perfetto L, Castagnoli L, Cesareni G. MINT, the molecular interaction database: 2009 update. *Nucleic Acids Res.*2010;**38**(Database issue):D532–539.

[117] Keshava Prasad TS, Goel R, Kandasamy K, Keerthikumar S, Kumar S, Mathivanan S, Telikicherla D, Raju R, Shafreen B, Venugopal A. et al. Human Protein Reference Database--2009 update. *Nucleic Acids Res.* 2009;**37**(Database issue):D767–772.

[118] Lopes CT, Franz M, Kazi F, Donaldson SL, Morris Q, Bader GD. Cytoscape Web: an interactive web-based network browser. Bioinformatics. 2010 Jul 23.

[119] Avila-Campillo I, Drew K, Lin J, Reiss DJ, Bonneau R. BioNetBuilder: automatic integration of biological networks. Bioinformatics. 2007 Feb 1;23(3):392-3. Epub 2006 Nov 30.

[120] Konieczka JH, Drew K, Pine A, Belasco K, Davey S, Yatskievych TA, Bonneau R, Antin B. BioNetBuilder2.0: bringing systems biology to chicken and other model organisms. BMC Genomics. 2009 Jul 14;10 Suppl 2:S6.

[121] Xia T, Dickerson JA. OmicsViz: Cytoscape plug-in for visualizing omics data across species. Bioinformatics. 2008 Nov 1;24(21):2557-8. Epub 2008 Sep 8.

[122] Ferro A, Giugno R, Pigola G, Pulvirenti A, Skripin D, Bader GD, Shasha D. NetMatch: a Cytoscape plugin for searching biological networks. Bioinformatics. 2007 Apr 1;23(7):910-2.

[123] Kanehisa M, Goto S. KEGG: kyoto encyclopedia of genes and genomes. Nucleic Acids Res. 2000 Jan 1;28(1):27-30.

[124] Kelley BP, Yuan B, Lewitter F, Sharan R, Stockwell BR, Ideker T. PathBLAST: a tool for alignment of protein interaction networks. Nucleic Acids Res. 2004 Jul 1;32(Web Server issue):W83-8.

[125] Smith, Temple F.; and Waterman, Michael S. (1981). Identification of Common Molecular Subsequences. Journal of Molecular Biology 147: 195–197.

[126] Lipman, DJ; Pearson, WR (1985). Rapid and sensitive protein similarity searches. *Science* **227** (4693): 1435–41.

[127] Pearson, WR; Lipman, DJ (1988). Improved tools for biological sequence comparison. Proceedings of the National Academy of Sciences of the United States of America 85 (8): 2444–8. doi:10.1073/pnas.85.8.2444.

[128] Johnson M, Zaretskaya I, Raytselis Y, Merezhuk Y, McGinnis S, Madden TL. NCBI BLAST: a better web interface. *Nucleic Acids Res.* 2008;**36**:W5–W9.

[129] Ye J, McGinnis S, Madden TL. BLAST: improvements for better sequence analysis. Nucleic Acids Res. 2006;34:W6–W9.

[130] Needleman, Saul B.; and Wunsch, Christian D. (1970). "A general method applicable to the search for similarities in the amino acid sequence of two proteins". Journal of Molecular Biology 48 (3): 443–53.

[131] Paul D. Thomas, Michael J. Campbell, Anish Kejariwal, Huaiyu Mi, Brian Karlak, Robin Daverman, Karen Diemer, Anushya Muruganujan, Apurva Narechania. 2003. PANTHER: a library of protein families and subfamilies indexed by function. Genome Res., 13: 2129-2141.

[132] Christian Klukas and Falk Schreiber: Dynamic exploration and editing of KEGG pathway diagrams. Bioinformatics 2007 23: 344-350.

[133] Hu, Z. Mellor, Snitkin, S. E., & DeLisi, C. (2008). VisANT: an integrative framework for networks in systems biology, Briefings in Bioinformatics, 2008;9:317-325.

[134] Hu, Z., et al., (2009) VisANT 3.5: multi-scale network visualization, analysis and inference based on the gene ontology. 2009 37: W115-W121.

[135] P. Holleis, T. Zimmermann, D. Gmach, Drawing Graphs Within Graphs, Journal of Graph Algorithms and Applications, JGAA, Vol. 9, No. 1, pp. 7-18, 2005.

[136] Opgen-Rhein, R., Strimmer, K (2007). From correlation to causation networks: a simple approximate learning algorithm and its application to high-dimensional plant gene expression data. *BMC Syst. Biol*. **1**, 37.

[137] Kauffman SA (1969). Metabolic stability and epigenesis in randomly constructed genetic nets. *Journal of Theoretical Biology*, **9**:3273-3297.

[138] K. Glass and S. A. Kauffman (1973). The logical analysis of continuous, nonlinear biochemical control networks. *J. Theoret. Biol*., vol. **39**, pp. 103–129.

[139] S. A. Kauffman (1974): The large scale structure and dynamics of genetic control circuits: an ensemble approach. *J. Theoret. Biol.*, vol. **44**, pp. 167–190.

[140] Kim H, Lee JK, Park T (2007). Boolean networks using the chi-square test for inferring large-scale gene regulatory networks. *BMC Bioinformatics*, **8**:37.

[141] Antonov AV, Tetko IV, Mader MT, Budczies J, Mewes HW (2004) Optimization models for cancer classification: extracting gene interaction information from microarray expression data. Bioinformatics 20: 644–652.

[142] Chi JT, Rodriguez EH, Wang Z, Nuyten DS, Mukherjee S, et al. (2007) Gene expression programs of human smooth muscle cells: tissue-specific differentiation and prognostic significance in breast cancers. PLoS Genet 3: 1770–1784.

[143] Choi JK, Yu U, Yoo OJ, Kim S (2005) Differential coexpression analysis using microarray data and its application to human cancer. Bioinformatics 21: 4348–4355.

[144] Golub TR, Slonim DK, Tamayo P, Huard C, Gaasenbeek M, et al. (1999) Molecular classification of cancer: class discovery and class prediction by gene expression monitoring. Science 286: 531–537.

[145] Yang Y, Adelstein SJ, Kassis AI (2009) Target discovery from data mining approaches. Drug Discov Today 14: 147–154.

[146] Huang LT (2009) An integrated method for cancer classification and rule extraction from microarray data. J Biomed Sci 16: 25.

[147] Gong P, Guan X, Inouye LS, Pirooznia M, Indest KJ, et al. (2007) Toxicogenomic analysis provides new insights into molecular mechanisms of the sublethal toxicity of 2,4,6-trinitrotoluene in *Eisenia fetida*. Environ Sci Technol 41: 8195–8202.

[148] Gong P, Guan X, Inouye LS, Deng Y, Pirooznia M, et al. (2008) Transcriptomic analysis of RDX and TNT interactive sublethal effects in the earthworm *Eisenia fetida*. BMC Genomics 9: Suppl 1S15.

[149] Kuperman RG, Simini M, Siciliano SD, Gong P (2009) Effects of energetic materials on soil organisms. In: Sunahara GI, Lotufo GR, Kuperman RG, Hawari J, editors. Ecotoxicology of Explosives. Boca Raton, FL: CRC Press. pp. 35–76.

[150] Falciani F, Diab AM, Sabine V, Williams TD, Ortega F, et al. (2008) Hepatic transcriptomic profiles of European flounder (*Platichthys flesus*) from field sites and computational approaches to predict site from stress gene responses following exposure to model toxicants. Aquat Toxicol 90: 92–101.

[151] Nota B, Verweij RA, Molenaar D, Ylstra B, van Straalen NM, et al. (2010) Gene expression analysis reveals a gene set discriminatory to different metals in soil. Toxicol Sci 115: 34–40.

[152] Wang RL, Bencic D, Biales A, Lattier D, Kostich M, et al. (2008) DNA microarray-based ecotoxicological biomarker discovery in a small fish model species. Environ Toxicol Chem 27: 664–675.

[153] Ankley GT, Daston GP, Degitz SJ, Denslow ND, Hoke RA, et al. (2006) Toxicogenomics in regulatory ecotoxicology. Environ Sci Technol 40: 4055–4065.

[154] Moens LN, van der V, Van RP, Del-Favero J, De Coen WM (2006) Expression profiling of endocrine-disrupting compounds using a customized Cyprinus carpio cDNA microarray. Toxicol Sci 93: 298–310.

[155] Poynton HC, Zuzow R, Loguinov AV, Perkins EJ, Vulpe CD (2008) Gene expression profiling in Daphnia magna, part II: validation of a copper specific gene expression signature with effluent from two copper mines in California. Environ Sci Technol 42: 6257–6263.

[156] Svendsen C, Owen J, Kille P, Wren J, Jonker MJ, et al. (2008) Comparative transcriptomic responses to chronic cadmium, fluoranthene, and atrazine exposure in *Lumbricus rubellus*. Environ Sci Technol 42: 4208–4214.

[157] Gong P, Pirooznia M, Guan X, Perkins EJ (2010) Design, Validation and Annotation of Transcriptome-Wide Oligonucleotide Probes for the Oligochaete Annelid *Eisenia fetida*. PLoS ONE 5(12): e14266.

[158] Edgar R, Domrachev M, Lash AE (2002) Gene Expression Omnibus: NCBI gene expression and hybridization array data repository. Nucleic Acids Res 30: 207–210.

[159] Yu C, Zavaljevski N, Desai V, Johnson S, Stevens FJ, et al. (2008) The development of PIPA: an integrated and automated pipeline for genome-wide protein function annotation. BMC Bioinformatics 9: 52.

[160] Lu Y, Han J (2003) Cancer classification using expression data. Information Systems 28: 243–268.

[161] Yu L, Liu H (2004) Efficient feature selection via analysis of relevance and redundancy. Journal of Machine Learning Research 5: 1205–1224.

[162] Boutros PC, Okey AB (2005) Unsupervised pattern recognition: an introduction to the whys and wherefores of clustering microarray data. Brief Bioinform 6: 331–343.

[163] Saeys Y, Inza I, Larranaga P (2007) A review of feature selection techniques in bioinformatics. Bioinformatics 23: 2507–2517.

[164] Wang Y, Tetko IV, Hall MA, Frank E, Facius A, et al. (2005) Gene selection from microarray data for cancer classification–a machine learning approach. Comput Biol Chem 29: 37–46.

[165] Rocke DM, Ideker T, Troyanskaya O, Quackenbush J, Dopazo J (2009) Papers on normalization, variable selection, classification or clustering of microarray data. Bioinformatics 25: 701–702.

[166] Jeffery IB, Higgins DG, Culhane AC (2006) Comparison and evaluation of methods for generating differentially expressed gene lists from microarray data. BMC Bioinformatics 7: 359.

[167] Anand A, Suganthan PN (2009) Multiclass cancer classification by support vector machines with class-wise optimized genes and probability estimates. J Theor Biol 259: 533–540.

[168] Hawkins DM (2004) The problem of overfitting. J Chem Inf Comput Sci 44: 1–12.

[169] Suzuki T, Honda M, Matsumoto S, Sturzenbaum SR, Gamou S (2005) Valosine-containing proteins (VCP) in an annelid: identification of a novel spermatogenesis related factor. Gene 362: 11–18.

[170] Mosser DD, Caron AW, Bourget L, Meriin AB, Sherman MY, et al. (2000) The chaperone function of hsp70 is required for protection against stress-induced apoptosis. Mol Cell Biol 20: 7146–7159.

[171] Arcuri F, Papa S, Meini A, Carducci A, Romagnoli R, et al. (2005) The translationally controlled tumor protein is a novel calcium binding protein of the human placenta and regulates calcium handling in trophoblast cells. Biol Reprod 73: 745–751.

[172] Southby J, Gooding C, Smith CW (1999) Polypyrimidine tract binding protein functions as a repressor to regulate alternative splicing of alpha-actinin mutally exclusive exons. Mol Cell Biol 19: 2699–2711.

[173] Tonevitsky EA, Trushkin EV, Shkurnikov MU, Akimov EB, Sakharov DA (2009) Changed profile of splicing regulator genes expression in response to exercise. Bull Exp Biol Med 147: 733–736.

[174] Jorgensen R, Merrill AR, Andersen GR (2006) The life and death of translation elongation factor 2. Biochem Soc Trans 34: 1–6.

[175] Trabucchi M, Briata P, Garcia-Mayoral M, Haase AD, Filipowicz W, et al. (2009) The RNA-binding protein KSRP promotes the biogenesis of a subset of microRNAs. Nature 459: 1010–1014.

[176] Song H, Mugnier P, Das AK, Webb HM, Evans DR, et al. (2000) The crystal structure of human eukaryotic release factor eRF1–mechanism of stop codon recognition and peptidyl-tRNA hydrolysis. Cell 100: 311–321.

[177] Gong P, Basu N, Scheuhammer AM, Perkins EJ (2010) Neurochemical and electrophysiological diagnosis of reversible neurotoxicity in earthworms exposed to sublethal concentrations of CL-20. Environ Sci Pollut Res Int 17: 181-186.

[178] Orton RJ, Sturm OE, Vyshemirsky V, Calder M, Gilbert DR, Kolch W (Dec 2005). Computational modelling of the receptor-tyrosine-kinase-activated MAPK pathway. The Biochemical journal 392 (Pt 2): 249–61.

[179] Walker FO (2007). "Huntington's disease". *Lancet* **369**(9557): 218

[180] Kremer B (2002). "Clinical neurology of Huntington's disease". In Bates G, Harper P, and Jones L. Huntington's Disease – Third Edition. *Oxford: Oxford University Press*. pp. 28–53.

[181] Akutsu T, Miyano S, Kuhara S (1999). Identification of genetic networks from a small number of gene expression patterns under the Boolean network model. *Pacific Symposium on Biocomputing*, **4**:17-28.

[182] M. Brun, E. R. Dougherty, I. Shmulevich (2005). Steady-State Probabilities for Attractors in Probabilistic Boolean Networks. *Signal Processing*, **85**, 1993–2013.

[183] Werhli, A.V., Husmeier, D (2007). Reconstructing gene regulatory networks with Bayesian networks by combining expression data with multiple sources of prior knowledge. *Stat. Appl. Genet. Mol. Biol.*, **6**:Article 15.

[184] Needham, C.J., Bradford, J.R., Bulpitt, A.J.,Westhead, D.R (2007). A primer on learning in Bayesian networks for computational biology. *PLoS Comput. Biol.* **3** (8), e129.

[185] Murphy, K. and Mian, S (1999). Modelling gene expression data using dynamic Bayesian networks. *Technical report, Computer Science Division, University of California, Berkeley, CA.*

[186] Z. Ghahramani (2002). Graphical Models: Parameter Learning. The handbook of Brain Theory and Neural Networks (2nd edition).

[187] R. Greiner and W. Zhou (2002). Structural extension to logistic regression: Discriminant parameter learning of belief net classifiers. In *AAAI*.

[188] H. Wettig, P. Grünwald, T. Roos, P. Myllymäki, and H. Tirri (2003). When discriminative learning of Bayesian network parameters is easy. In *IJCAI2003*, pages 491-496.

[189] P. Kontkanen, P. Myllymäki, T. Silander, and H. Tirri (1999). On supervised selection of Bayesian networks. In *UAI99*, pages 334-342.

[190] A. Ng and M. Jordan (2001). On discriminative versus generative classifiers: A comparison of logistic regression and naive Bayes. In *NIPS*.

[191] Murphy, K (2002). Dynamic Bayesian Networks: Representation, Inference and Learning. PhD dissertation, University of California, Berkeley.

[192] Bayes Net Toolbox. http://www.cs.berkeley.edu/~murphyk/Bayes/bnt.html

[193] S. Liang, S. Fuhrman, et al (1998). Reveal, a general reverse engineering algorithm for inference of genetic network architectures. *Pac Symp Biocomput*: 18-29.

[194] Yu,H., Luscombe,N.M., Qian,J. and Gerstein,M (2003). Genomic analysis of gene expression relationships in transcriptional regulatory networks. *Trends Genet,* **19**, 422–427.